# Class III HD-ZIP transcription factors in patterning and differentiation of the vascular system in *Arabidopsis*

A dissertation submitted to the
UNIVERSITY OF NEUCHATEL
for the degree of
Doctor of Natural Sciences

Presented by MICHAEL ILEGEMS
from the Institute of Biology, Laboratory of Plant Physiology

Accepted on the recommendation of
Prof. Felix Kessler, thesis director
Dr. Pia Stieger, thesis supervisor
Prof. John Bowman
Dr. Philippe Reymond
the 31 March 2008

*Keywords*: class III HD-ZIP, AtHB8, revoluta, vascular system, kanadi, auxin, microRNA, development, Arabidopsis thaliana

*Mots-clefs:* HD-ZIP de classe III, AtHB8, revoluta, système vasculaire, kanadi, auxine, microARN, developement, Arabidopsis thaliana

Université de Neuchâtel

FACULTE DES SCIENCES
Secrétariat-Décanat de la faculté
- Rue Emile-Argand 11
- CP 158
- CH-2009 Neuchâtel

# IMPRIMATUR POUR LA THESE

## Discovering the role of auxin and class III HD-ZIP transcription factors in the patterning and differentiation of the vascular system in Arabidopsis

**Michael ILEGEMS**

UNIVERSITE DE NEUCHATEL

FACULTE DES SCIENCES

La Faculté des sciences de l'Université de Neuchâtel,
sur le rapport des membres du jury

M. F. Kessler (directeur de thèse),
Mme P. Stieger, MM. P. Reymond (Université de Lausanne)
et J. Bowman (Melbourne)

autorise l'impression de la présente thèse.

Neuchâtel, le 8 mai 2008

Le doyen :
F. Kessler

UNIVERSITE DE NEUCHATEL
FACULTE DES SCIENCES
Secrétariat - décanat de la faculté
Rue Emile-Argand 11 - CP 158
~~CH~~-2009 Neuchâtel
felix Kessler

# Contents

# Abstract

The plant vascular system connects the different plant organs. This network not only allows the transport of water, nutrients and signaling molecules, but also provides a support to the plant stature. The formation of the vascular system depends on the procambium, also called vascular stem cells. To produce the principal conducting tissues phloem and the xylem, procambium cells are tightly regulated by hormonal and genetic signals. An effective interplay between the abaxial and adaxial dorsoventral signals is needed to obtain a properly developed vascular system.

The work presented here focuses on a family of transcription factors, the class III homeodomain leucine zipper (HD-ZIP III) that are involved in vascular system differentiation. Two members of this class, *AtHB8* and *AtHB15*, are expressed in the procambium and protoxylem. In this approach, class III HD-ZIPs were ectopically expressed throughout the plant. Post-transcriptional regulation of these genes normally occurring by microRNAs was omitted by mutating the microRNA target site in the class III HD-ZIP transgenes. The role of *AtHB8* in xylem differentiation as well as its post-transcriptional regulation by microRNAs was confirmed in this study. Moreover, this approach suggested that almost all class III HD-ZIP transcription factors share the same functions in adaxial identity and vascular differentiation and differ only in their expression pattern.

In the second part of this work, vascular development of plants with reduced class III HD-ZIPs or ectopic expression of an antagonist, *KANADI1* (*KAN1*), in the procambium was studied. The reduction of class III HD-ZIPs in this tissue resulted in an enlargement of procambial tissues and wider auxin distribution. The ectopic expression of *KAN1* in procambium cells inhibited the formation of the vascular system. Polar auxin transport (PAT) was affected by the ectopic expression of *KAN1*. These observations suggest that class III HD-ZIPs regulate the vascular system development by promoting xylem differentiation, while PAT is affected by the ectopic expression of *KAN1*.

# Résumé

Le système vasculaire connecte les différents organes de la plante. Ce réseau permet non seulement le transport d'eau, de produits de la photosynthèse et de molécules signale, mais fourni également un support physique à la plante. La mise en place du système vasculaire se fait à partir du procambium, les cellules souches du système vasculaire. Un fin contrôle par des signaux hormonaux ou génétiques régule la différentiation du procambium en tissus conducteurs du système vasculaire : le xylème et le phloème.

Afin d'élucider les mécanismes qui régulent la différentiation du système vasculaire, une famille de facteurs de transcription, les homeodomaine leucine-zippers de classe III (HD-ZIP III), a été étudiée dans ce travail. Deux membres de cette famille, *AtHB8* et *AtHB15*, sont exprimés dans le procambium et le protoxylème du système vasculaire. L'expression de HD-ZIPs III sous une forme résistante à la régulation post-transcriptionnelle par des microARNs a permis de confirmer leur rôle dans la maturation du système vasculaire de la plante. De plus, les fonctions de quatre facteurs de transcription HD-ZIP III se sont révélées similaires: Ils peuvent réguler la différentiation du système vasculaire et définir une identité dorsoventrale de type adaxiale. La différence entre ces gènes réside ainsi dans leur région d'expression.

Dans la deuxième partie de ce travail, l'établissement du système vasculaire a été étudié grâce à un système réduisant les HD-ZIPs III ou exprimant leur antagoniste, *KANADI1* (*KAN1*), dans le procambium. La réduction des HD-ZIPs III dans ce tissu résulta en un élargissement du procambium et en une distribution plus large d'auxine. L'expression de *KAN1* dans ce tissu inhiba la formation du système vasculaire et affecta le transport d'auxine. Ces observations suggèrent que les HD-ZIP III régulent le développement du système vasculaire en promouvant sa différentiation en xylème, alors que *KAN1* affecte la distribution d'auxine.

# List of abbreviations

| | |
|---|---|
| % (v/v) | ml/100ml |
| % (w/v) | g/100ml |
| *ACT* | *ACTIN* |
| *AGO* | *ARGONAUTE* |
| AHP | histidine phosphotransfert protein |
| *APL* | *ALTERED PHLOEM DEVELOPMENT* |
| ARF | auxin response factor |
| ARR | nuclear response regulator |
| *AS1* | *ASYMETRIC LEAFS 1* |
| *At* | *Arabidopsis thaliana* |
| ATP | adenosine triphosphate |
| *AUX1* | *AUXIN RESISTANT 1* |
| *Aux/IAA* | *AUXIN/INDOLE-3-ACETIC ACID* |
| *BDL* | *BODENLOS* |
| bp | base pairs |
| BR | brassinosteroid |
| *BRI1* | *BRASSINOSTEROID INSENSITIVE 1* |
| *BRL1* | *BRI1-LIKE1* |
| CaMV | cauliflower mosaic virus |
| cDNA | complementary DNA |
| *CLE* | *CLV3/ESR-related* |
| *CLV* | *CLAVATA* |
| Col | Columbia |
| *CRC* | *CRAB CLAW* |
| *CRE* | *CYTOKININ RESPONSE* |
| *CUC* | *CUP-SHAPED COTYLEDON* |
| DAG | days after germination |
| DNA | desoxyribonucleic acid |
| dNTP | desoxy nucleotide triphosphate |
| *DCL* | *DICER* |
| DR5 | synthetic auxin response element |
| *DRN* | *DORNROESCHEN* |
| *DRNL* | *DORNROESCHEN-LIKE* |
| dsRNA | double stranded RNA |
| DTT | 1,4-dithio-DL-threitol |
| *E. coli* | *Escherichia coli* |
| EDTA | ethylenediamine-N,N,N',N'-tetraacetic acid |
| *En-2* | *Enkheim-2* |
| EST | expressed sequence tag |

| | |
|---|---|
| *ETT* | *ETTIN* |
| *FIL* | *FILAMENTOUS FLOWERS* |
| gDNA | genomic DNA |
| GFP | green fluorescent protein |
| gof | gain of function |
| GS | goat serum |
| GUS | 5-Bromo-4-Chloro-3-Indoxyl-β-D glucuronic acid |
| *HCA* | *HIGH CAMBIAL ACTIVITY* |
| HD-ZIP | homeo domain leucin-zipper |
| His6 | hexahistidinyl-tag |
| IAA | indole-3-acetic acid |
| *ICU4* | *ICURVATA4* |
| *INO* | *INNER NO OUTER* |
| *KAN* | *KANADI* |
| *KNOX* | *KNOTTED homeodomain* |
| kb | kilo base pairs |
| kDa | kilo Dalton |
| LB | T-DNA left boarder or Luria-Bertani |
| LC-MSMS | liquid chromatography tandem mass-spectrometry |
| Ler | Landsberg erecta |
| LhG4 | *lac*/*Gal4* domain II chimeric transcription factor |
| LLR-RLK | leucine-rich repeat receptor-like kinase |
| lof | loss of function |
| MAPK | mitogen-activated protein kinase |
| *MDR* | *MULTIDRUG RESISTANCE* |
| miRNA | micro RNA |
| *ML1* | *MERISTEMATIC LAYER 1* |
| *MP* | *MONOPTEROS* |
| mRNA | messenger RNA |
| MS | Murashige and Skoog |
| n.a. | not available |
| NAA | naphthylacetic acid |
| NAC | NAM, ATAF1/2 and CUC2 |
| Ni-NTA | nickel-nitrilotriacetic acid |
| NPA | 1-N- naphthylphtalamic acid |
| *NST* | *SECONDARY WALL THICKENING PROMOTING FACTOR* |
| pat | polar auxin transport |
| PBS | phosphate-buffered saline |
| PCR | polymerase chain reaction |
| PGP | p-glycoproteins |
| *PHB* | *PHABULOSA* |
| *PHV* | *PHAVOLUTA* |
| *PID* | *PINOID* |
| *PP2A* | *PROTEIN PHOSPHATASE 2A* |
| *PXY* | *PHLOEM INTERCALATED WITH XYLEM* |
| RB | T-DNA right boarder |
| RdRp/RDR | RNA-dependent RNA polymerases |
| *REV/IFL1* | *REVOLUTA / INTERFASCICULAR FIBERLESS1* |
| RISC | RNA induced silencing complex |
| RNA | ribonucleic acid |
| rRNA | ribosomal RNA |

| | |
|---|---|
| *RS2* | *ROUGH SHEATH 2* |
| RT | room temperature |
| RT-PCR | reverse transcription-PCR |
| SAM | shoot apical meristem |
| SDS | sodium dodecyl sulfate |
| SDS-PAGE | SDS-polyacrylamide gel electrophoresis |
| SEM | scanning electron microscopy |
| siRNA | short interfering RNA |
| *SND1* | *SECONDARY WALL–ASSOCIATED NAC DOMAIN 1* |
| ssRNA | single stranded RNA |
| START | Steroidogenic Acute Regulatory protein-related lipid-Transfer |
| *STM* | *SHOOT MERISTEMLESS* |
| tasiRNA | trans-acting siRNA |
| *TDIF* | *TREACHERY ELEMENT DIFFERENTIATION INHIBITORY FACTOR* |
| TE | treachery elements |
| T-DNA | transfer DNA |
| *TIR1* | *TRANSPORT INHIBITOR RESPONSE 1* |
| tricine | N-tris(hydroxymethyl)methylglycine |
| Tris t | Tris(hydroxymethyl)aminomethane |
| TX-114 | triton X-114 |
| UTR | untranslated region |
| UV | ultra violet |
| Vb | vascular bundle |
| *VDN* | *VASCULAR RELATED NAC-DOMAIN* |
| *WOL* | *WOODEN LEG* |
| wt | wild type |
| *WUS* | *WUSCHEL* |
| *YAB* | *YABBY* |
| YEB | yeast extract broth |
| *ZPR* | *LITTLE ZIPPER* |

| | |
|---|---|
| Upper case, italic | gene, wild type allele (e.g. *AtHB8*) |
| Lower case, italic | mutant allele (e.g. *athb15*) |
| Upper case | protein (e.g. AtHB8) |
| : | fusion of two proteins (e.g. PIN1:GFP) |
| :: | promoter-coding sequence fusion (e.g. *AtHB8*::AtHB8 wt) |
| >> | binary transactivation system promoter>>gene coding sequence association (e.g. REV>>AtHB8) |
| -∂*miR* | Placed after a gene, this particle indicates that a point mutation in the miRNA binding site is present. |

# Chapter 1
# Introduction

## 1.1 The importance of the plant vascular system

The plant vascular system is the organ that allows the transport of water and nutrients throughout the plant. What appears to be a basic function also played a fundamental role in evolution. The possibility to transport water over long distances and the mechanical resistance provided by the vascular system represented a major progress during the process of dry land colonization by the first plants millions of years before our era. Tissue rigidity allowed plants to grow vertically, what provided not only an enhanced photosynthetic surface, but also an important advantage for sunlight competition. This new strategy resulted in the production of the currently most abundant biomass on the planet: wood. Wood is one of the key raw and renewable materials of today's industry, used for construction, combustion and paper production. In addition to the major environmental and economical value of the forest, it has been shown that wood formation is one of the major sinks for atmospheric carbon dioxide (Plomion et al., 2001).

This introduction on plant vascular system development has the following structure: After a morphological description of the tissue, key elements of vascular setup, maintenance and differentiation are reviewed. Roles of plant hormones as well as genes defining vascular identity are described for the different stages of vascular development.

## 1.2 Morphology of the plant vascular system

The vascular tissue of the adult plant is generated continuously from apical meristems.

Organized in vascular bundles, the vascular tissue is divided in three parts. The phloem distributes products of photosynthesis as well as proteins, peptides and mRNA. The xylem conducts water and minerals from the soil to the aerial parts. These two tissues are generated from the vascular meristematic tissue called procambium. In plants where secondary growth occurs, phloem and xylem are also generated later by the cambium. The exact mechanisms triggering the transition between procambium and cambium have not been determined yet. Morphologically, the (pro)cambium presents cytoplasm dense elongated cells tightly ordered in a transversal structure in the center of the vascular bundles (Nelson and Dengler, 1997). Divisions of (pro)cambial cells along the axis separating xylem and phloem increase the plant circumference. Together with divisions along the central-peripheral axis, these two events enlarge the stem diameter. Divisions on the abaxial (away from the meristem) side of the (pro)cambium produce the phloem. The phloem is composed of long conducting sieve elements associated with their companion cells, non-conducting parenchyma cells and fibers. Together, the sieve elements form the sieve tube, the conducting element of the phloem. Contrary to tracheary elements, sieve elements are living cells conserving their nucleus and separated from one another by sieve plates (Fukuda, 2004). Opposite to the phloem, xylem, also known as wood, develops in the adaxial (near the meristem) region from the (pro)cambium. Wood is composed of tracheary elements for transport of water and solutes, fibers for mechanical resistance and parenchyma. The tracheary elements are composed of tracheids and vessels. Vessels in angiosperms can be of two types: protoxylem and metaxylem. Protoxylem vessels with annular and spiral secondary wall thickenings form by differentiation from the procambium. Protoxylem is often mature and functional before the surrounding tissue, but is also frequently destroyed at the end of the maturation of surrounding tissues. On the other hand, metaxylem vessels with reticulate and pitted thickenings differentiate from cambium and mature at the same time as the surrounding tissues (Demura and Fukuda, 2007). The maturation of xylem cells is divided into four steps: 1) Cell expansion; 2) Formation of the secondary cell wall, a process

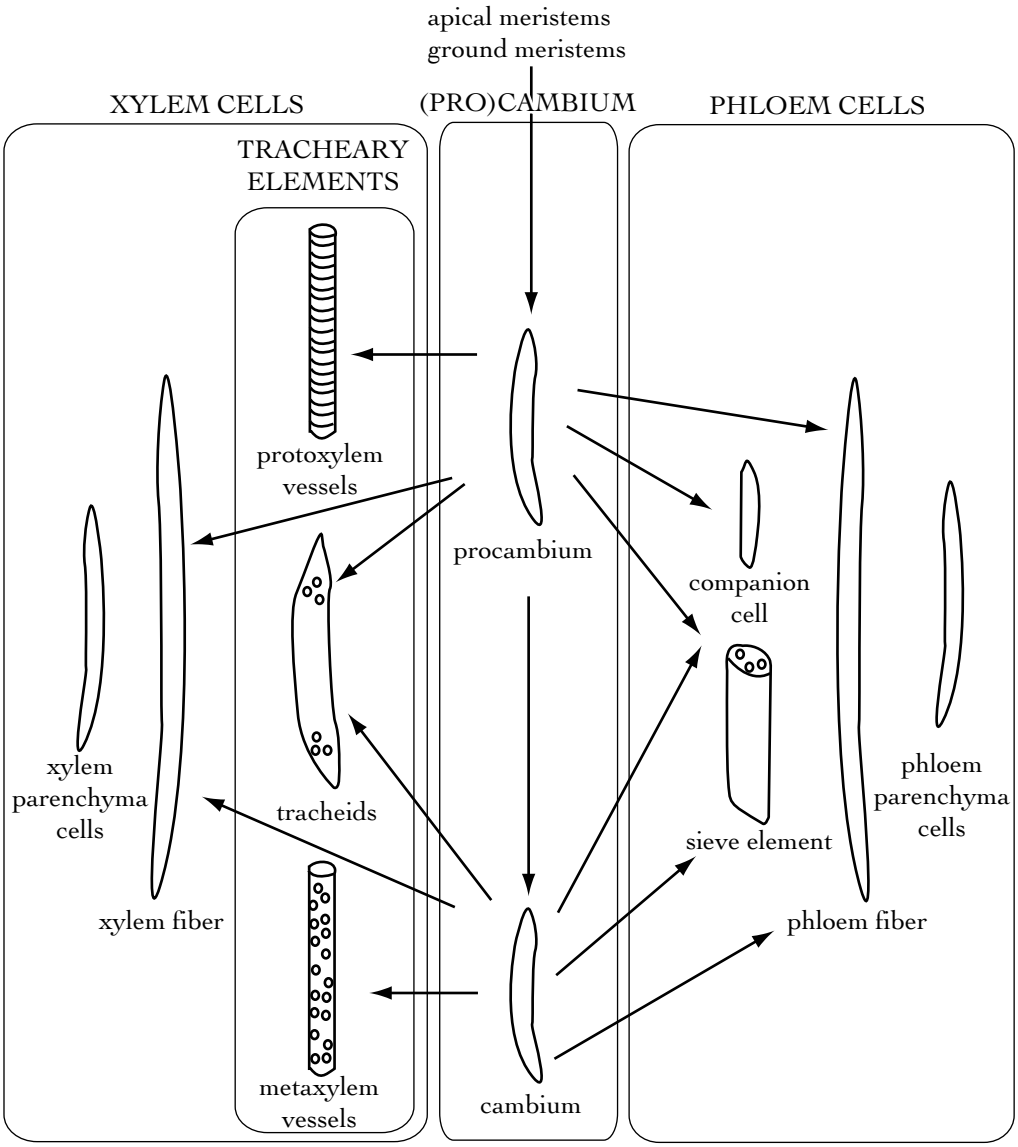


**Figure 1.1: Schematic representation of vascular system formation.** Cells from the (pro)cambium and their daughter cells can differentiate into phloem cells and xylem cells. Xylem cells are constituted of tracheary elements (tracheids and vessels), fibres and parenchyma. Phloem cells are constituted of sieve elements and their associated companion cell, fibres and parenchyma.

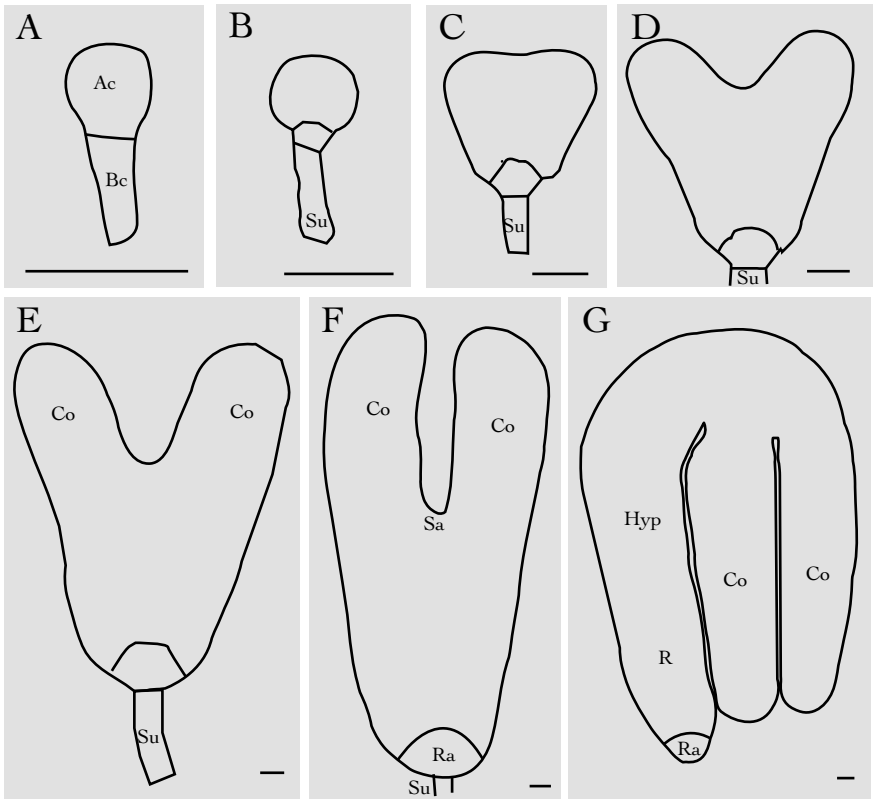


**Figure 1.2: Arabidopsis thaliana embryo development.** The embryogenesis is characterized by a well-defined pattern of cell divisions. Successive steps of embryogenesis are described here. One cell embryo (A); early globular (B); heart stage (D); late heart stage (E); torpedo stage (F); mature embryo (G). Ac, apical cell; Bc, basal daughter cell; Co, cotyledon; Hyp, hypocotyl; R, radicle; Ra, root apex; Su, suspensor. Scale bar is approximately 25 µm.

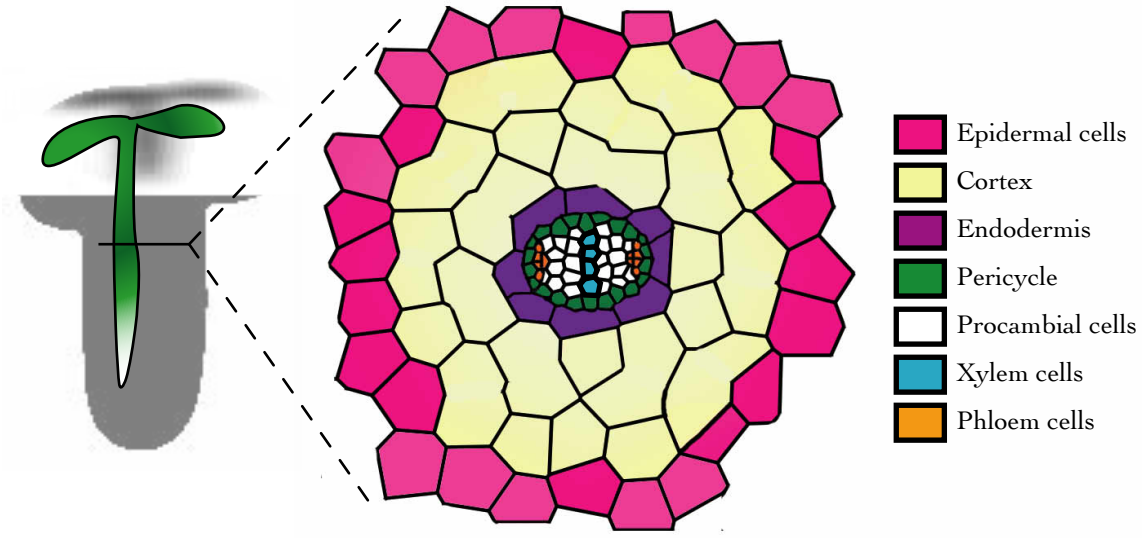


**Figure 1.3: Organization of the vascular system in the hypocotyl of Arabidopsis thaliana seedlings.** The approximate level of the cross-section is shown by the line on the seedling scheme.

that is dependent on the biosynthesis of polysaccharides and cell wall proteins; 3) Lignification of the cell wall; 4) Senescence that allows the cells to be emptied to form a tube (Plomion et al., 2001).

The different components of the vascular system in the adult plant are schematically presented in figure 1.1. This arrangement, predictably, begins its establishment during embryogenesis (Figure 1.2) (Ye et al., 2002; Scarpella et al., 2004). A correct patterning of all early actors of plant differentiation is necessary for an accurate embryogenesis and postembryonic development of the plant body and the vascular system. Distinct developmental potentials distinguish the cells derived from the upper, middle and lower region of the globular embryo. The apical region develops into cotyledons and the shoot apical meristem (SAM) at the heart stage. On the other hand, the central region differentiates into the hypocotyl and the major part of the root. Finally, the apical cells of the suspensor become the quiescent center and columella of the root. A correct signal patterning results in the establishment of the three main tissues in the embryo: epidermis, ground and vascular tissue. These latter are organized in radial layers with superimposition of apical-basal and radial pattern elements.

In the following sections, patterning signals will be presented in the form of plant hormones and developmental genes, principally transcription factors, affecting vascular system differentiation. Patterning signals are roughly classified by their corresponding vascular localization, procambium, phloem and xylem. Occasionally, parallels to tissue patterning in other organs are drawn.

## 1.3 Auxin, regulator of procambium cell establishment

Among the plant hormones that were shown to induce vascular differentiation, the most important is certainly auxin. This phytohormone not only induces vascular differentiation, but a local application of auxin can also induce the transformation of parenchyma cells into a continuous and oriented vascular strand (Sachs, 1981). This section describes how polar auxin transport influences vascular development.

### 1.3.1 Discovery of the plant hormone auxin

The effects of the plant hormone auxin were first described more than 100 years ago by Charles and Francis Darwin. They observed that a growth stimulus, induced by light, and generated at the tip of a coleoptile was transmitted to the growth zone (Darwin and Darwin, 1881). At this time, the signal was not identified. However, some years later, the presence of a growth-promoting chemical was confirmed in the tip of the *Avena sativa* coleoptile. Went isolated it and demonstrated that it was able to promote the elongation of the coleoptile without light (Went, 1928). This chemical was thus named from the Greek word "auxein" translated as "to grow".

The chemical structure of auxin, indole-3-acetic acid (IAA) was determined in the 1930s (Thimann, 1935). Since then, several other auxins were identified or synthesized. The common feature of active auxins is the 0.5nm distance separating a positively charged aromatic group and a negatively charged carboxyl group (Taiz and Zeiger, 2006).

### 1.3.2 Auxin signaling

Since its identification, roles of auxin in plant development have been extensively studied. The set of genes regulated by the presence of auxin affects many developmental processes that range from germination to senescence of the plant. Regulation of apical dominance, floral bud development, phyllotaxy, formation of lateral and adventive roots and vascular differentiation are the most cited regulatory effects of auxin (Taiz and Zeiger, 2006). It is therefore not surprising that synthetic auxin has been widely used from agricultural applications to military warfare (Murphy, 2005). In the next paragraph, the most studied auxin signaling pathway, involving *AUXIN/INDOLE-3-ACETIC ACID* (*Aux/IAA*) and *AUXIN RESPONSE FACTORS* (*ARF*) genes, is described.

ARFs are transcription factors that, as indicated by their name, modulate auxin response of genes downstream in the auxin signaling/response pathway. ARF proteins can be either activators or repressors. Their state is dependent on the ratio of the glutamine amino acid in their central domain (Tiwari et al., 2003). Aux/IAA proteins, whose family includes 29 different members in the *Arabidopsis thaliana* genome, bind to ARFs via two domains

allowing heterodimerization (Hagen and Guilfoyle, 2002). This association results in the inhibition of ARF activity. AUX/IAA proteins contain a specific domain that can be ubiquitinated. Ubiquitination of AUX/IAAs leads to a rapid degradation of these proteins by the 26S proteasome. Therefore, modulation of gene transcription by ARFs is dependent on ubiqitination of AUX/IAA proteins. Ubiquitination of AUX/IAAs occurs upon auxin binding to the "F-box" receptor present in the TRANSPORT INHIBITOR RESPONSE 1 (TIR1) proteins (Dharmasiri et al., 2005a; Dharmasiri et al., 2005b; Kepinski and Leyser, 2005). TIR1 proteins are part of the $SCF^{TIR1}$ ubiquitin ligase complex that, when activated by auxin, ubiquitinate AUX/IAA repressor proteins. This regulation system guarantees that ARFs present in cells only activate or repress auxin-related genes in the presence of the phytohormone. The MONOPTEROS (MP/ARF5) transcription factor and auxin response inhibitor BODENLOS (BDL/IAA12) are two well-known components of the ARF-AUX/IAA regulation mechanism. When active, MP/ARF5 promotes vascular development and therefore facilitates auxin flux (Jenik and Barton, 2005). The homozygous *mp* mutant does not develop a root and the vascular system is altered (Berleth and Jurgens, 1993). These alterations are highly similar to those observed in the *bdl-1* dominant mutant that is not regulated by the $SCF^{TIR1}$ ubiquitin ligase complex (Hamann et al., 2002). Thus, in the absence of auxin in wild-type plants MP/ARF5 transcriptional activation is inhibited though an interaction with BDL/IAA12. It has been shown recently that a third actor, *TOPLESS*, interacted with BDL/IAA12 to repress MP/ARF5 (Szemenyei et al., 2008).

### 1.3.3 Auxin transport

The pivotal role of auxin in different developmental processes implies that its transport and presence is tightly regulated. Although auxin is amphiphatic, its transport by diffusion is marginal. The difference of pH between the cytosol of the cells (pH 7.2) and the apoplast (pH ≅ 5) signifies that auxin, a weak acid (pKa = 4.75), is partially anionic within the apoplast. Considering these chemiosmotic parameters, auxin can freely enter the cells, but needs an active efflux to prevent remaining trapped within cells. The localization of the auxin efflux and influx carriers defines a route for auxin (Rubery and Sheldrake,

1974; Raven, 1975). Influx of auxin can occur via the AUXIN RESISTANT 1 (AUX1) $2H^+$ -$IAA^-$ symporter (Bennett et al., 1996; Swarup et al., 2001). The active influx provided by AUX1 symporter is thought to prevent diffusion of auxin in neighbouring cells, thereby maintaining an optimal flux (Swarup et al., 2001; Hellmann et al., 2003; Reinhardt et al., 2003).

Two families of proteins were shown to be determinant in regulating auxin efflux, *PIN FORMED (PIN)* and *MULTIDRUG RESISTANCE (MDR)-p-glycoproteins (PGP)*. Composed of 8 members in *Arabidopsis*, PIN proteins contain multiple potential transmembrane domains. The PIN protein localization on specific sides of the plasma membrane supports the polar transport model in which they are guiding auxin flow (Galweiler et al., 1998; Friml et al., 2003). Plants with a mutation in *PIN1* have been shown to phenocopy plants cultivated with the 1-N-naphthylphtalamic acid (NPA) auxin transport inhibitor (Okada et al., 1991). Although PIN2 and PIN7 reduce auxin retention in heterologuous yeast models (Blakeslee et al., 2005) and are similar to bacterial transporters (Galweiler et al., 1998), PIN proteins are considered as auxin efflux facilitators rather than auxin efflux carriers (Blilou et al., 2005; Benjamins and Scheres, 2008). The other proteins known to mediate auxin efflux, PGPs, are membrane proteins of a family including 5 members (Murphy et al., 2000; Brown et al., 2001; Gil et al., 2001; Noh et al., 2001; Murphy et al., 2002; Noh et al., 2003). Examination of mutants for PGPs shows that this class of proteins is necessary for polar auxin transport (pat) (Noh et al., 2001). Furthermore, interactions have been observed between PGPs and PINs as well as a broad expression pattern overlap (Blakeslee et al., 2005). PIN1, PIN2, PGP1, PGP2 and PGP4 display a high affinity for the NPA inhibitor of auxin transport (Noh et al., 2001; Murphy et al., 2002). Although the exact interaction between PGPs and PINs remains unknown, it has been suggested that PIN proteins modulate the activity of PGP transporters (Petrasek et al., 2006).

At the level of individual cells, correct orientation of the components of the auxin efflux complex is necessary to allow pat. Mutants with mislocalization of PIN proteins indicated that a correct phosphorylation state was required. The PINOID (PID) serine/threonine kinase and the PROTEIN PHOSPHATASE 2A (PP2A) are involved in this mechanism as they were

proposed to be involved in vesicular trafficking of PIN proteins (Garbers et al., 1996; Michniewicz et al., 2007).

Auxin transport seems to depend on several self-regulatory mechanisms. With experiments involving artificial vascular differentiation, Sachs (Sachs, 1981; Sachs, 1991) proposed an "auxin canalization theory". Diffusion of auxin induces the establishment of an active transport of auxin in certain cells, promoting their conductivity for auxin. In turn, the higher auxin flux creates a canal in the activated cells favouring their differentiation into procambium. It has been proposed that this regulatory mechanism would also be responsible for other developmental processes such as recovery after wounding, vascular venation, establishment of the embryo axis and organogenesis (Berleth and Sachs, 2001). Recent evidence has shown that the Aux/IAA-ARF pathway and *PIN1* is involved in this process (Sauer et al., 2006).

### 1.3.4 Auxin localization

Although all plant tissues appear to be able to synthesize auxin, the SAM and young leaves seem to be primary sites of auxin production (Ljung et al., 2005). However, exact localizations of auxin biosynthesis remain more or less unknown (Benjamins and Scheres, 2008). The localization of enzymes involved in auxin biosynthesis indicates that meristems, young primordia, vascular tissues, and reproductive organs are the primary sites of biosynthesis (Boerjan et al., 1995; Seo et al., 1998; Cheng et al., 2006, 2007). To localize auxin, constructs combining identical or near-identical promoter regions of auxin inducible genes (GH3, SAUR, DR5, 2xDO) are used with a reporter gene such as the β-glucuronidase (*GUS)* or green fluorescent protein (*GFP*) (Ulmasov et al., 1997; Murphy, 2005). The localization of auxin is further complicated as more than 99% of it is covalently linked with small molecules such as glucose or larger molecules such as peptides (Park et al., 2001). These molecules are biologically inactive but both amide and sugar linked IAAs can be released by hydrolysis (Bartel, 2005).

## 1.4 Maintenance of cambium activity

As the procambium is at the origin of the functional vascular system, its orientation, localization, reticulation, continuity and maintenance are of first importance. Identity and characteristics of procambium are preserved by several factors including antagonistic signals provided by the abaxial and adaxial regions, polar auxin transport and cytokinins (Fukuda, 2004; Scarpella and Meijer, 2004; Carlsbecker and Helariutta, 2005). It also appears that meristematic tissues, such as the SAM and procambium, share some signaling pathways to maintain their stem cell population. Thus, techniques as gene trapping, often lead to the discovery of few new cambium specific genes. (Nagawa et al., 2006). Common features of SAM and cambium are described after the next section on SAM establishment and maintenance.

### 1.4.1 Cytokinins and cambium identity

Cytokinins were identified in the course of research on factors stimulating plant cell division. When separated from the whole plant, few organs will continue to grow on a nourishing medium. However, the culture of other plant cells was shown to be possible in the presence of auxin and coconut milk (Caplin and Steward, 1948). It was shown later that cytokinin, an aminopurine derivative, was responsible for cell divisions (Miller et al., 1955). Since then, cytokinins were shown to be involved in many other aspects of plant development such as leaf senescence, apical dominance, chloroplast biogenesis or floral development. Some pathogens, such as *Agrobacterium tumefaciens*, also use cytokinins to influence plant growth (Taiz and Zeiger, 2006).

Cytokinins have an important role in procambium establishment and maintenance, as a cytokinin receptor mutant, *wooden leg/cytokinin response* (*wol/cre1*), presents a reduced procambium in embryos and its root vascular system is mainly composed of xylem cells. The study of WOL/CRE1, present in root procambium, demonstrated the role of cytokinins in procambial cell divisions (Mahonen et al., 2000; Inoue et al., 2001) and indicated that cytokinins act as negative regulators of protoxylem differentiation. A signaling cascade, including WOL/CRE1, *Arabidopsis thaliana* HISTIDIN KINASE2 (AtHK2) and AtHK3 as cytokinin receptor, has been proposed. The

active cytokinin receptors interact with histidine phosphotransfert proteins (AHPs) through the action of phosphorelays. AHPs are then translocated from the cytosol to the nucleus and activate the nuclear response regulators (ARRs) transcription activators. The active ARRs can then bind to cis element of target genes (Hwang and Sheen, 2001; Kakimoto, 2003; Mahonen et al., 2006). Other cytokinin-related genes such as *HIGH CAMBIAL ACTIVITY* (*HCA*) have been shown recently to be involved in the regulation of cambium development (Pineau et al., 2005) demonstrating the importance of this phytohormone in cambial activity.

### 1.4.2 Shoot apical meristem and (pro)cambium, the struggle of meristematic tissues

At each end of the apical-basal axis of the plant, meristematic tissues provide undifferentiated cells to form the plant tissues throughout the development. Another meristematic region, the procambium, provides the necessary cells to develop a vascular system. By following the formation of the SAM, we can observe that some mechanisms are shared between these two meristematic tissues.

The formation of the SAM in the early embryo is linked with a peak in auxin concentration. However, the auxin efflux from this region is later needed for its further development (Hardtke et al., 2004). In this central region, the activity of *CUP-SHAPED COTYLEDON* (*CUC*) genes, belonging to the class of NAC-domain transcription factors, and *SHOOT MERISTEMLESS* (*STM*), a KNOTTED1 (KNOX) family gene, define the intercotyledonary zone. A faster expansion in the lateral regions of the embryo gives to the embryo its heart shape (Aida et al., 1997; Aida et al., 1999; Aida et al., 2002; Vroemen et al., 2003). Later on, the expression pattern of *STM* is reduced to a more central region defining the SAM (Long et al., 1996; Long and Barton, 1998). As lateral organs develop, *KNOX* expression is reduced (Long et al., 1996; Kerstetter et al., 1997; Bowman and Eshed, 2000; Vollbrecht et al., 2000). To maintain the identity of the SAM the expression of *WUSCHEL* (*WUS*) in a small sub-apical region appears to be essential (Haecker and Laux, 2001). The expression of WUS is tightly controlled by the *CLAVATA (CLV)* genes. CLV1 is a receptor-like kinase (RLK) with an extracellular leucine-rich (LRR) domain (LRR-RLK),

that presents an extracellular ligand binding domain, a trans-membrane domain and an intracellular kinase domain. CLV1 dimerises with CLV2, a highly similar protein lacking the kinase domain. When activated by CLV3, a CLV3/ESR-related (CLE) peptide, the CLV1-CLV2 heterodimer activates a mitogen-activated protein kinase (MAPK) cascade to repress *WUS* gene expression. WUS limits its own patterning by promoting *CLV3* expression. Mutants of *CLV* genes present an enlarged meristem, while the *wus* mutant fails to produce a SAM. This precise control keeps the expansion of the SAM in a state of equilibrium. Daughter cells either maintain the stem cell population or provide cells which are at the origin of all aerial components of the plant formed after germination (Clark, 2001; Nakajima and Benfey, 2002). Interestingly, the SAM is not the only meristematic tissue whose maintenance is regulated by CLE peptides, as *CLV3* is also involved in cambium maintenance. The main features of the family of CLE peptides are a small size (<14kD), a secretion signal at their amino end, and a 14 amino acid-long CLE motif (Fiers et al., 2007). Beside the common CLE motif, CLE peptides have few sequence similarities. Thus, their function may vary. Some CLE peptides induce cell differentiation, such as *CLV3* that promotes xylem differentiation. Others, like the TRACHEARY ELEMENT DIFFERENTIATION INHIBITORY FACTOR (TDIF) that suppress xylem development, inhibit cell differentiation (Ito et al., 2006). Another LRR-RLK involved in procambium activity, PHLOEM INTERCALATED WITH XYLEM (PXY), has been identified, although no associated CLE peptides have been identified yet. Vascular bundles of the stem in *pxy* mutants are flattened instead of exhibiting the common triangle-shape with intermixed phloem and xylem. *PXY* is proposed to play a role in vascular meristem polarity (Fisher and Turner, 2007).
Thus, different combinations of CLE peptides and LRR-RLK receptors seem to maintain the meristematic function of both SAM and procambium.

## 1.5 Transversal pattering; phloem and abaxial identity

Although the phloem is morphologically and functionally well defined, few factors that define phloem identity are known (Fukuda, 2004; Sieburth and Deyholos, 2006). However, based on its location, it appears that phloem and

abaxial identity are linked. Genes defining abaxial identity in the vascular system and other regions of the plant as well as phloem specific genes are described in this section.

### 1.5.1 *YABBYs* and *KANADIs* defining abaxial identity

The set of genes that are required for a correct abaxial patterning includes the *YABBY (YAB)* genes (Bowman and Eshed, 2000), as mutants missing one or more of these zinc finger proteins develop organs with adaxial characteristics (Bowman et al., 2002). The *YAB* gene family encodes six putative transcription factors with two major patterns of expression. *FILAMENTOUS FLOWER* (*FIL*), *YAB2* and *YAB3* expression is restricted to the abaxial domain of lateral organs of the vegetative or reproductive phase (Bowman et al., 2002; Watanabe and Okada, 2003). Expression of others *YABs* such as *CRAB CLAW* (*CRC*) and *INNER NO OUTER* (*INO*) is limited to floral organs. Ectopic expression of *FIL*, *YAB3* or *CRC* results in tissue abaxialisation (Eshed et al., 1999; Siegfried et al., 1999; Sawa et al., 2006). The role of *YABs* in defining lateral organs is further supported by the fact that they repress expression of *KNOX* genes (Kumaran et al., 2002). In contrary, *FIL* expression is reduced by the class III HD-ZIP transcription factor PHABULOSA (PHB) (See chapter 1.6) (Siegfried et al., 1999). Additionally, when *YAB* mutants are combined with mutants of the *KANADI* (*KAN*) family, the phenomenon of lateral organ adaxialization is further accentuated (Eshed et al., 2004). The four KAN proteins, KAN1, KAN2, KAN3, KAN4/ABERRANT TESTA SHAPE, are the only GARP-type transcription factors known to promote abaxial cell fate (Eshed et al., 2001; Bowman et al., 2002; McAbee et al., 2006). As for *YABBY* genes, mutants of *KAN* have severe abaxial identity defects (Eshed et al., 2001; Kerstetter et al., 2001). *KAN1*, *KAN2* and *KAN3* are involved in dorsoventral identity of leaves and vascular bundles. Only *KAN1* and *KAN2* seem to have the same function in flowers (Eshed et al., 2001). Patterning overlap grants a certain redundancy between certain members of the *KAN* family. This overlap is more limited for the *KAN4* gene, as its role is limited to ovule and embryo development (Izhaki and Bowman, 2007). Inversely, ectopic expression of *KAN* genes in the region of the leaf primordia induces the growth of abaxial

tissues in adaxial regions, reduces lateral lamina growth and affects the vascular system (Eshed et al., 2001).

Several genes have been shown to modulate *KAN* expression. Class III HD-ZIP transcription factors (see chapter 1.6) interact antagonistically with *KAN* genes (Eshed et al., 2004). On the other hand, some ARFs such as ETTIN (ETT) and ARF4 are necessary to *KANs* to promote abaxial identity (Pekker et al., 2005). This interplay between auxin and *KANADI* genes is not limited to ARFs, as it appears that they restrict the localization of PIN proteins (Izhaki and Bowman, 2007).

### 1.5.2 More phloem-specific genes

*KANADI* genes are involved in abaxial identity. *KAN1, KAN2* and *KAN3* are expressed in the corresponding region of the vascular system, the phloem (Emery et al., 2003). Other proteins, such as the MYB-coiled-coil transcription factor ALTERED PHLOEM DEVELOPMENT (APL), appear to be more phloem specific. The *APL* expression pattern is specific to companion cells and proto- and metaphloem sieve elements. The *apl* mutant presents tracheary elements in phloem regions. The sucrose-$H^+$ symporter gene *AtSUC2* (Truernit and Sauer, 1995), that is often used as a companion cell specific marker, is not expressed in *apl* mutants. This absence of phloem in *apl* is seedling lethal. On the other hand, the ectopic expression of *APL* in xylem region delays tracheary element differentiation but was not sufficient to induce ectopic production of phloem. Thus it appears that expression of APL is required but not sufficient to promote phloem identity. APL seems also to prevent the development of xylem specific cells in phloem regions (Bonke et al., 2003).

Several other phloem specific genes are known or have been identified such as the plasma membrane proton pump ($H^+$-ATPase) AHA3 however, few are known to define phloem identity (Zhao et al., 2005).

## 1.6 Transversal patterning: xylem and adaxial identity

In this section, signals linked to xylem formation are presented. Xylem is adaxialy located within the plant. Among the genes specifically expressed in

the adaxial region, some are determinant for xylem differentiation. The class III HD-ZIP transcription factors belong to these genes, and constitute the main topic of this work. Expression pattern, structural domains, functions and mutant phenotypes are thus described in detail. Finally, complementary signals for xylem differentiation, such as other genetic and hormonal factors are also studied.

### 1.6.1 The role of Class III HD-ZIP in vascular differentiation

While the class III HD-ZIP transcription factors *REVOLUTA/INTERFACICULAR FIBERLESS1* (*REV/IFL1*), *PHAVOLUTA/AtHB9* (*PHV/AtHB9*) and *PHB/AtHB14*, are expressed in meristematic tissues and adaxial regions of lateral organs and vasculature, *AtHB8* and *AtHB15/CORONA/INCURVATA4* (*AtHB15/CRN/ICU4*) appear to be more vascular system specific (Fukuda, 2004). As vascular cells originate from both the SAM and root apical meristem, class III HD-ZIP transcription factors play a key role throughout the process of vascular differentiation.
The over-expression of *AtHB8* or its *Zinnia* ortholog, *ZeHB10*, induces xylem tissue and tracheary element (TE) formation in vascular bundles (Baima et al., 2001; Ohashi-Ito et al., 2005). In addition to vascular differentiation, constitutive expression of *AtHB8* induces the formation of hyponastic leaves. On the other hand expression of *REV Zinnia* orthologs, *ZeHB11* or *ZeHB12*, in *Arabidopsis* suggested that REV is involved in the formation of procambium and xylem precursor cells but not in the differentiation of TE. This was supported by microarray data, as no TE-specific genes were induced by *ZeHB12* over-expression, while BR-related genes and genes of the lignin monomer pathway were induced (Ohashi-Ito et al., 2005). *In vitro* data indicate that the *AtHB15* ortholog in *Zinnia*, *ZeHB13*, is expressed during TE differentiation. Several class III HD-ZIP transcription factors have been shown to be targets of BR signaling (Ohashi-Ito and Fukuda, 2003).

### 1.6.2 Structure of the Class III HD-ZIPs

The class III homeodomain (HD) leucin zipper (ZIP) transcription factor family is composed of five members: *REV*, *PHV*, *PHB*, *AtHB8* and *AtHB15* (Talbert et al., 1995; McConnell et al., 2001; Zhong and Ye, 2001; Emery et al., 2003). Gene sequences (Figure 1.5) and functional domains (Figure 1.4 A) are

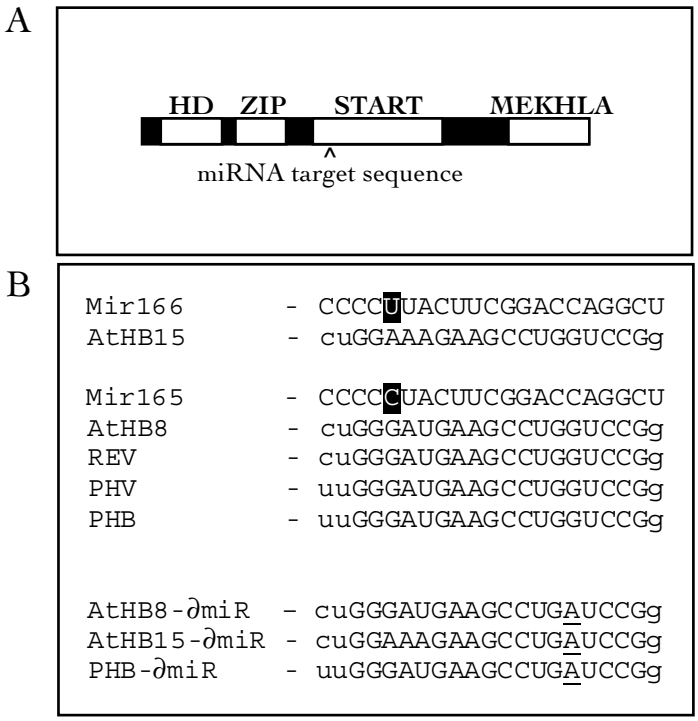


**Figure 1.4: Domains and miRNA binding sites of Class III HD-ZIP transcription factors.** (A) Schematic representation of functional domains of class III HD-ZIP transcription factors: Homeo domain (HD) for DNA binding; Leucin zipper (ZIP) for homo/hetero-dimerization; The putative sterol/lipid binding domain Steroidogneic Acute rugulatory protein-related lipid transfert (START); a C-terminal MEKHLA domain containing a PAS domain; A miRNA target sequence for *miR165* and *miR166* is present in the START domain. (B) miRNA target sequences of the class III HD-ZIP transcription factors and the corresponding *miR165/166*. Sequences are ordered by the closest matching sequences. The unconserved base between *miR165* and *miR166* is shown in black. The altered miR target site of class III HD-ZIPs used in this study are shown on the lower part (*AtHB8-∂miR, AtHB15-∂miR, PHB-∂miR*). The non-silent mutation is underlined.

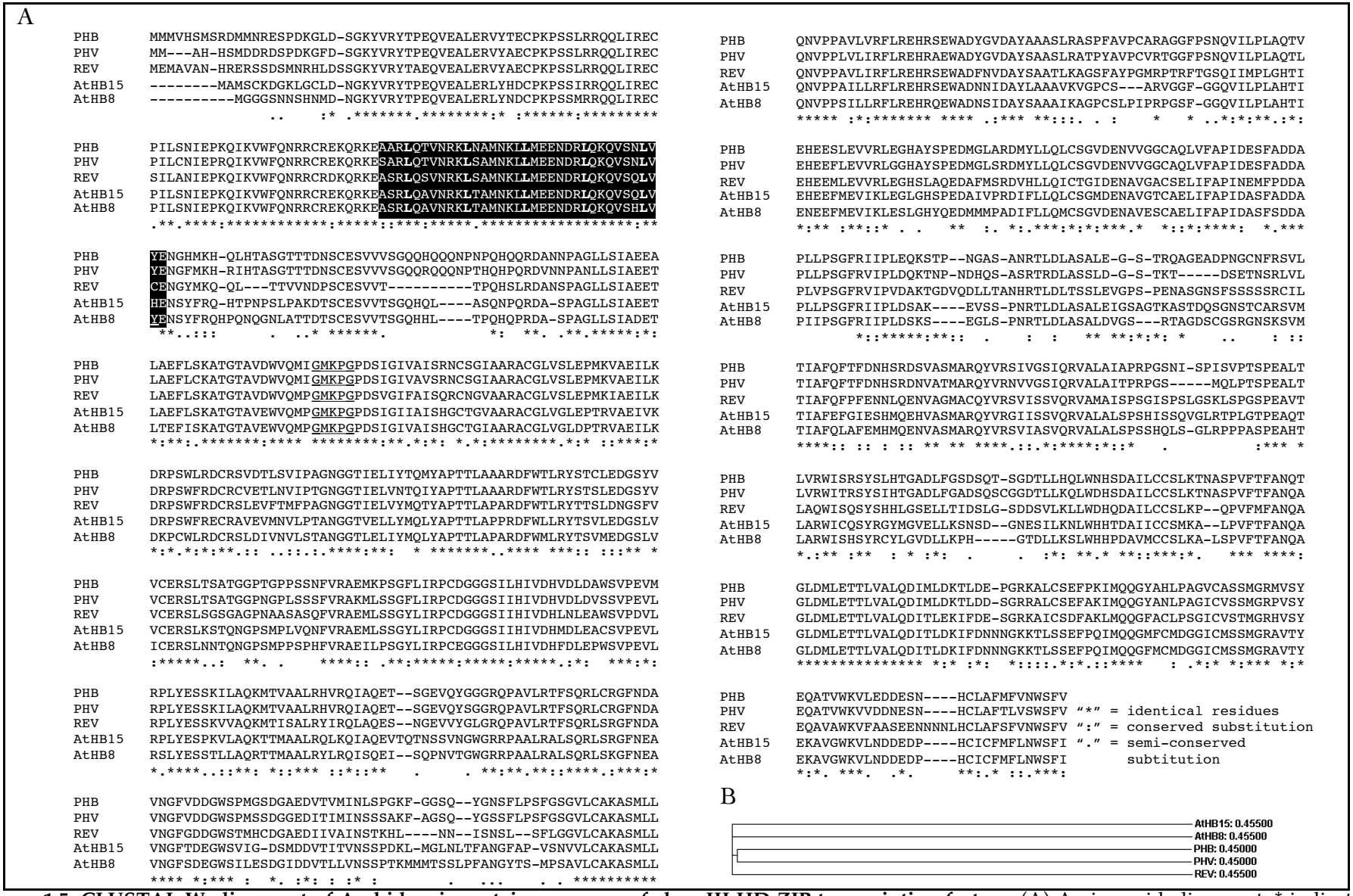


**Figure 1.5: CLUSTAL-W alignment of Arabidopsis protein sequence of class III HD-ZIP transcription factors.** (A) Amino acid alignment, * indicates a perfect match between sequences. The leucin zipper is highlighted in black. The translated miR165/166 site is underlined. (B) Phylogram of the aligned sequences. Made with TCOFFEE Version_5.05 [http://www.tcoffee.org]

highly conserved in this family of TFs. Ancestors of class III HD-ZIP appear to have been present in plants before the emergence of the charophycean green algae (Floyd et al., 2006). In total, four classes of HD-ZIP exist and are only found in the plant kingdom. While the four classes of HD-ZIP present a ZIP domain, this domain differs from one class to the other (Sessa et al., 1998; Wenkel et al., 2007). HD-ZIPs are composed of a leucine zipper domain, a homeodomain, a StAR (Steroidogenic Acute Regulatory protein)-related lipid-Transfer (START) domain and, specific to class III HD-ZIP, a MEKHLA domain (Mukherjee and Burglin, 2006) (Figure 1.4 A). The leucine zipper can form homo- and hetero- dimmers. Heterodimers formed with the LITTLE ZIPPER (ZPR) class of proteins has been reported to reduce the activity of *REV* while bound to DNA. Moreover, over-expression of *ZPR* results in phenotypical alterations similar to those observed in class III HD-ZIP loss of function (lof) mutants. ZPR have been proposed to be regulatory elements of class III HD-ZIPs as *ZPR* expression is induced by class III HD-ZIP proteins (Wenkel et al., 2007; Kim et al., 2008). The START domain, named after the lipid/sterol binding domain occurring in mammalian proteins, is a motif that binds sterols or phospholipids (Ponting and Aravind, 1999) as well as a wide range of other compounds such as RNAs or antigens in mammalian cells (Iyer et al., 2001). In animals, some proteins presenting a START domain are involved in gene expression regulation by binding steroid hormones (Laudet and Gronemeyer, 2002). Since class III HD-ZIP transcription factors are localised in the nucleus, the START domain could also be involved in sterol/lipid-induced signal transduction (Schrick et al., 2004). Additional protein-protein interactions occur as all members of the family interact with the AP2 domain of DÖRNROSCHEN (DRN) and DÖRNROSCHEN-LIKE (DRL) via their C-terminal regions (Chandler et al., 2007). Besides the ability to bind DNA and to dimerize, several domains were proposed to have regulatory functions (Sessa et al., 1998). The START domain is a putative sterol binding domain as similarities to the mammalian sterol/lipid binding domain were observed (Ponting and Aravind, 1999). The C-terminal MEKHLA domain is composed of a PAS domain considered to be a physiological status detector (light, oxygen and redox potential) in the cell (Gilles-Gonzalez and Gonzalez, 2004). The discovery of a sequence complementary to the miRNAs miR165/166 in the START domain (Figure 1.4

B) suggested that this class of transcription factors is post-transciptionally regulated by miRNAs (See chapter 1.7) (Reinhart et al., 2002; Rhoades et al., 2002).

### 1.6.3 Expression pattern of the class III HD-ZIPs

Class III HD-ZIPs are principally expressed adaxially, however some variation occurs between the members. *REV* is expressed since the 16 cells stage of the embryo. In later stages of embryogenesis, *REV* is restricted to the central region and adaxial side of the cotyledons. After germination, *REV* is expressed in all the plant aerial meristems, adaxial regions of lateral organs and the vasculature (McConnell et al., 2001; Otsuga et al., 2001; Emery et al., 2003). The expression pattern of *PHB* in embryo is similar to *REV* expression. In the SAM, the *PHB* expression pattern is restricted to the adaxial regions and the center of the meristem (McConnell et al., 2001). With *PHV, PHB* is also present in xylem and adaxial regions of lateral organs. The expression pattern of *PHV* is similar to *PHB* and *REV,* although shortly delayed. (Emery et al., 2003). The *AtHB15* expression pattern is restricted to procambial cells of all plant parts although slightly reduced in leaves (Ohashi-Ito and Fukuda, 2003; Ochando et al., 2006). Expression of AtHB8 is restricted to the central domain of embryos and is then present in procambium and xylem precursor cells of the plants from roots to flowers. *AtHB8* is not present in meristems (Baima et al., 1995; Fukuda, 2004). The expression pattern of class III HD-ZIPs appears to be restricted to the adaxial region of the leaf at least partially by microRNAs (miRNAs) (see chapter 1.7) (Kidner and Martienssen, 2003; Tang et al., 2003). With their meristematic and vascular localization, it is no wonder that class III HD-ZIPs expression is also influenced by auxin as *REV, PHV, AtHB8* and *AtHB15* mRNA levels are induced by auxin (Baima et al., 1995; Zhou et al., 2007).

### 1.6.4 Class III HD-ZIP mutants

Lof-mutations in single genes of class III HD-ZIPs have limited effects on leaf development, however, lof-mutations in multiple genes will result in an abaxialisation of the organs (Prigge et al., 2005). Only REV loss of function mutants induces phenotypic defects in leaves, axillary meristems and

inflorescences. Defects in auxin transport and stem cell specification are also observed (Talbert et al., 1995; Zhong et al., 1997; Otsuga et al., 2001; Zhong and Ye, 2001). Double *phb phv* or *athb8 athb15* mutants don't present any particular phenotype compared to wild-type plants. Multiple combinations of loss of function mutants of class III HD-ZIP genes, result in a wide panel of different defects, demonstrating either redundancy or opposite functions of the genes depending on the organ in which they are expressed. As an example *rev athb15* and *rev athb8* double mutants have the same phenotype as *rev* mutants. But *rev athb8 athb15* triple mutants produce more flowers than *rev* single mutants, suggesting an antagonistic effect between AtHB15-AtHB8 and REV in this organ. Multiple class III HD-ZIP mutants including $rev^{+/-}$ have a dwarf phenotype (Prigge et al., 2005). Another multiple mutant of interest is the *phb phv rev* triple mutant. This plant has an abaxially radialized cotyledon, underlining the importance of this set of genes in the adaxial identity of tissues (Emery et al., 2003).

Dominant gain of function (gof) mutations affecting regulation by miRNAs (Chapter 1.7) result in the adaxialisation of the leaves. Plants expressing *REV* with an altered miRNA-binding site (*rev-10d*) reducing complementarity to miR165/166 present amphivasal (i.e xylem cells enclosing a central phloem cylinder) vascular bundles in the inflorescence stem (Emery et al., 2003). Plants expressing *PHB and PHV* with an altered miRNA binding site (respectively *phb-1d* and *phv-1d*) present adaxialized leaves (McConnell and Barton, 1998; McConnell et al., 2001). Similar events were observed after *AtHB15* gof expression (Kim et al., 2005; Ochando et al., 2006). In addition to the gof mutants, mRNA cleaved at the miRNA site has been detected *in vivo* for the five members of class III HD-ZIPs (Emery et al., 2003; Mallory et al., 2004).

### 1.6.5 Brassinosteroids and xylem identity

It's not the putative sterol-binding domain of class III HD-ZIP, but rather the several mutants of the brassinosteroid (BR) pathway presenting discontinuous vasculature, that revealed the role of this hormone in vascular differentiation (Fukuda, 2004). Besides photomorphogenesis and cell elongation (Clouse and Sasse, 1998), BRs also affect xylem differentiation (Nagata et al., 2001).

Procambial cells have been shown to produce BRs while differentiating into tracheary elements (Yamamoto et al., 2001; Fukuda, 2004). Mutant plants for the BRs membrane-localized leucine-rich repeat receptor-like kinase (LRR-RLK) BRASSINOSTEROID INSENSITIVE 1 (BRI1) and BRI1-LIKE1 (BRL1) presenting reduced xylem and increased phloem confirmed the importance of BR in transverse patterning of the vasculature. Additionally, the triple BR LRR-RLK mutants *bri1 brl1 brl3* have reduced phloem and xylem suggesting that this pathway can also affect more global vascular differentiation factors (Cano-Delgado et al., 2004). BRs are present in all plant tissues with a higher concentration in apical regions of the shoot. It should be noted that no long distance transport of BRs has been observed (Shimada et al., 2003; Symons and Reid, 2004; Montoya et al., 2005).

### 1.6.6 NAC domain transcription factors and xylem vessel differentiation

Recently, transcriptome analysis of *in vitro* xylem element formation systems in *Arabidopsis* and *Zinnia* revealed that NAC domain (for NAM, ATAF1/2, and CUC2) transcription factors were involved in xylem differentiation (Kubo et al., 2005; Ohashi-Ito et al., 2005). Procambium and cambium differentiate on the adaxial side into protoxylem and metaxylem vessels respectively. The *VASCULAR RELATED NAC-DOMAIN6* and *7* (*VDN6*/*VDN7*) promote the differentiation of these two tissues respectively (Kubo et al., 2005). The *vdn6* and *vdn7* mutants present reduced protoxylem and metaxylem vessels in the root vascular system of *Arabidopsis*. In addition to *VDN1*-*VDN7*, another class of NAC proteins is involved in the establishment of the vasculature. The SECONDARY WALL–ASSOCIATED NAC DOMAIN 1 (SND1) protein is a transcription factor involved in the deposition of the secondary cell wall in interfascicular and xylary fibers (Zhong et al., 2006). Members of the *NAC SECONDARY WALL THICKENING PROMOTING FACTOR* (*NST*) were also shown to regulate secondary wall deposition in anthers and interfascicular fibers (Mitsuda et al., 2005; Mitsuda et al., 2007). These regulators seem to be also present in the genome of woody plants such as poplar. This further supports that wood formation mechanisms can be studied in herbaceous plants such as *Arabidopsis.*

## 1.7 Developmental genes regulation by micro RNAs

MicroRNAs (miRNAs) are short RNA molecules that mediate gene expression by complementary base pairing to their mRNA products. They often post-transcriptionally regulate developmental genes, by limiting their domain of mRNA distribution or by clearing the presence or their target mRNA in differentiated tissues. To do so miRNAs either affect transcription, translation or mRNA stability.

First identified in *Caenorhabditis elegans*, miRNAs have since then been found in the genome of Arabidopsis thaliana and several other metazoa (Reinhart et al., 2002). Widespread in the plant kingdom, these short RNAs have been detected in plant species ranging from Selaginella to flowering plants (Floyd and Bowman, 2004).

### 1.7.1 Post transcriptional regulation by siRNAs and miRNAs

Although similar to the action of short-interfering RNAs (siRNA) that target viruses and transposons, miRNAs do not target foreign but endogenous RNA. The siRNA pathway is a cytoplasmic process that targets double stranded RNA (dsRNA). In addition to viruses with dsRNA, replicating single stranded RNA (ssRNA) viruses and the secondary structures they form, or RNA from loci presenting inverted repeats, share this feature (Hannon, 2002). dsRNAs are recognized and cleaved by multi-domain RNaseIII-like enzymes called DICER (DCL). Viral and endogenous siRNA is processed by DCL2 and DCL3 respectively in *Arabidopsis* (Xie et al., 2004). However, when one of the DCLs is deficient, another DCL can more or less compensate its activity (Moissiard and Voinnet, 2006). dsRNA can also be produced endogenously by RNA-dependent RNA polymerases (RdRp/RDR) that will use single stranded RNA as template. RDRs share similarities with DNA-dependent RNA polymerase (Iyer et al., 2003). These double stranded RNAs (dsRNA) will then be treated in the siRNA pathway generating secondary siRNAs (Chapman and Carrington, 2007). The dsRNAs used as template for miRNAs differ from those used for siRNA. In the miRNA pathway, endogenous precursors of a length of 90-100 nucleotides presenting imperfectly paired hairpin structures

are cleaved into 21-22bp products by DCL1 proteins (Hutvagner and Zamore, 2002).

The 21-24bp short RNAs generated by the different dicers are associated with an ARGONAUTE (AGO) protein and additional proteins to form the RNA induced silencing complex (RISC). AGO proteins bind RNA as well as provide an RnaseH domain. Target RNA interacts by base pairing to mRNA containing complementary (siRNA) or nearly complementary sequences (miRNA) in one of the grooves of AGO. 10 different AGO proteins are present in *Arabidopsis*. For siRNA, this binding is suggested to recruit RDR proteins. The RISC-RNA interaction will either block translation, induce cleavage or modify transcriptional regulation of the targeted transcript (Kidner and Martienssen, 2003). Epigenetic events such as methylation of DNA have been shown to be linked with miRNAs leading to transcriptional regulation (Bao et al., 2004). The details of miRNA mechanisms present some variation from plants to animals but are very often linked with organism development (Baulcombe, 2004; Kidner and Martienssen, 2005; Park et al., 2005; Voinnet, 2005; Henderson and Jacobsen, 2007). Other similar mechanisms such as trans-acting siRNA, involving RDR proteins, are also important in development, but have only been described in plants for the moment (Peragine et al., 2004; Bartel, 2005).

Other differences between the plant and animal miRNA pathway exist. While animal pre-miRNAs are processed in both nucleus and cytoplasm (Bartel, 2004), plant pre-miRNAs are processed in the nucleus (Papp et al., 2003). The *HYPONASTIC LEAVES1* (*HYL1*) dsRNA binding protein is involved in this process. Interestingly, the *hyl1* mutant phenotype is similar to the dominant *icu4* mutant (Lu and Fedoroff, 2000).

The miRNA and siRNA pathways are presented in a simplified schema in figure 1.7.

### 1.7.2 miRNAs in *Arabidopsis*

Since their discovery, several miRNAs have been identified in *Arabidopsis*. A large number of miRNAs and their targets have also been predicted by computational methods and confirmed by northern blot (Wang et al., 2004; Zhang, 2005). In some cases, as for class III HD-ZIP-related miRNAs, several

loci encode the same miRNA, however pre-miRNA and promoter sequences vary from one copy to the other. Thus, the expression patterns of several miRNAs, as miR165 and miR166 (Jung and Park, 2007), have been determined by studying the expression of promoter-GUS marker genes and have confirmed that these several loci have different expression patterns.

Gene regulation by miRNAs has been demonstrated in several cases by the expression of a gene with an altered miRNA target sequence, or gain of function construct (gof) (McConnell 1998; Emery et al., 2003; Laufs et al., 2004; Kim et al., 2005, Tang et al., 2003). The involvement of *KAN* proteins regulating class III HD-ZIPs via *miR165/166* has often been suggested but has not yet been established. No miRNA has been shown to regulate *KAN* mRNA stability yet, however coactivators of KAN are regulated by a pathway combining mi- and siRNAs (Pekker et al., 2005; Fahlgren et al., 2006). In this pathway, called trans-acting siRNA (ta-siRNA), the miRNA facilitates the cleavage of a non-coding RNA, the ta-siRNA. The cleaved product then forms a double stranded RNA that is then incorporated into the siRNA machinery (Allen et al., 2005; Bartel, 2005).

## 1.8 Proximodistal growth - another growth axis

The several genes and phytohormones affecting the development of the vascular system presented here are schematically summarized in Figure 1.6. A correct split into an abaxial and adaxial region seems to be essential for a proper establishment of the vascular system. However, as in the apical-basal axis where SAM cells need to differentiate into procambium and cambium, lateral differentiation is also necessary to establish a proximodistal axis.

The SAM is composed of several zones and layers. The central zone is the most apical and central region where slow stem cell divisions are occurring. Around it, on the surface, the peripheral zone generates leaf primordia. Bellow, the rib zone produces the central tissues of the stem. The uppermost layer of cells contributes to the epidermis while the two lower layers are responsible for internal tissues (Bowman and Eshed, 2000). The localization of the new primordia around the peripheral zone determines the phyllotaxy of the plant. While auxin is transported in the epidermis toward the SAM, the flux is disturbed at the level of young primordia that act as auxin sinks. The

resulting peak in auxin concentration in the adjacent region is responsible for initiation of new primordia (Reinhardt et al., 2003). The initiation of new primordia will be dependent on auxin efflux carriers, while influx carriers will only influence their proper localization (Stieger et al., 2002).

In young primordia, the central zone identity genes will be repressed to allow leaf-fate events to take place. The *ASYMETRIC LEAVES 1* (*AS1*) gene has this role in proximo-distal differentiation as it downregulates genes of the *KNOX* family (Lin et al., 2003; Byrne, 2005). This role is supported by the phenotype of the maize *AS1* ortholog mutant, *rough sheath 2* (*rs2*). The leaves of *rs2* mutant present stem or petiole characteristics almost up to the distal end (Tsiantis et al., 1999). Others characteristics of *AS1* mutants are the presence of adaxial laminar outgrowth due to ectopic expression of *KNOX* genes as in *nsphan* tobacco ortholog (Sakamoto et al., 2001; Byrne, 2005). *AS1* does not only promote proximo-distal differentiation, but also adaxial identity. Indeed, the *AS1 Antirrhinum* mutant ortholog, *phantastica* (*phan*) present abaxialized leaves (Waites and Hudson, 1995). *AS1* is also known to repress *YABBY* genes (Kumaran et al., 2002).

## 1.9 Transactivation system

In this work, the transactivation system developed by Moore and colleagues (Moore et al., 1998) was used. This system allows expressing a gene of interest in a specific pattern by crossing two transgenic plant lines. In the plant line defining the expression pattern, a transgene contains the promoter of a gene of interest followed by the sequence of a chimeric transcription factor *LhG4*. *LhG4* is composed of a transcription activation domain II from the *Gal4* gene of *Saccharomyces cerevisiae* fused to the *lac*-repressor. The *lac* repressor is mutated to provide increased affinity to its operator sequence. Multiple repeats of the *lac* operator sequence precede the coding sequence of the gene of interest in the second transgenic plant line. Thus, when the two lines are crossed, the LhG4 transcription factor is produced in the desired pattern and will activate the transcription of the gene of interest by binding to the *lac* domain (Figure 1.8). This system has the advantage to study multiple combinations of promoter-operator expression, as well as for the study of transgenes that induce plant sterility.

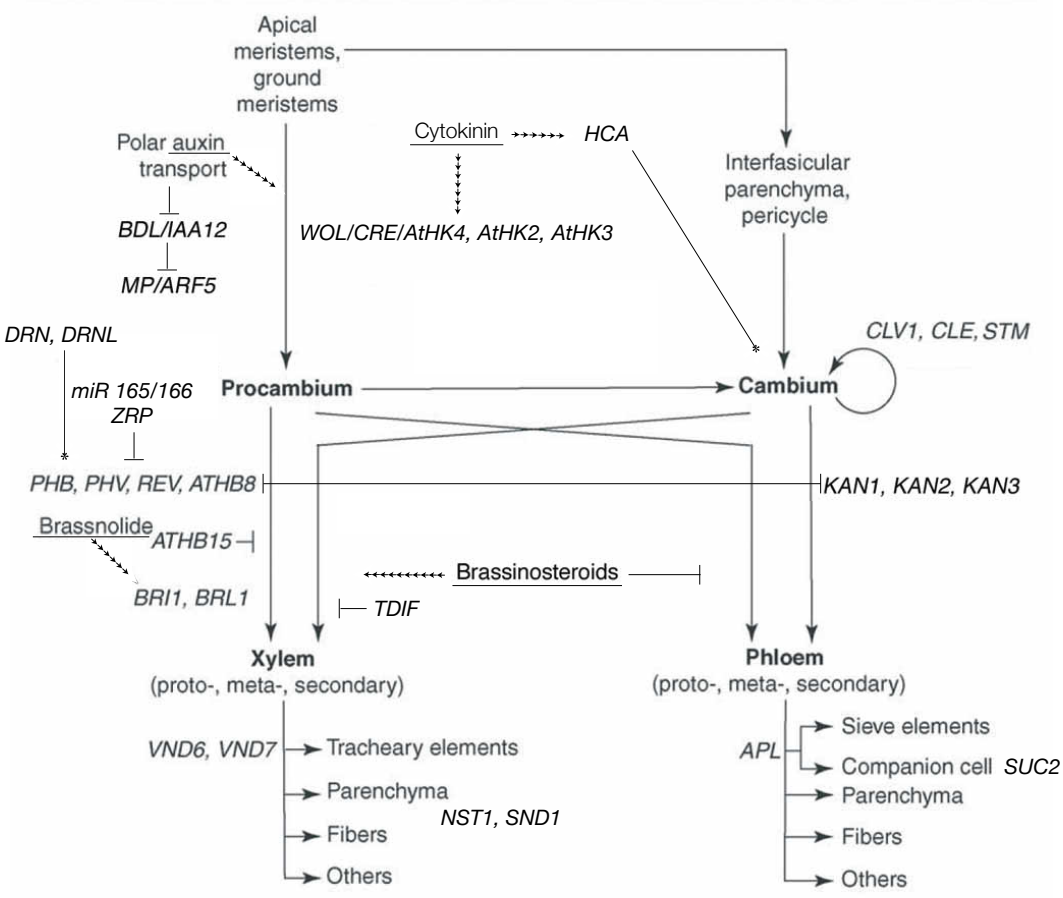


**Figure 1.6: Genes and signal molecules that influence vascular differentiation.** In this scheme, interactions between the genes (in uppercase italics) and phytohormones (underlined) described in the introduction are resumed. Arrows indicate transitions between cell types. Genes are shown next to the processes with which they are associated during differentiation of the different cell types. Some of the genes/phytohormones might affect additional cell types. Multiple arrows indicate multiple indirect processes. T-bars indicate inhibition. Star-arrows indicate interactions. Scheme adapted from Sieburth and Deyholos, 2006 and Demura and Fukuda, 2007.

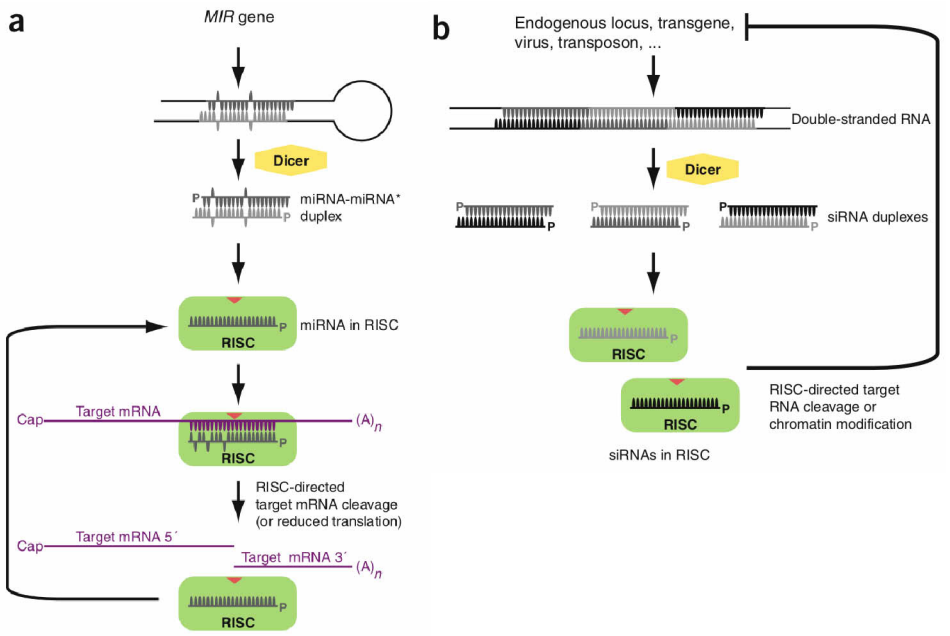


**Figure 1.7 MicroRNAs and short interfering RNAs.** (A) MicroRNA primary transcripts include imperfectly paired hairpins that are processed by a Dicer ribonuclease to form the miRNA-miRNA duplex. One of the two miRNA is incorporated within the RISC complex. The target mRNA pairs with the miRNA and is cleaved by the ARGONAUTE protein. (B) siRNA formation results from Dicer action on long double-stranded RNA molecules derived from endogenous loci, viruses, transposons or transgenes. siRNAs are incorporated into the RISC, where they directly target RNA cleavage or chromatin modification of the locus from which they were transcribed, or very closely related loci. Scheme and legend from Bartel 2005.

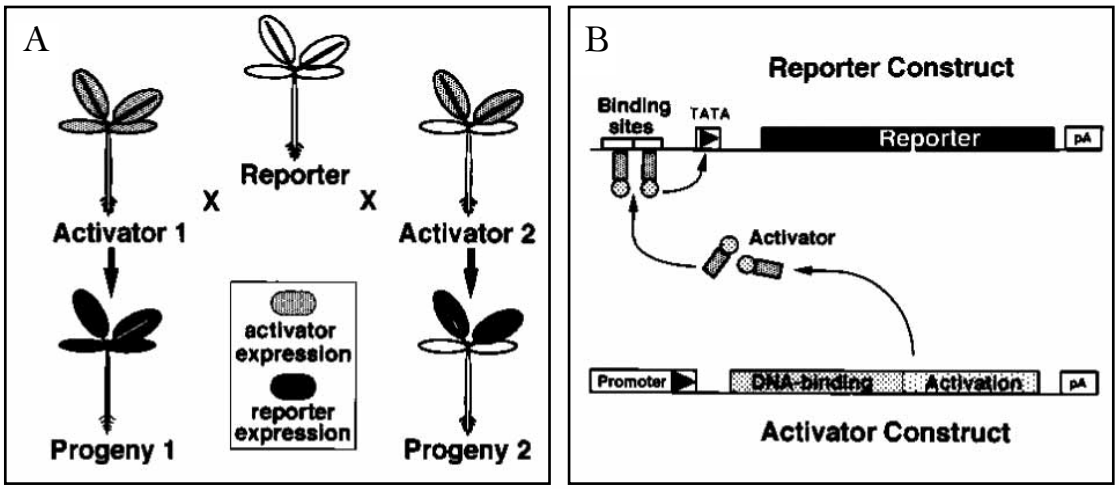


**Figure 1.8: Principles of the binary transactivation system.** (A) A reporter gene linked to a novel promoter is silent when first introduced into reporter plants. Transgene expression is induced by crossing to activator lines that express a heterologous transcription factor that specifically recognizes the transgene promoter. The pattern of reporter gene expression will reflect the pattern of activator expression, allowing a gene of interest to be expressed under a variety of regimes simply by crossing to an appropriate activator line. (B) Schematic representation of activator and reporter constructs. In the reporter construct the reporter or gene-of-interest is linked to a minimal promoter (TATA) that lacks intrinsic transcriptional activity. Upstream of this promoter are binding sites for a transcription factor with a DNA-binding specificity that is not found in plants. The activator construct expresses a transcription factor that possesses this novel DNA-binding specificity and also has the ability to activate transcription in plants. This transcription factor is expressed from a plant promoter that will give the desired characteristics of reporter expression. Scheme and legend from Moore et al. 1998.

## 1.10 Objectives of this work

Wood plays a central role in our ecosystem. This role is predicted to be even more important in the decades to come. Thus, a precise understanding of wood development is essential. One class of transcription factors was shown to play a central role in vascular system differentiation: the class III HD-ZIPs. However, the exact functions of this class of genes and the regulatory mechanisms in which they are involved still need to be determined. One of the identified factors regulating several class III HD-ZIPs is the post transcriptional regulation by *miR165* and *miR166*. Other factors, such as *KANADI* genes were shown to negatively affect class III HD-ZIP expression.

The aim of the first part of the presented thesis is to further characterize the role of the class III HD-ZIP gene *AtHB8* in the formation of the vascular tissue. To this end, a *AtHB8* sequence with a modified *miR165*/*166* complementary site (*AtHB8-∂miR*) to prevent post-transcriptional regulation by the miRNA machinery will be expressed under the control of different promoters in Arabidopsis plants. Expression of *AtHB8-∂miR* in the *AtHB8* expression pattern will allow determining the role of *miR165*/*166* on *AtHB8* mRNA stability. Expression of *AtHB8-∂miR* in the pattern of other class III HD-ZIPs will allow to draw parallels between the functions of the different members of this family. I will focus in particular on the effect of this ectopic expression on the differentiation of the vascular system.

In the second part of this thesis, the roles of class III HD-ZIPs and *KAN1* during the establishment of the vascular system will be studied. Therefore, class III HD-ZIP mRNAs will be reduced by expressing *miR165* in procambium cells. The transcription factor and class III HD-ZIP antagonist *KAN1* will also be expressed in the same pattern. The effect of ectopic *KAN1* and altered levels of class III HD-ZIPs on vascular differentiation will be studied. A particular focus will be made on interactions of class III HD-ZIPs and KAN1 with the plant hormone auxin.

# Chapter 2

# Results

## 2.1 The role of the Class III HD-ZIP transcription factor *AtHB8* in the development of the vascular system in *Arabidopsis thaliana*.

### 2.1.1 AtHB8 affects the differentiation of xylem cells

In previous studies, a class III HD-ZIP transcription factor, *AtHB8,* was identified as an important actor in the process of vascular development. Its properties in xylem differentiation were carefully studied (Baima et al., 1995). However, knowledge of gene post-transcriptional silencing by miRNAs was not available when *AtHB8* was first described. Since then, it has been shown that members of the class III HD-ZIP transcription factors share a miRNA target site for post-transcriptional regulation (Jones-Rhoades *et al*., 2003; Tang *et al.,* 2003; Emery *et al.,* 2003; Mallory *et al.,* 2004; Kim *et al*., 2005; Williams *et al*., 2005; Jung and Park, 2007). In order to gain additional insights on the effect of *AtHB8* in plant development, we expressed the coding sequence of *AtHB8* with a point mutation in the miRNA target site (Figure 1.4) under the control of the endogenous promoter: *AtHB8::AtHB8-∂miR.* This non-silent mutation changing a glycine to an aspartic acid is identical to the described gof mutation in *REV*: *rev-10d* (Emery et al., 2003). Note that, as the cDNA sequence was used here instead of the full sequence, the intron separating the miRNA cleavage site in the endogenous gene is not present in this construct.

Plants transformed with *AtHB8::AtHB8* (coding sequence of *AtHB8* under the control of the *AtHB8* promoter) were used as controls. Four homozygous F2 lines were identified by segregation analysis for the two constructs (data not shown). A segregation ratio (sensitive : resistant) on selective media close to 1:3 of the parental lines suggested a single insertion locus in these lines (data not shown). No conspicuous alterations in phenotype were observed between *AtHB8::AtHB8-∂miR*, *AtHB8::AtHB8* and untransformed *Landsberg erecta* (*Ler*) plants (data not shown). Quantification of *AtHB8* mRNA (Figure 2.1 A) in young seedlings (15 DAG) by semi-quantitative RT-PCR suggested that none of the four *AtHB8::AtHB8-∂miR* lines had a higher steady state level of *AtHB8* mRNA than *AtHB8::AtHB8*. Moreover, real time quantitative PCR confirmed this result for two lines as *AtHB8* mRNA level was comparable in one *AtHB8::AtHB8* and one *AtHB8::AtHB8-∂miR* line (Figure 2.1 B). Although not strikingly higher than untransformed *Ler*, the higher level of *AtHB8* mRNA in *AtHB8::AtHB8* and *AtHB8::AtHB8-∂miR* lines implies that the transgenes were active. The comparable expression level of *AtHB8* between *AtHB8::AtHB8-∂miR* and *AtHB8::AtHB8* does not allow to affirm that *AtHB8* is post-transcriptionaly regulated by miRNAs. However, if further results indicate that *AtHB8* is regulated by *miRNA*, the present result would suggest that the overlap between the *AtHB8* and *miR165/166* expression pattern is limited.

Since *AtHB8* is specific to the vascular system, vascular tissue formation was analyzed in *AtHB8::AtHB8-∂miR* lines. Cross-sections of the inflorescence stems of *AtHB8::AtHB8* and *AtHB8::AtHB8-∂miR* lines 6 weeks after sowing were made. About 15 plants were analyzed for each line. The number of vascular bundles was not significantly different between two *AtHB8::AtHB8-∂miR* lines and each control (two *AtHB8::AtHB8* lines and untransformed *Ler* plants) ($p>0,05$) (Figure 2.1 C). Additionally, the number of protoxylem strands per vascular bundle was also highly comparable between the same five lines (Figure 2.1 D). Semi-thin cross-sections of the stems were made to compare vascular bundle morphology (Figure 2.1 E,F). Differentiated xylem (dx) cells present in the first two rows of cells next to cambial cells in *AtHB8::AtHB8* (dx=8.92 ± 2.01, n=48) and *AtHB8::AtHB8-∂miR* (dx=2.67 ± 2.00, n=38) were significantly different ($p<0,0001$, unpaired t-test) in the n vascular

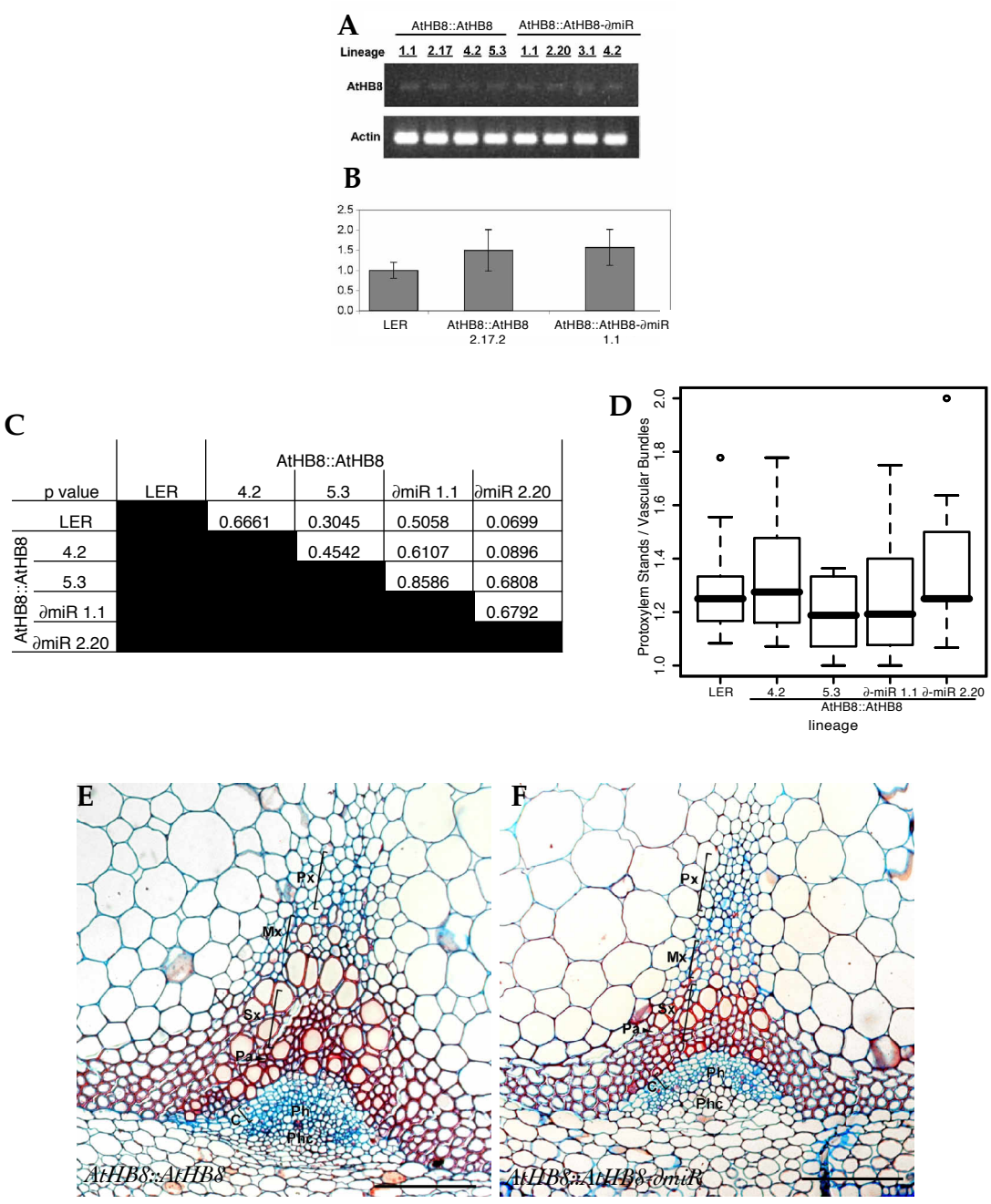


**Figure 2.1: Characterization of *AtHB8::AtHB8-∂miR* transformants.** (A) Level of *AtHB8* mRNA in 15DAG *AtHB8::AtHB8* and *AtHB8::AtHB8-∂miR* lines compared by semi-quantitative PCR. *ACTIN2* was used as reference gene. (B) Level of *AtHB8* mRNA in 15DAG seedlings measured by real-time PCR in triplicate. The ribosomal *S16* gene was used as control. (C) Number of vascular bundles in the inflorescence stem of 6 week old plants normalized to the diameter of the stem/size of the shoot. (D) Boxplot of the number of protoxylem strands per vascular bundle in inflorescence stems of the same plants. 5µm transversal sections of the inflorescence stem of 6 week old *AtHB8::AtHB8* 2.17.2 used here as control (E) and *AtHB8::AtHB8-∂miR* 1.1 (F). Coloration with safranine orange counterstained with astra blue. The scale bar represents 100µm in E-F. C, cambium; Mx, metaxylem; Pa, parenchyma; Ph, phloem; Phc, phloem cap cells; Px, protoxylem; Sx, secondary xylem.

bundles tested. Note that, phloem cap cells were usually less dense in *AtHB8::AtHB8-gof* than in controls (Figure 2.1 E,F).

To summarize, *AtHB8* mRNA levels in young seedlings were highly similar between *AtHB8::AtHB8* and *AtHB8::AtHB8-∂miR* plants. The major morphological changes observed in the dominant mutants of the four other class III HD-ZIPs were not observed in *AtHB8::AtHB8-∂miR* plants. Moreover, the endogenous regulation of *AtHB8* expression by miRNAs appears to neither have an effect on the number of vascular bundles nor on the number of protoxylem strands formed as these were comparable in *AtHB8::AtHB8* and *AtHB8::AtHB8-∂miR*. However, more differentiated metaxylem cells adjacent to cambium were found in the controls than in *AtHB8::AtHB8-∂miR* plants, suggesting a role for *AtHB8* in defining the identity of young developing xylem cells.

### 2.1.2 Constitutive expression of *AtHB8*

Limited morphological differences were observed between the controls and *AtHB8::AtHB8-∂miR* plants compared to gof mutations of other class III HD-ZIP members. Thus, we hypothesized that the pattern of expression of *AtHB8* limited the effect of *AtHB8-∂miR*. To further characterize *AtHB8* in a gof context, an over-expression approach was chosen. We expressed the *AtHB8* native and gof sequences under the control of the constitutive cauliflower mosaic virus (CaMV) 35S promoter and the RuBisCO small subunit (RSSU) terminator (Figure 2.2 A). Transformants were selected on phosphinothricin-containing media and are referred to as *35S::AtHB8*, *35S::AtHB8-δ mir* and *p3300* respectively. 24 primary transformants were identified on selection medium and homozygous F2 lines containing a single insertion locus were identified by segregation analysis (data not shown). For several lines, 35S::*AtHB8* seedlings growing on MS medium (Figure 2.2 C) and adults growing on soil exhibited leaf hyponasty (stronger growth on the lower (abaxial) side of a plant part) in standard growth conditions (Figure 2.2 E) compared to control p3300 transformants (Figure 2.2 B and D respectively). Expression of *AtHB8* was assayed by real time quantitative RT-PCR in 2 *35S::AtHB8* and 2 35S::*AtHB8-∂miR* homozygous lines and a *Ler* control. Mutation in the putative *AtHB8* miRNA cleavage site of the transgene was

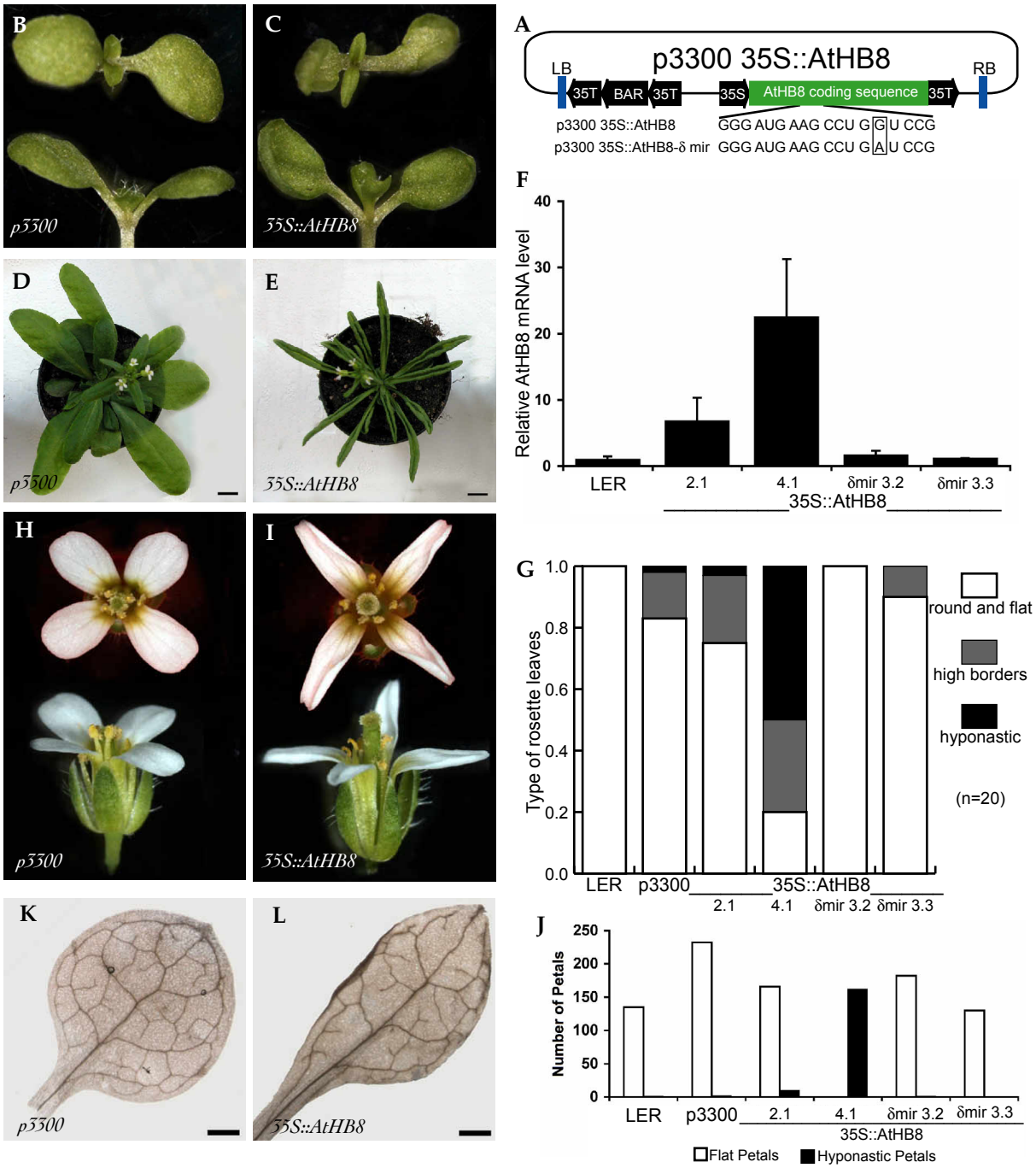


**Figure 2.2: Characterization of the *35S::AtHB8* transformants.** Scheme (A) of the construct used for plant transformation. The coding sequence of *AtHB8* was inserted in the binary p3300 vector. A non-silent mutation was present in the miRNA binding site of the p3300 *35S:AtHB8-∂mir*. The vector contained the BAR gene (phosphinotricin acetyl transferase) for basta resistance under the control of the CaMV 35S promoter (35S) and the CaMV 3'UTR (35T, polyA signal) for selection. LB and RB are T-DNA left and right boarders respectively. Plants transformed with p3300 were used as controls (B,D,H,K) and compared to plants expressing *35S::AtHB8* (C,E,I,L). 15DAG F2 seedling (B,C), level of *AtHB8* mRNA in homozygous transformant lines measured by real-time PCR in triplicate (F). The ribosomal *S16* gene was used for normalization, expression is relative to p3300. Rosette leaves of 6 week old plants (D,E) were classified in 3 categories: round and flat – corresponding to wild type leaves; high border – leaf margins were higher than the midvein; hyponastic – no visible lateral margins of the leaf due to a strong hyponasty (G). On flowers (H,I) of 8 week old plants petal hyponasty (J) was quantified (petals were counted on the flowers of 2 to 4 plants). Vein patterning in leaf (K,L). Scale bar 1cm (E,F), 1mm (H,I).

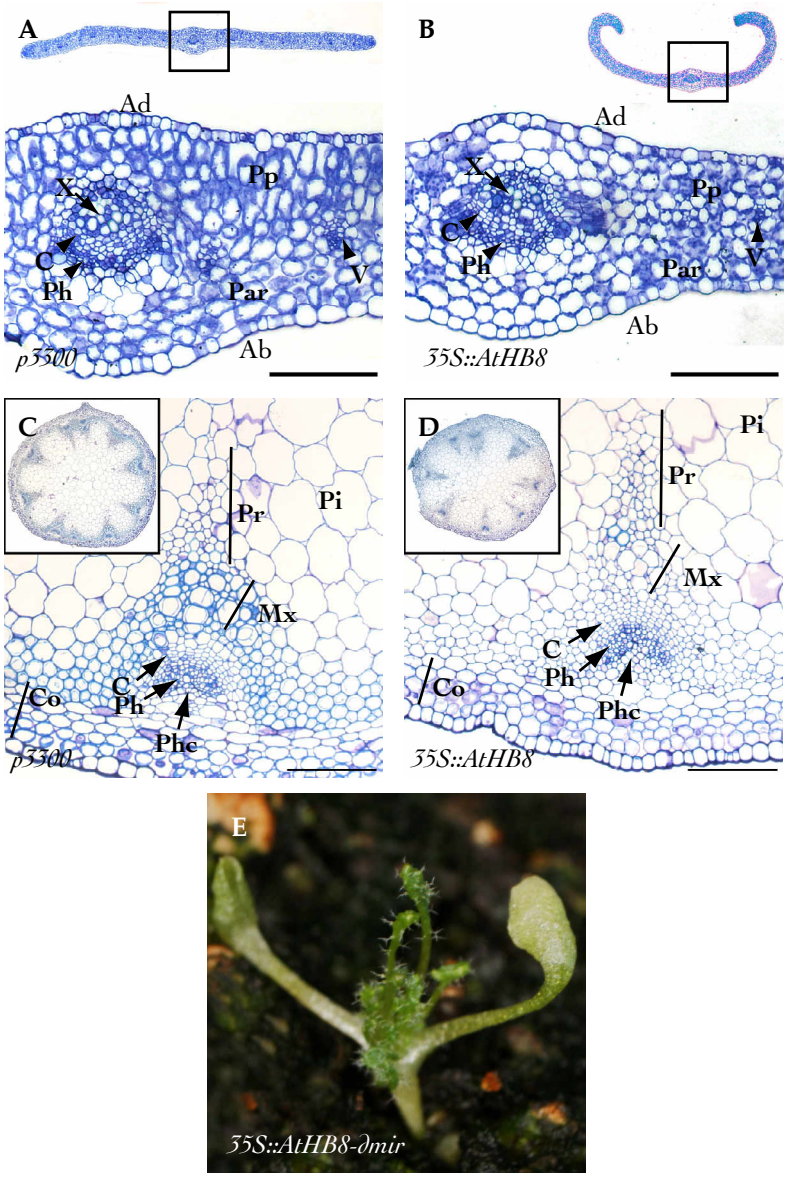


**Figure 2.3: Characterization of the *35S::AtHB8* transformants (2).** Transversal 5µm section of a 2 cm long cauline leaf of 5 week old p3300 controls (A) and *35S::AtHB8* plants (B). Picture centred on the midvein of the leaf. General view of the leaf (A,B, insert). Note the absence of ordered palysadic parenchyma in B. (C-D) Inflorescence stem cross section. Picture centred on a typical vascular bundle of p3300 control (C) or *35S::AtHB8* (D) plant. Sterile 21DAG F0 *35S::AtHB8-∂mir* seedling (E). Sections A-D were stained with toludine blue. Scale bar in A-D is 100µm. Ab, abaxial side of the leaf; Ad, adaxial side of the leaf; C, cambium; Co, cortex; Mx, metaxylem; Par, parenchyma; Ph, phloem; Phc, phloem cap cells; Pi, pith; Pp, palysadic parenchyma; Pr, protoxylem; V, secondary vein; X, xylem.

verified by sequencing in 4 lines (data not shown). As shown in figure 2.2 F, only in the 35S::*AtHB8* lines the abundance of *AtHB8* mRNA was higher than in control samples. No homozygous *35S::AtHB8-δ miR* lines showed an altered phenotype, or had a higher level of *AtHB8* mRNA than the control. Although these homozygous lines were selected on herbicide, the part of the construct constitutively expressing *AtHB8* was considered as silenced.

The abundance of *AtHB8* transcript correlated with the longitudinal hyponasty of rosette leaves of 6 weeks old plants (Figure 2.2 G). Flowers of *35S::AtHB8* plants also presented hyponastic petals (Figure 2.2 I) compared to controls (Figure 2.2 H). This feature also correlated with the amount of *AtHB8* mRNA (Figure 2.2 J). Several *35S::AtHB8* lines presented similar hyponastic features. The *35S::AtHB8* 4.1 line was selected for further characterization since it showed the most severe phenotypical alterations and higher *AtHB8* mRNA levels. Although the leaves hyponasty affected its general shape (Figure 2.2 K,L), the number of secondary veins branching the mid vein was not significantly changed (data not shown). This result suggested that the cause of leaf hyponasty was not due to altered vein pattering. Therefore, transversal sections of leaves were made in order to obtain additional insights on tissue organization in hyponastic leaves (Figure 2.3 A,B). *AtHB8* over-expression altered the organization of palisade parenchyma as shown on semi-thin transversal sections of cauline leaves. Instead of the long cells perpendicular to the leaf surface (Figure 2.3 A, Pp), palisade parenchyma cells in *35S::AtHB8* leaves (Figure 2.3 B, Pp) were exhibiting a circle shape, characteristic for leaf spongy parenchyma cells. However, vascular bundles did not show major modifications compared to wild type. As previously described (Baima et al., 2001), leaf margin cells were of high density (data not shown), suggesting a high division rate. To explore the impact of constitutive expression of AtHB8 on the vascular system, semi-thin cross sections of the basis of the stem of 7 week old control and 35S::*AtHB8* 4.1 plants were made. No major reorganization of the vascular bundles, such as amphivasal vascular bundles, was observed (Figure 2.3 C,D insert). The presence of the *35S::AtHB8* construct altered cell differentiation at the level of the vascular bundles compared to *p3300* controls (Figure 2.2 C,D). Similarly as in *AtHB8::AtHB8-∂miR* lines, xylem cell differentiation and lignification was reduced in *35S::AtHB8* lines.

Additionally to the homozygous 35S::*AtHB8-∂miR* silenced lines, one 35S::*AtHB8-∂miR* primary tranformant exhibited an altered phenotype (Figure 2.3 E). A strong transversal and longitudinal hyponasty of the cotyledons occurred and leaves were partially radialized. Plant size was reduced and bolting was not initiated in standard growth conditions. Due to the similarities with the *phv* gof mutant (McConnell et al., 2001) and other plants expressing *AtHB8* in various patterns described in section 2.1.4, this plant is not considered as a transformation outlier, but as representative of plants expressing *35S::AtHB8-∂miR*.

These results suggest that, when ectopically expressed, AtHB8 triggers important development alterations such as lateral organs hyponasty and reduced xylem maturation. However, when *AtHB8-∂mir* is ubiquitously expressed, additional alterations occur, supporting a model where miRNAs post-transcriptionaly regulate *AtHB8*. The similarity to the dominant *phv-1d* mutant phenotype, also suggests that, when expressed in a comparable pattern, *AtHB8-∂miR* could trigger the same downstream genes. Therefore, it was decided to study the similarities between *AtHB8* and other members of this family of transcription factors. Thus, plants constitutively expressing *AtHB15* were generated and *AtHB8-∂miR* was expressed in the pattern of others class III HD-ZIPs.

### 2.1.3 Plants constitutively expressing *AtHB8* or *AtHB15* present closely related phenotypes

As *AtHB8-∂miR* expression in the *AtHB8* pattern generated subtle effects on vasculature, the effects of *AtHB8* and *AtHB15* on plant development were compared by using the ubiquitously expressed CaMV 35S promoter.

We designed constructs encoding the *AtHB15* and AtHB15 *gof* sequences under the control of the constitutive cauliflower mosaic virus (CaMV) 35S promoter and the RuBisCO small subunit (RSSU) terminator. 35S::*AtHB15-∂miR* presents the same sequence modification as *AtHB8::AtHB8-δ mir* (Figure 2.4A). Transformants were selected on phosphinothricin-containing media and are denoted *35S::AtHB15* and *35S::AtHB15-∂miR*, respectively. Primary transformants were identified on selection media and homozygous F2 lines

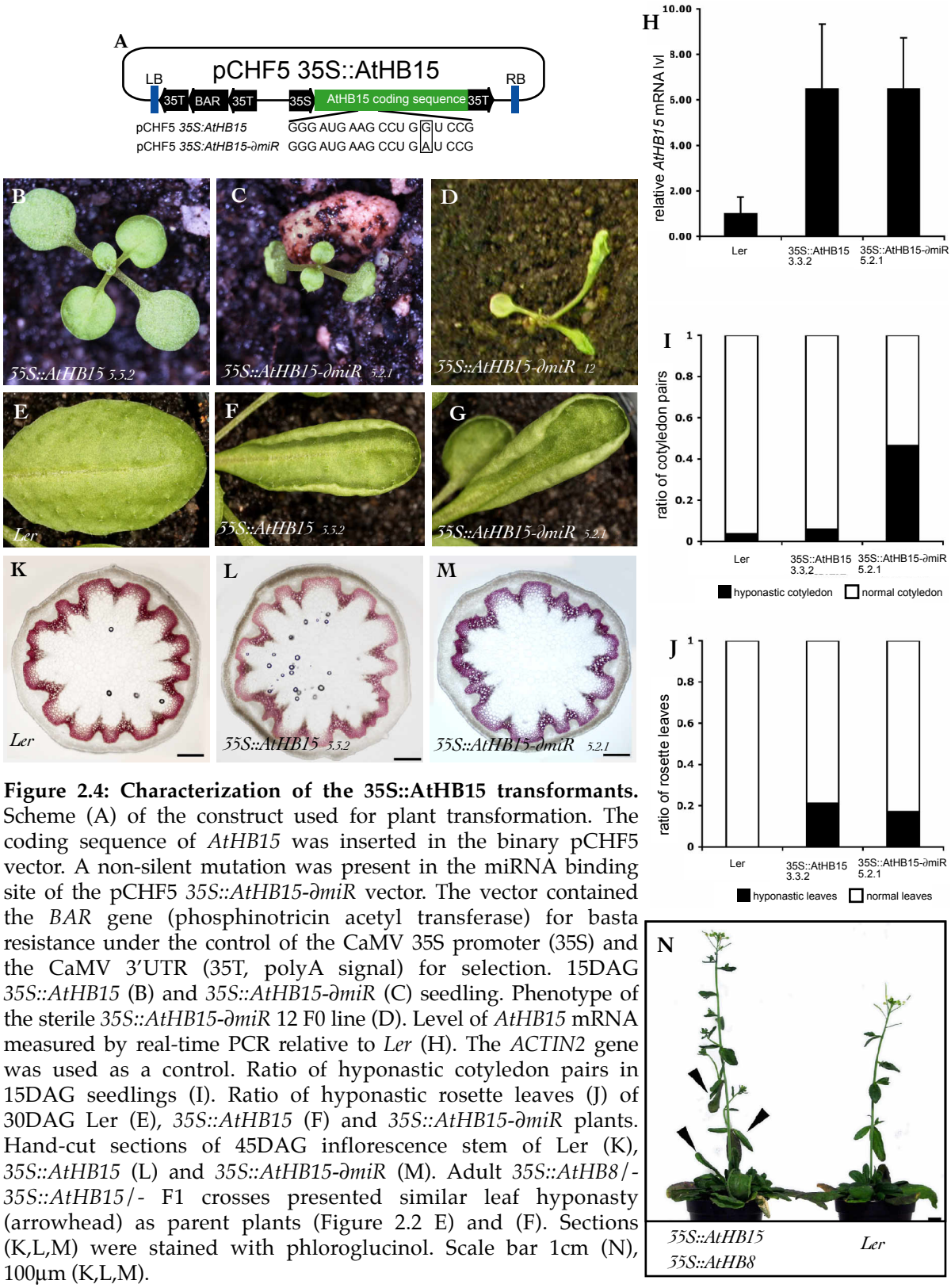


**Figure 2.4: Characterization of the 35S::AtHB15 transformants.** Scheme (A) of the construct used for plant transformation. The coding sequence of *AtHB15* was inserted in the binary pCHF5 vector. A non-silent mutation was present in the miRNA binding site of the pCHF5 *35S::AtHB15-∂miR* vector. The vector contained the *BAR* gene (phosphinotricin acetyl transferase) for basta resistance under the control of the CaMV 35S promoter (35S) and the CaMV 3'UTR (35T, polyA signal) for selection. 15DAG *35S::AtHB15* (B) and *35S::AtHB15-∂miR* (C) seedling. Phenotype of the sterile *35S::AtHB15-∂miR* 12 F0 line (D). Level of *AtHB15* mRNA measured by real-time PCR relative to *Ler* (H). The *ACTIN2* gene was used as a control. Ratio of hyponastic cotyledon pairs in 15DAG seedlings (I). Ratio of hyponastic rosette leaves (J) of 30DAG Ler (E), *35S::AtHB15* (F) and *35S::AtHB15-∂miR* plants. Hand-cut sections of 45DAG inflorescence stem of Ler (K), *35S::AtHB15* (L) and *35S::AtHB15-∂miR* (M). Adult *35S::AtHB8/-35S::AtHB15/-* F1 crosses presented similar leaf hyponasty (arrowhead) as parent plants (Figure 2.2 E) and (F). Sections (K,L,M) were stained with phloroglucinol. Scale bar 1cm (N), 100µm (K,L,M).

containing a single insertion locus were identified by segregation analysis (data not shown). Sequence of the miRNA binding site of *AtHB15* in both *35S::AtHB15* and *35S::AtHB15-∂miR* transgene was confirmed by sequencing (data not shown). *35S::AtHB15* seedlings (Figure 2.4 B) exhibited no particular cotyledon phenotype compared to wild type (Figure 2.4I). Although *35S::AtHB15-∂miR* seedlings grown on 0,5 MS medium (Figure 2.3 C) presented hyponastic cotyledons (Figure 2.4 I) mRNA levels of both *35S::AtHB15* and *35S::AtHB15-∂miR* were comparable and elevated when compared with the *AtHB15* mRNA level of *Ler* (Figure 2.4 H). *35S::AtHB15* and *35S::AtHB15-∂miR* adults plants grown on soil exhibited transversal leaf hyponasty (Figure 2.4J) in standard growth conditions (Figure 2.3 F,G) compared to *Ler* (E). Note that for clarity reasons only two homozygous lines are shown here (*35S::AtHB15 3.3.2* and *35S::AtHB15-∂miR* 5.2.1), but similar results were obtained for 2 additional *35S::AtHB15* and *35S::AtHB15-∂miR* lines. Additionally, a sterile *35S::AtHB15-∂miR* F0 plant (Figure 2.4 D) with a phenotype comparable with *35S::AtHB8-∂mir* was found. Thus, it was considered that the *35S::AtHB15-∂miR* homozygous line 5.2.1 was presenting an intermediate phenotype. Similarly to *35S::AtHB8* plants, no major reorganization of the vascular bundles occurred between *35S::AtHB15*, *35S::AtHB15-∂miR* and controls (Figure 2.4 K-M). These results suggest that when expressed in the CaMV 35S pattern, *AtHB8* and *AtHB15* trigger comparable phenotypical alterations. To support this hypothesis, *35S::AtHB8* and *35S::AtHB15* were crossed (Figure 2.3 N**)**. Phenotype of *35S::AtHB8* / - *35S::AtHB15* / - plants was not altered compared to parent plants, petal hyponasty excepted. The stability of observed phenotype, either in presence of high levels of AtHB8, AtHB15 or both AtHB8 and AtHB15, suggest a situation where both transcription factors have closely related targets and where saturation occurs.

### 2.1.4 AtHB8 phenocopies other class III HD-ZIPs

The phenotypical similarity between 35S::*AtHB8-∂mir* (Figure 2.3E), 35S::*AtHB15-∂miR* (Figure 2.4D) and *phv-1d* (McConnell et al., 2001) plants suggested that some class III HD-ZIPs might have similar functions. However, the CaMV promoter is not suited to compare the function of these

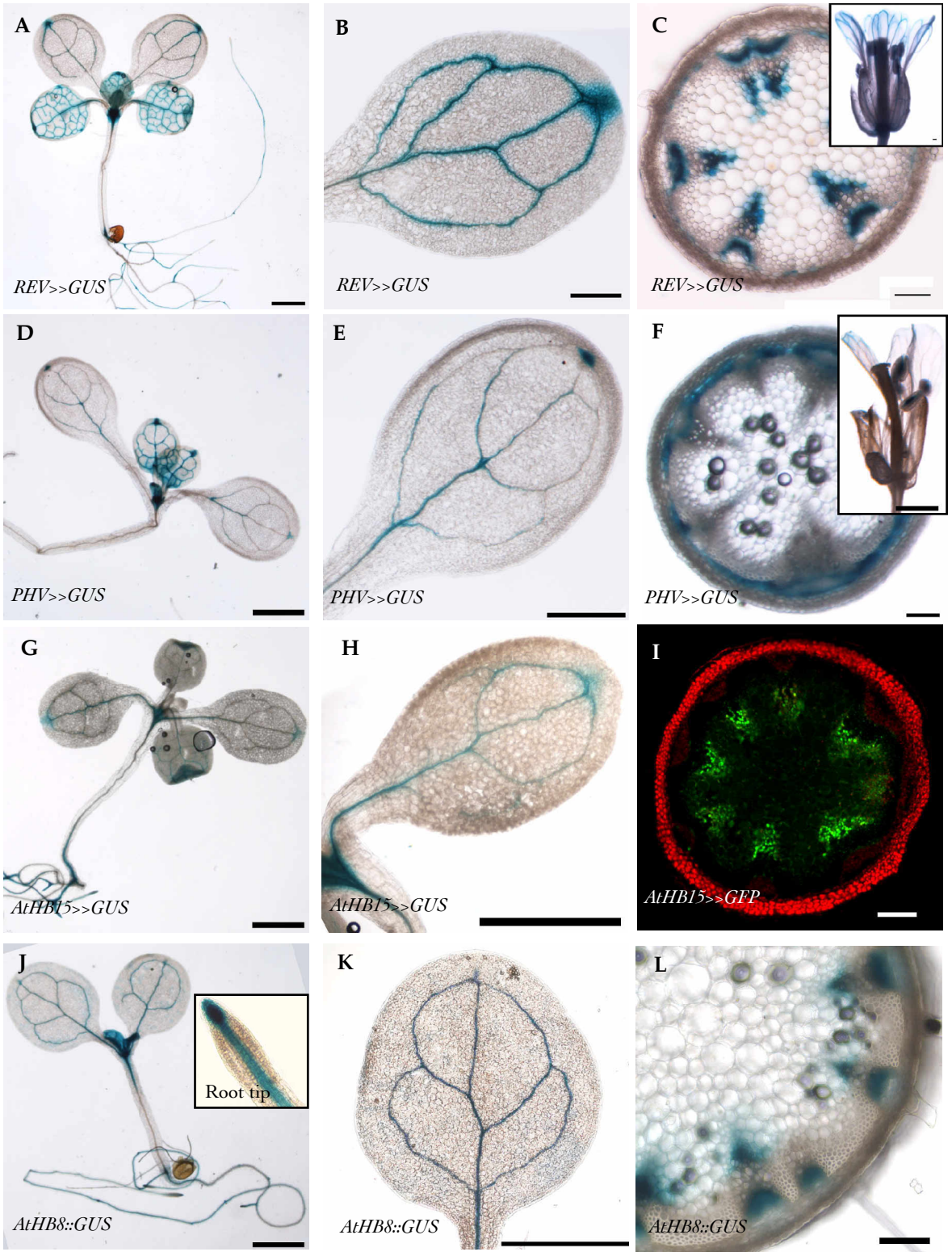


**Figure 2.5: Expression pattern of promoters used for transactivation and *AtHB8::GUS* expression pattern.** *REV>>GUS* (A-C), *PHV>>GUS* (D-F), *AtHB15>>GUS* (G-H) and *AtHB8::GUS* (J-L). GUS reactions were made on 15 DAG seedlings (A-B, G-H, J-K) or 4-6 week old inflorescence stems and flowers (C,F,I,L). Entire seedling (A,D,G,J), detail of the cotyledon (B,E,H,K) and transverse sections of the inflorescence stem (C,F,I,L). Insert in picture J showed root tip of the seedling. Confocal microscopy observation of *AtHB15>>GFP* inflorescence stem (I). Scale bar is 1mm in A,B,D,E,G,H,J,K, 100µm in C,F,I,L.

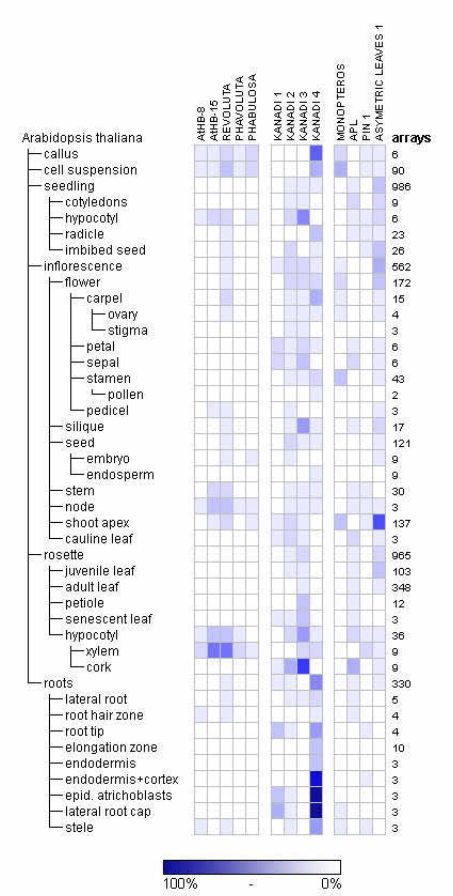


**Figure 2.6: Spatial expression patterns of class III HD-ZIPs and other genes of interest.** Expression profile of class III HD-ZIPs, KANs and other genes of interest in different organs and developmental stages. Public microarray data were analysed using the Genevestigator software (Zimmermann et al. 2004). The blue-white heat map reflects signal intensity values, maximum signal intensity of 100% was indicated in dark blue and no signal was indicated by 0% in white. The number of microarrays used for each profile was indicated in the last column.

transcription factors as few transformants are obtained and constitutive expression enhances the probability to study secondary effects. Thus, more specific promoters were selected to compare primary effects of class III HD-ZIPs on vascular tissue, leaf and flower formation. The transactivation system developed by Moore et al. (Moore et al., 1998) was used to express gain of function sequences of *AtHB8*, *AtHB15* and *PHABULOSA* (*PHB*) in the expression pattern of *AtHB15*, *PHAVOLUTA (PHV)*, *REVOLUTA (REV)* and *ASYMMETRIC LEAFS 1 (AS1)*.

The operators of the transactivation system used here, 10Op::*ATHB8-∂mir*, 10Op::*ATHB15-∂mir* and 10Op::*PHB-∂mir*, have the same point mutation in the miR165 binding site as the *AtHB8::AtHB8-∂mir* construct (Figure 1.4 B). To evaluate the expression patterns of the promoters used in the binary transactivation system, LhG4 activator lines were crossed with reporter lines containing either the ß-glucuronidase gene (GUS) 10Op::*GUS* (Figure 2.5 A-H) or the green fluorescent protein gene 10Op::*GFP* (Figure 2.5 I). To prevent saturation, the GUS reaction was stopped after 3 hours, therefore irregularities in the staining can occur. Note that miR165 cleavage sites were not added to the GUS sequence or to the GFP sequence. The *AtHB8* expression pattern is shown here for information purpose (Figure 2.5 J-L). The promoters (noted here *pGENE NAME*) *pREV*, *pPHV*, *pAtHB15* and *AtHB8::GUS* showed activity in the vascular system of the seedlings. Morever, *pREV*, *pPHV* and *AtHB8::GUS* presented activity in young developing leaves. *pREV*, *pPHV* and *pAtHB15* were also active in hydatodes at the tip of the cotyledons. In the inflorescence stem of adult plants, *pREV* and *AtHB8::GUS* were active in protoxylem, cambium and interfascicular cambium (data not shown); *pAtHB15* was active in protoxylem; *pPHV* was active in cambium and interfascicular cambium. In flowers, *pREV* was active in all the vasculature, petal blades and anther. On the other hand, *pPHV* was only active in the stamen stalk and the stamen and a faint activity was observed at the distal region of the petal blades. The expression patterns of *pREV*, *pPHV* and *pAtHB15* are coherent with the previous description of the class III HD-ZIP transcription factors (McConnell et al., 2001; Otsuga et al., 2001; Emery et al., 2003; Ohashi-Ito and Fukuda, 2003; Ochando et al., 2006).

To gain additional insight on the expression pattern of the genes studied, we analyzed publicly available microarray data using the Genevestigator toolbox

(Zimmermann et al., 2004); (http://www.genevestigator.ethz.ch/). The class III HD-ZIP transcription factor expression patterns were compared to the activity of other genes active during the development of the vascular system and to genes of general interest (Figure 2.6). Normalized signal of all class III HD-ZIP genes was low, as expected for a family of transcription factors. With the set of oligos printed on the microarrays, *REV* was the class III HD-ZIP gene with the strongest and most widespread expression. The near background signal is relatively conserved between all class III HD-ZIP genes in the conditions studied. While class III HD-ZIPs signals were weak and presented many overlapping patterns, *KANADI* genes produced strong and varied signals on theses microarrays. The expression comparison for these two families in the hypocotyl confirms the accuracy of some arrays: *REV* and *AtHB15* were highly expressed in the xylem and *KAN2* and *KAN3* were expressed in the cork. It should be noticed that micro array data and promoter activity tested with the LhG4/pOP transactivation system should not be compared directly, as post-transcriptional regulation might occur, especially for class III HD-ZIPs.

*REV*, *PHV*, *AtHB15* and *AtHB8* expression patterns defined in previous and published research were described in the introduction. Reporter gene assays and microarray data brought additional information on the expression pattern of these four genes in this section. These three sources of evidences will be used in a complementary way to analyze further results.

### 2.1.5 Expression of class III HD-ZIP gain of function in procambium

To determine the effects of AtHB8 and to compare its function with the function of PHB in the development of the vascular system, *AtHB8-∂miR* and *PHB-∂miR* sequences were expressed in the *AtHB15* pattern using the transactivation system (Moore et al., 1998) (Figure 2.7). In a first step, the *AtHB8* mRNA was quantified in plants with the *AtHB15>>AtHB8-∂miR* construct to confirm ectopic expression. Real time PCR confirmed ectopic expression, as *AtHB8* mRNA level was elevated in *AtHB15>>AtHB8-∂miR* plants ($AtHB8_{\text{expression}} = 2.64 \pm 0.69$) when compared with *AtHB8* mRNA content of control plants ($AtHB8_{\text{expression}} = 1.00 \pm 0{,}15$). To determine the effect of *AtHB15>>AtHB8-∂miR* on vascular development, hypocotyl cross sections of

15 DAG seedlings were made (Figure 2.7 B). Compared to hypocotyl sections of pATHB15::LhG4 used as controls (Figure 2.7A), expression of *AtHB15>>AtHB8-∂miR* had only a weak influence on hypocotyl vascular conformation. The stele contained an increased number of differentiated xylem cells (Figure 2.7 B). The same observations were made for *AtHB15>>PHB-∂miR* plants (Figure 2.7 C). At the level of the entire seedling, *AtHB15>>AtHB8-∂miR* and *AtHB15>>PHB-∂miR* presented hyponastic cotyledons and first leaves (Figure 2.7 E,F) compared to *pATHB15::LhG4* (Figure 2.7 D) control seedlings. This similar phenotype suggests that *PHB* and *AtHB8* had similar effects on leaf and vascular tissue differentiation, when expressed under the control of the *AtHB15* promoter. To test if *AtHB8-∂miR* expression in procambial cells influences phloem differentiation, *APL* expression pattern was studied in *AtHB15>>AtHB8-δ miR* plants. The unaltered pattering of *APL::GUS* in *AtHB15>>AtHB8-δ miR* (Figure 2.7 G), suggested that presence of AtHB8 in procambium does not interfere with phloem establishment and continuity. Later during development, it was observed that several *AtHB15>>AtHB8-δ miR* plants presented trumpet-shaped leaves (Figure 2.7 H, arrowhead and left panel I) or cabbage-like structures (Figure 2.7 I, right panel). Trumpet-shaped leaves and cabbage-like structures were either formed in a prolongation of rosette leaf midvein or from the center of the rosette. A new pedicel sometimes supported these structures. These alterations suggested a modification in dorsoventral identity as similar structures are observed in plants with class III HD-ZIP-*KANADIs* imbalance (Emery et al., 2003; Eshed et al., 2004). Adaxial surface of leaves of the *kan1 kan2 kan4* multiple mutant are shown here for comparison (Figure 2.7 K). As *YABBY* mutants were also shown to produce ectopic tissues on leaf blades (Kumaran et al., 2002), the mRNA levels of the *FIL* gene were measured in *AtHB15>>AtHB8-∂miR* seedlings ($AtHB8_{expression} = 1.05 \pm 0.15$) and were not significantly different from FIL mRNA levels in control plants ($AtHB8_{expression} = 1.00 \pm 0.05$). No ectopic growth was observed during preliminary observations of the *AtHB15>>PHB-∂miR* adult plants (n=4) (Figure 2.7 J). Hand sections of the inflorescence stem of *AtHB15>>AtHB8-∂miR* and *AtHB15>>PHB-∂miR* adult plants were made. No major modifications occurred at the level of organization of the vascular system in

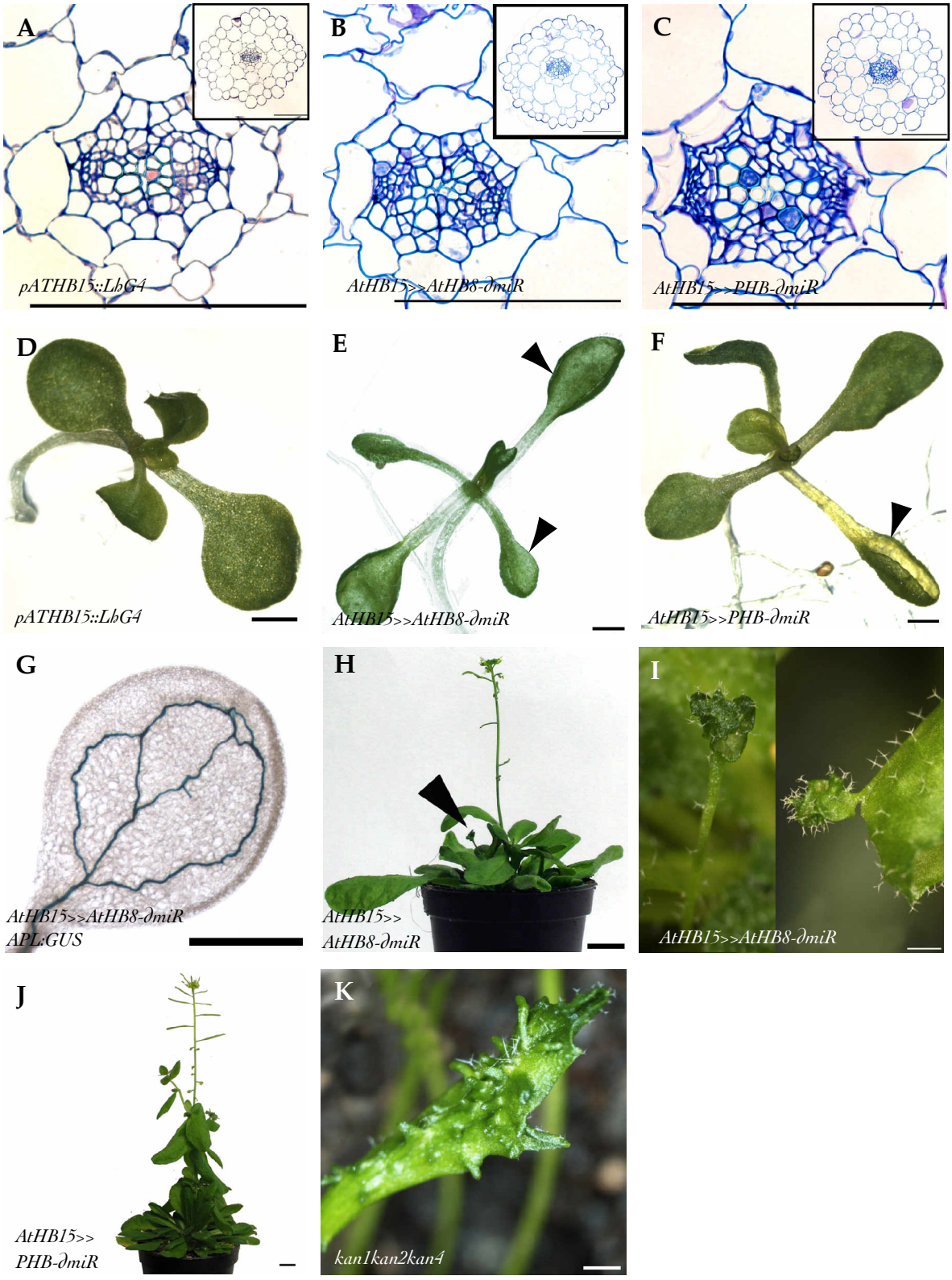


**Figure 2.7. Expression of *AtHB8-∂miR* and *PHB-∂miR* in the *AtHB15* expression pattern.** Control *ATHB15::LhG4* seedlings (A,D), *AtHB15>>AtHB8-∂miR* (B,E,G-I), *AtHB15>>PHB-∂miR* (C,F,J) and *kan1kan2kan4* mutant (K). Semi-thin transversal section through the hypocotyl of 15DAG seedlings (A-C). Compared to control (D), some 15DAG seedlings presented hyponastic cotyledons (arrowhead, E-F). 45DAG *AtHB15>>AtHB8-∂miR* plants presented trumpet-shaped leaves (H, arrowhead, I left panel) and cabbage-like structures (I, right panel). No ectopic structures developed on the leaf of *AtHB15>>PHB-∂miR* plants (J). Ectopic structures on the surface of *kan1kan2kan4* triple mutants (K). Sections A-C were stained with toludine blue. The scale bars represent 100µm in A-C, 1mm in D-G.I,K and 1cm in H and J.

inflorescence stems of *AtHB15>>AtHB8-∂miR* and *AtHB15>>PHB-∂miR* plants (data not shown).

In summary, these results suggest that both PHB and AtHB8 can influence vascular system differentiation as more differentiate xylem cells in the vascular system of the hypocotyl were observed in *AtHB15>>AtHB8-∂miR* and *AtHB15>>PHB-∂miR* than in controls. The seedling phenotype of the *AtHB15>>AtHB8-∂miR* and *AtHB15>>PHB-∂miR* line is very similar to mutants with an *AtHB15* sequence resistant to miRNA cleavage (*icu4-1*) (Ochando et al., 2006). Although leaf surface alterations were not described for *icu4-1* mutants, these modifications were observed on plants with constitutive expression of the *icu4-1* sequence (Ochando et al., 2006). Additional adult plant observations and RNA quantification are still required for *AtHB15>>PHB-∂miR* plants. These observations suggest that AtHB8, AtHB15 and PHB transcription factors induce similar alterations when present in the *AtHB15* expression pattern.

### 2.1.6 The *phv-1d* mutant can be phenocopied by ectopic *AtHB8* or *PHB* expression

We previously showed that constitutive expression of gof *AtHB15* and *AtHB8* leads to phenotypes similar to the *PHV* gof mutant *phv-1d* (McConnell *et al.* 2001). Moreover, *AtHB8-δ miR* and *PHB-δ miR* induced similar phenotype alterations when expressed under the control of the *AtHB15* promoter, which is expressed mainly in the vascular system and in meristematic tissues (Ohashi-Ito and Fukuda, 2003; Prigge et al., 2005; Ochando et al., 2006). The resulting phenotype was comparable to *icu4-1* mutants. To further explore the possibility that several class III HD-ZIPs could have redundant functions, we expressed *AtHB8-∂miR* and *PHB-∂miR* in the *PHV* pattern in order to determine if they phenocopied *phv-1d* (McConnell et al., 2001).

Since *PHV* is expressed in the vascular system and in the adaxial part of the leaves, we first searched for alterations in the vascular system to compare AtHB8 and PHB function. The anatomy of the vasculature in the hypocotyl of *PHV>>AtHB8-δ miR* (Figure 2.8 A) and *PHV>>PHB-δ miR* (Figure 2.8 B) seedlings was comparable to the vascular anatomy of controls (Figure 2.7 A), suggesting that no particular influences on the differentiation of the different

cell types in the vascular system occurred when *AtHB8* was expressed in the *PHV* pattern. On the other hand, seedling morphology was identical for *PHV>>AtHB8-δ miR* (Figure 2.8 C) and *PHV>>PHB-δ miR* (Figure 2.8 D). First leaves phenotypes varied from hyponastic to radialized for *PHV>>AtHB8-∂miR* and *PHV>>PHB-∂miR* seedling. The epidermis of radialized leaves of *PHV>>AtHB8-δ miR* (Figure 2.8 F), *PHV>>PHB-δ miR* (Figure 2.8 G) plants had a similar texture to epidermal cells at the adaxial leaf surface of wild type plants (Figure 2.8 E) although the height of the cells seems to be reduced. The reduced height of the epidermal cells appears to be a petiole feature, as visible on controls leaf petiole (Figure 2.8 J). Moreover, texture of the epidermal cells was much more comparable between control petiole (Figure 2.8 J) and *PHV>>AtHB8-∂miR* (Figure 2.8 H), *PHV>>PHB-∂miR* (Figure 2.8 I) radialized leaf basis.

*PHV>>AtHB8-∂miR* and *PHV>>PHB-∂miR* adult plants had a reduced size and a retarded bolting. Rosette leafs were more dense than control. Moreover, multiple inflorescences stem of reduced stature developed simultaneously instead of the principal stem developing in controls (Figure 2.9 A and data not shown). This adult phenotype was similar to *35S::icu4-1* (Ochando et al., 2006). Both *PHV>>AtHB8-∂miR* (Figure 2.9 B) and *PHV>>PHB-∂miR* (Figure 2.9 C) could present cabbage-like structure on the leaf surface (arrowhead) and leaves with a trumpet shape (arrow). The cabbage-like structures developed on both leaves sides and were not systematically originating from veins. On these structures, trichomes were present in high density (Figure 2.9 B, bottom right). Similar adaxial traits were observed on the adaxial leaf surface of *phb-1d* mutants (McConnell et al. 2001, Figure 1F).

Flowers of both *PHV>>AtHB8-∂miR* (Figure 2.9 D) and *PHV>>PHB-∂miR* (Figure 2.9 E) plants had wild type, trumpet-shaped (arrowhead) and radialized petals (arrow). A direct comparison between controls and *PHV>>PHB-∂miR* or *PHV>>AtHB8-∂miR* vascular system of the stem is not possible due to retarded bolting and reduced diameter. However, no major alterations such as amphivasal vascular bundles were observed in the vascular system of inflorescence stem of *PHV>>AtHB8-∂miR* and *PHV>>PHB-∂miR* by hand-cut transverse sections (data not shown). Semi-thin sections on *PHV>>PHB-∂miR* inflorescence stem confirmed that no major alteration occurred (Figure 2.9 G) although it should not be directly compared to control

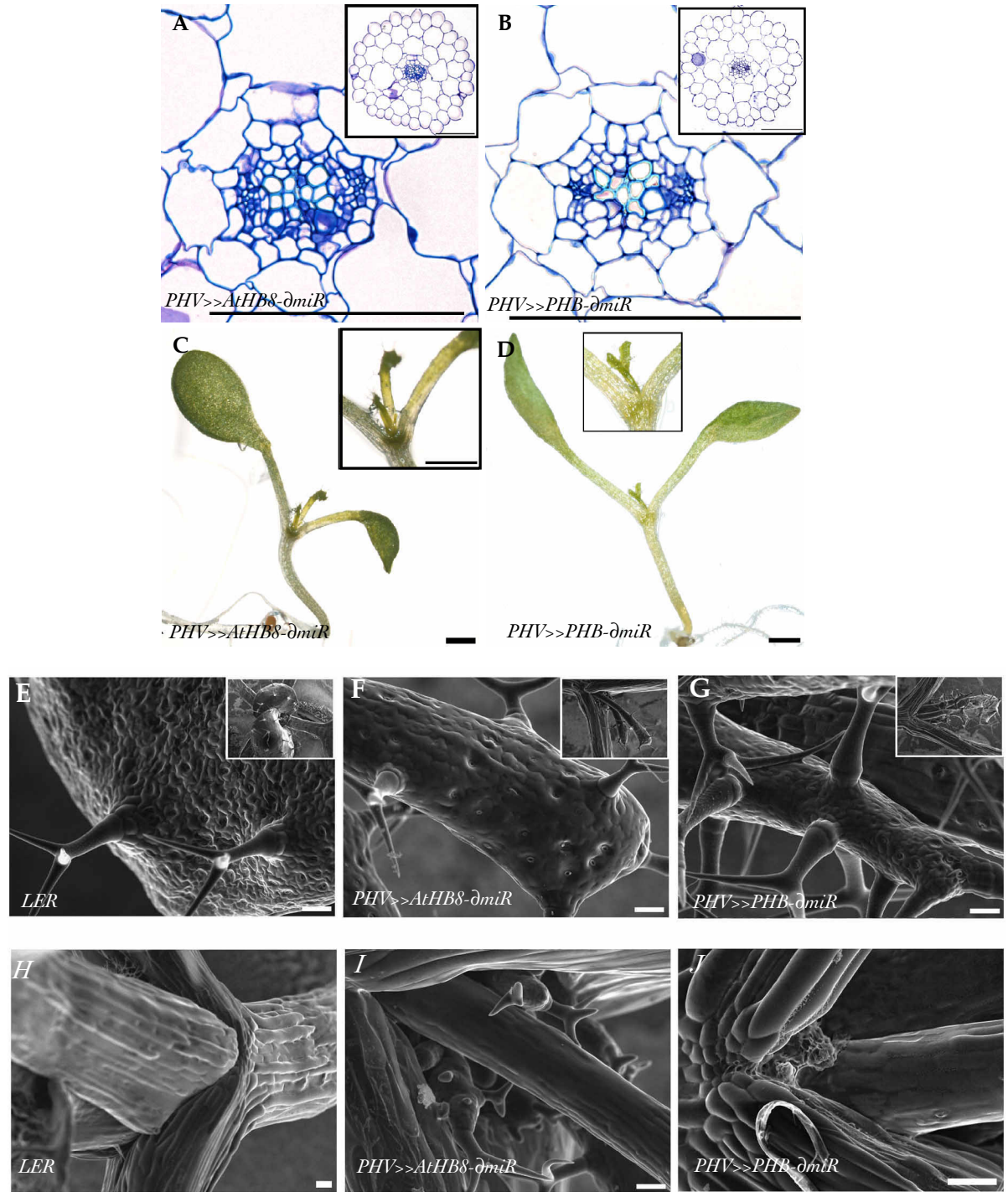


**Figure 2.8. Expression of *AtHB8-∂miR* and *PHB-∂miR* in the expression pattern of *PHV*.** 15DAG *PHV>>AtHB8-∂miR* (A,C,F,I) and *PHV>>PHB-∂miR* (B,D,G,J) seedlings. No major alterations were observed at the level of hypocotyl vasculature (A,B). First leaves presented various levels of radialization (inserts C,D). Scanning electron microscopy observation (E-J) showed that adaxial epidermal cells are comparable at the tip of the first leaves between control (E), *PHV>>AtHB8-∂miR* and *PHV>>PHB-∂miR* (F,G) although cell height was reduced. In the naturally radialized region of the petiole (H-J) the same cell height was observed. Sections A-D were stained with toludine blue. The scale bars represent 100µm in A,B,E-J 1mm in C-D.

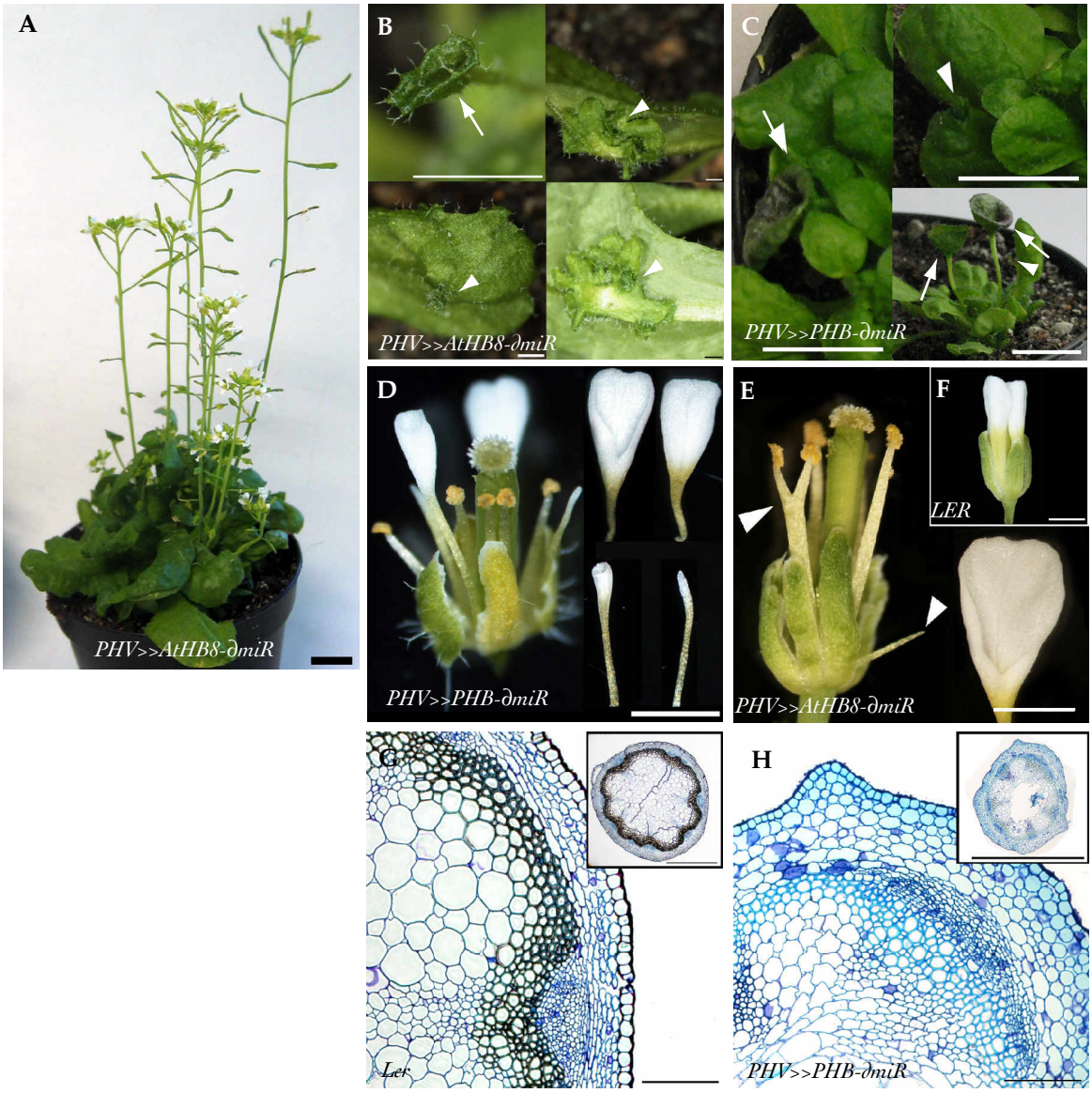


**Figure 2.9 Expression of *AtHB8-∂miR* and *PHB-∂miR* in the expression pattern of *PHV* in adult plants.** 60DAG *PHV>>AtHB8-∂miR* plant (A) had no main inflorescence stem. Both *PHV>>AtHB8-∂miR* (B) and *PHV>>PHB-∂miR* (C) presented altered leaf surface and trumpet leaf shape. Flowers of both *PHV>>AtHB8-∂miR* (D) and *PHV>>PHB-∂miR* (E) plants presented wild type, trumpet-shaped (arrowhead) and radialized petals (arrow) compared to controls (F). The vascular system of the stem of the inflorescence of *PHV>>PHB-∂miR* did not present major alterations (H) compared to controls (G). Sections G and H were stained with toludine blue. The scale bars represent 1cm in A and C, 1mm in B,D,E and 100µm in G and H.

(Figure 2.9 F) due to differences in diameter and in bolting time. The cambium and phloem presented cells of reduced size.

Taken together these results show that, when expressed in the *PHV* pattern, *AtHB8* and *PHB* gof can phenocopy the class III HD-ZIP *PHV* gof mutant. The results also indicate that, placed out of a vascular specific pattern, AtHB8 can induce alterations in non-vascular tissues.

### 2.1.7 *REVOLUTA* gain of function mutants cannot be phenocopied by ectopic expression of *AtHB8*

To further test if class III HD-ZIP proteins were exchangeable, *AtHB8* was expressed under the control of the *REV* promoter using the transactivation system and compared to the *rev-10d* dominant mutant.

One of the most striking characteristic of the *rev-10d* mutant is the frequently radialized and amphivasal vascular bundles in adult plants (Emery et al., 2003)(Figure 2.10 A). Organization of the vasculature in the hypocotyl of *rev-10d* (Figure 2.10 B) plants was also altered compared to controls as an increased number of xylem cells were present. Although *REV>>AtHB8-∂miR* presented similar alterations as *rev-10d* at the level of hypocotyl vasculature (Figure 2.10 E), the inflorescence stem had no amphivasal vascular bundles and was similar to wild type (Figure 2.10 D).

Additionally, *REV>>AtHB8-∂miR* seedlings had two (Figure 2.10 H, main) (29/45 seedling), three (Figure 2.10 H, detail) (12/45 seedling) or four cotyledons (4/45 seedling) and radialized leaves. The structure of epidermal cells of the radialized leaves (Figure 2.10 I) was comparable to *PHV>>AtHB8-∂miR* and *PHV>>PHB-∂miR* epidermal cells in radialized leaves (Figure 2.8 F,G). Meanwhile, *rev-10d* seedling presented either a wild-type (Figure 2.10 C, arrow) or dwarf appearance (Figure 2.10 C, arrowhead).

In the adult stage, *rev-10d* had dense rosette leaves and a retarded bolting occurred (data not shown). In *REV>>AtHB8-∂miR* adult plants, the phenotype ranged from plants with a dwarf rosette and retarded bolting to plants with a SAM producing several radial leaves depending on the 10Op::*AtHB8-∂miR* used (Figure 2.10 H). Additionally, while flowers of *rev-10d* were comparable to *wt* flowers (data not shown), only *REV>>AtHB8-∂miR* with a less severe phenotype (dwarf rosette) produced inflorescences (Figure 2.10 I). Flowers

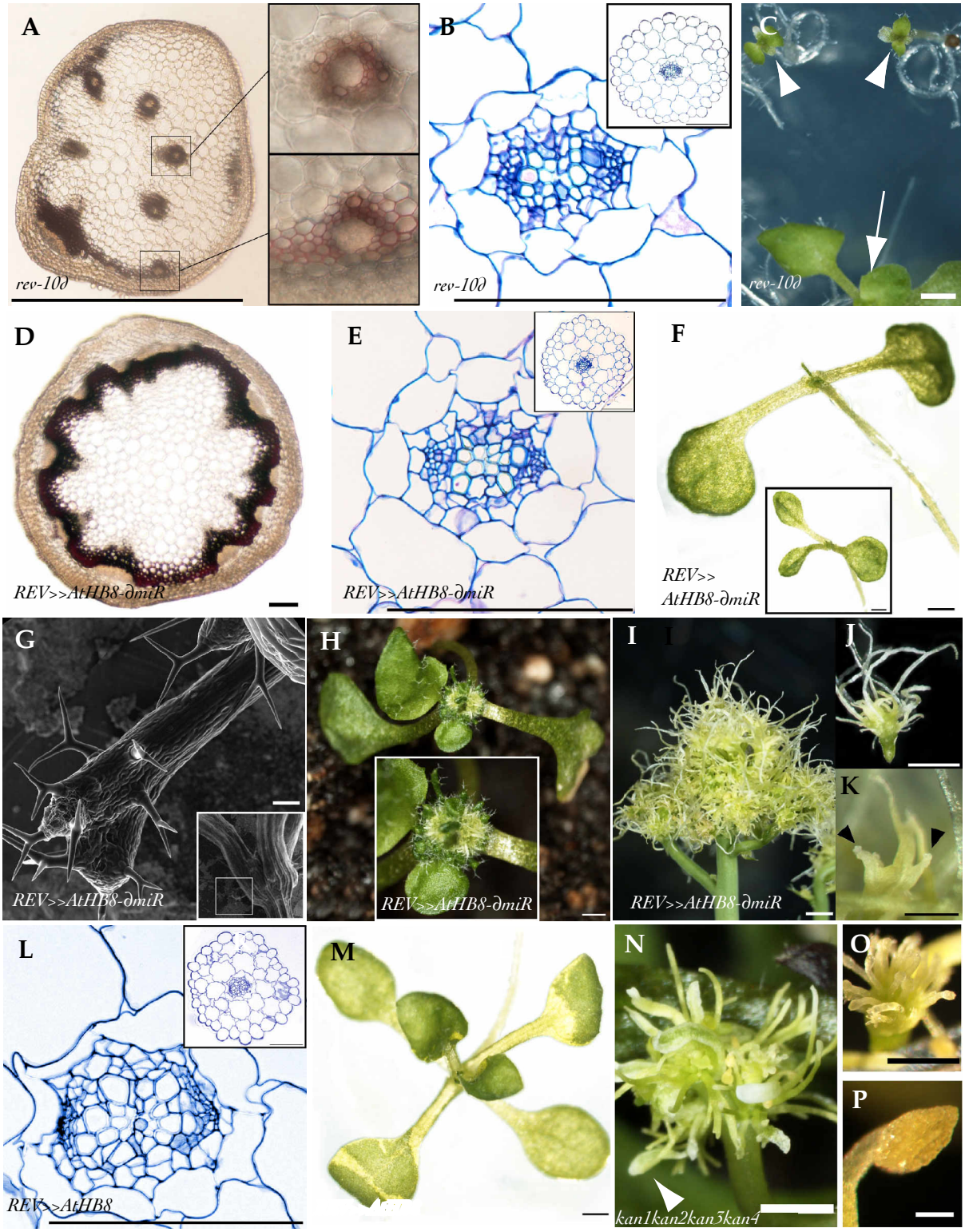


**Figure 2.10: Expression of *AtHB8-∂miR* in the *REV* pattern compared to the *rev-10d* gain-of-function mutant and *kan1kan2kan3kan4* quadruple mutant.** *rev-10d* gof mutants (A-C) are compared to plants expressing unaltered (L-M) and gof (D-K) *AtHB8* in the *REV* expression pattern using the transactivation system (Moore et al. 1998). Amphivasal vascular bundles were present in rev-10d mutants (A) while absent from *REV>>AtHB8-∂miR* inflorescence stems (D). Vascular system of 15DAG hypocotyl was similar in *rev-10d* (B), *REV>>AtHB8* (L) and *REV>>AtHB8-∂miR* (E). Seedlings of rev-10d were either similar to wild type (C, arrow) or of reduced size (C, arrowhead). *REV>>AtHB8-∂miR* seedlings presented unstable numbers of cotyledons (F, insert) and radialized leaves (F) with adaxial characteristics as shown with scanning electron microscopy (G). *REV>>AtHB8* seedlings presented narrow leaves (M). Adult *REV>>AtHB8-∂miR* presented adaxialized leaves (H). Inflorescences of *REV>>AtHB8-∂miR* plants (I) presented flowers with radialized structures (J) and altered carpels (arrowhead, K). Flowers of *kan1kan2kan3kan4* quadruple mutant also presented radialization (N), although carpel (O) and stamens (P) are formed. Sections were stained with phloroglucinol (A,D) or toludine blue (B,E,L). The scale bars represent 1mm in A,C,F,H,I,J,M,N, 100µm in B,D,E,G,L,P, 500µm in O and 250µm in K.

presented the general appearance of a "hydra": organs were radialized and undistinguishable from one another like tentacles (Figure 2.10 J). Some distorted flower organs presented a carpel feature, as structures resembling stigma were visible (Figure 2.10 K, arrowhead). Although similar, inflorescences of *k1k2k3k4* mutants (Figure 2.10 N) developed petals (Figure 2.10 N, arrowhead), structures identifiable as carpel with long stigmas (Figure 2.10 O) and stamens (Figure 2.10 P).

In summary our results suggest that *AtHB8* cannot be used to phenocopy the *rev-10d* dominant mutant.

To further verify that AtHB8 has a separate function than REV in the *REV* expression pattern, *AtHB8* cDNA with no mutations in the coding sequence was expressed in this pattern. The vasculature of *REV>>AtHB8* hypocotyls (Figure 2.10 L) was comparable to the vasculature in hypocotyls of *REV>>AtHB8-ðmiR* plants. Morphologically, first leaves of *REV>>AtHB8* seedling were narrow, pointy and directed upward compared to controls (Figure 2.10 M), This suggests that at least in leaves, AtHB8 was additive to REV.

These results suggest that the transcription factor REV has different targets than AtHB8. However, a functional 10op::*REV-ðmiR* construct is required for confirmation. Also, REV>>AtHB8 could be expressed in the *rev* loss of function mutant (*rev-9*) to warranty that the endogenous REV in addition to the ectopic AtHB8 does not trigger a more severe phenotype than *rev-10d*.

### 2.1.8 Expressed in the pattern of *AS1, AtHB8-ðmiR, AtHB15-ðmiR* and *PHB-ðmiR* induce comparable phenotypical alterations.

Several class III HD-ZIP transcription factors seem to share similar functions. To further confirm this hypothesis, the functions of AtHB8, AtHB15 and PHB were compared when expressed in the *AS1* expression pattern. Comparatively to *REV*, *PHB* or PHV that are expressed in the central axis of the embryo and in the adaxial part of the cotyledons (Prigge et al., 2005), AS1 is expressed in embryo cotyledons but not in its central axis (Byrne et al., 2000). After germination, *AS1* is expressed in primordia P0 to P4, procotyledon cambium and in flower primordia. This difference in expression pattern should allow to

draw additional conclusions on alteration induced by ectopic gof class III HD-ZIP expression.

Neither *AS1>>AtHB8* nor *AS1>>AtHB15* seedlings grown on MS medium, nor adults grown on soil exhibited a significantly altered phenotype in standard growth conditions (data not shown). Conversely, *AS1>>AtHB15-∂miR* (Figure 2.11 A), *AS1>>AtHB8-∂miR* (Figure 2.11 B) and *AS1>>PHB-∂miR* (Figure 2.11 C) seedlings displayed phenotypes comparable to the ones observed when *AtHB15-δ miR, AtHB8-∂miR and PHB-∂miR* were expressed in the *PHV* and *REV* expression patterns. Cotyledons also presented a proximo-distal hyponasty. As *AS1* is not active in the hypocotyl, only preliminary observations were made on the hypocotyl vascular system. No major reorganization in this tissue in *AS1>>AtHB8-∂miR* (Figure 2.11 D) and *AS1>>PHB-∂miR* (Figure 2.11 E) plants occurred. Adult plants presented a normal (Figure 2.11 G,H) to reduced size (Figure 2.11 G,H, arrowhead), with dense rosette leaves compared to controls (Figure 2.11 F). No bolting occurred for plants of reduced size with adaxial leaves in the standard growth condition (*AS1>>PHB-∂miR* and *AS1>>AtHB8-∂miR* strong line). Observation of hand-made transversal sections indicated that no major alterations occurred in the inflorescence stem of *AS1>>AtHB15-∂miR* and *AS1>>AtHB8-∂miR* plants (data not shown). Cabbage-like structures were present on the leaf of some adult *AS1>>AtHB8-∂miR* plants (Figure 2.11 I). Similarly, as when expressed in the *PHV* pattern, radialisation of petals occurred for both *AS1>>AtHB8-∂miR* (Figure 2.12 B, arrowhead) and *AS1>>AtHB15-∂miR* (Figure 2.12 C, arrowhead). When compared by scanning electron microscopy, the shape of epidermal cells of the tip of radialized petals of *AS1>>AtHB15-∂miR* plants (Figure 2.12 D) was intermediate between the cone shaped adaxial petal cells (Figure 2.12 E) and the round abaxial petal cells of LER (Figure 2.12 F). However, at the distal part of the *AS1>>AtHB15-∂miR* petals (Figure 2.12 G,H) and on the tip of certain petals (Figure 2.12 I), epidermis cells were rather similar to cells from the naturally radialized stalk of the stamen (Figure 2.12 J).

In summary, the ectopic expressions of *AtHB8-∂miR, AtHB15-∂miR* and *PHB-∂miR* in the *AS1* expression pattern induce similar alterations as in the *PHV* expression pattern. Differences between these two setups, due to variation in expression pattern are observed at the level of cotyledons.

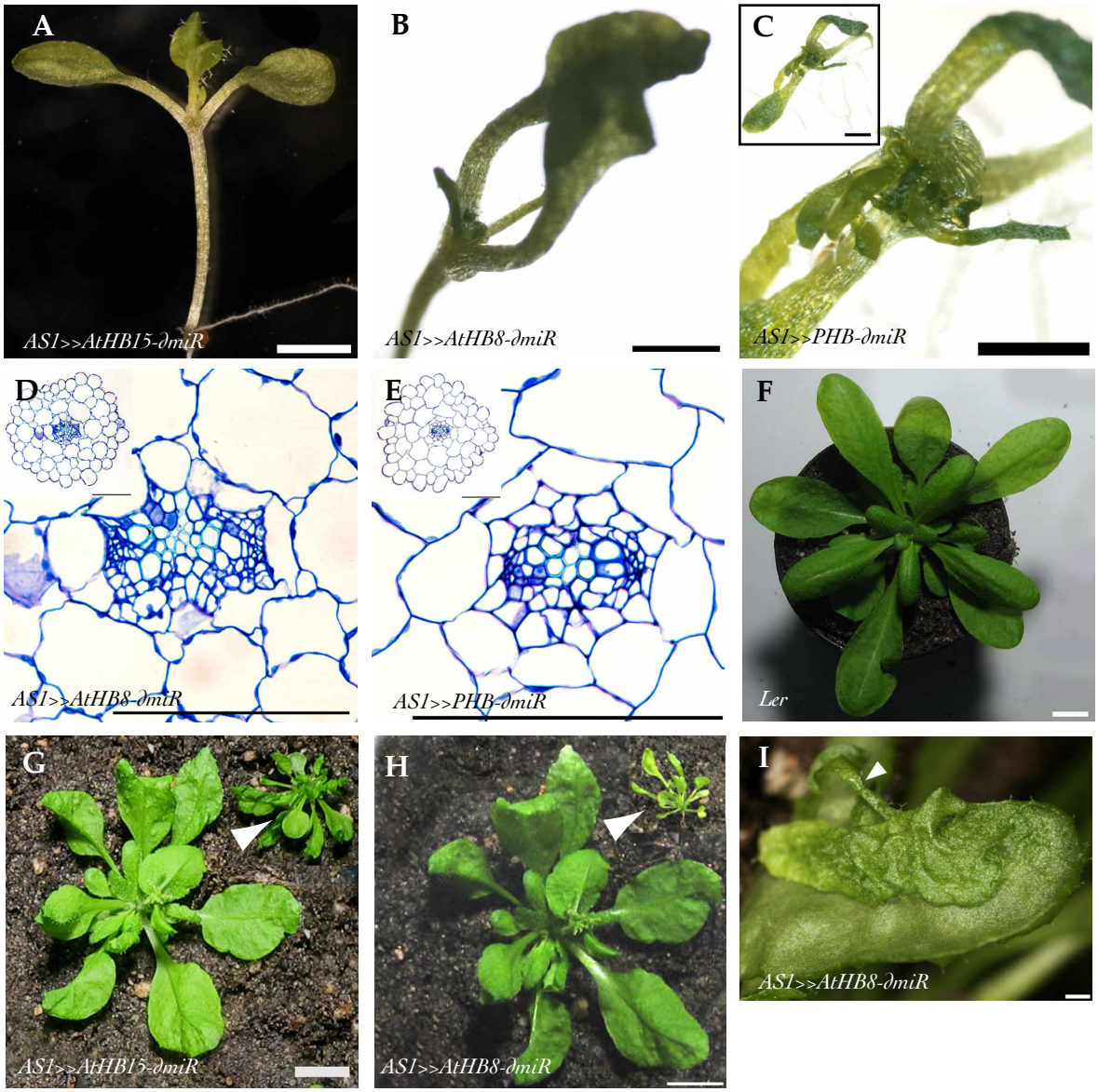


**Figure 2.11: Expression of *AtHB8-∂miR*, *AtHB15-∂miR* and *PHB-∂miR* in the *AS1* pattern.** First leaves presented radialized features when *AtHB15-∂miR* (A), *AtHB8-∂miR* (B) or *PHV-∂miR* (C) are expressed in the *AS1* expression pattern using the transactivation system (Moore et al. 1998) at 15DAG. No major alterations are observed in the vascular system of 15DAG hypocotyl of *AS1>>AtHB8-∂miR* (D) and *AS1>>PHV-∂miR* (E). Adult plants expressing *AS1>>AtHB8-∂miR* (G) and *AS1>>AtHB15-∂miR* (H) presented normal to reduced size (arrowhead) compared to untransformed Ler plants (F). Cabbage-like structures develop on the abaxial surface of *AS1>>AtHB8-∂miR* (I). Sections D and E were stained with toludine blue. The scale bars represent 1mm in A,B,C,N; 100µm in D,E and 1cm in F,G,H.

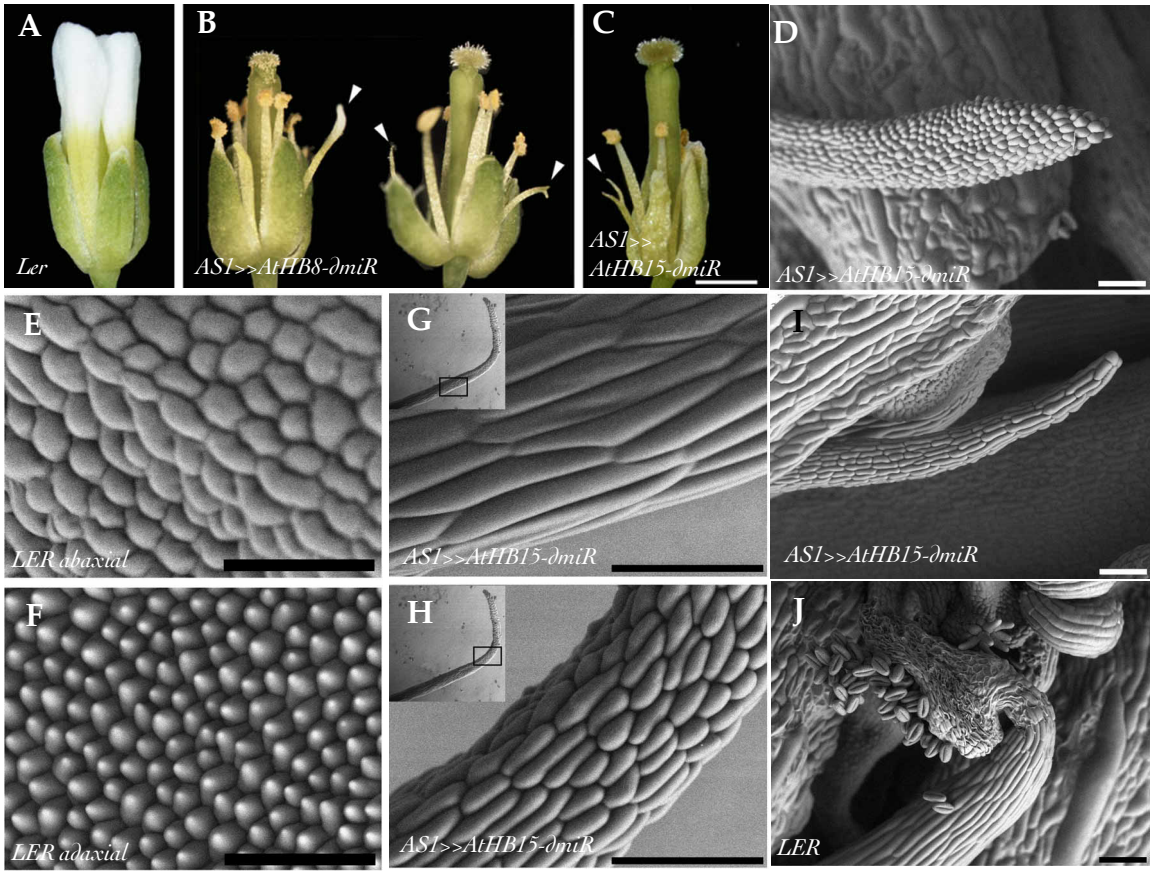


**Figure 2.12: Phenotype of *AS1>>AtHB8-∂miR* and *AS1>>AtHB15-∂miR* flowers.** Flowers of plants expressing *AtHB8-∂miR* (B) and *AtHB15-∂miR* (C) in the *AS1* expression pattern presented reduced to radialized petals (arrowhead) compared to wild type (A). Epidermis of control petals (E,F) and stamens (J) was compared to the epidermis of radial (G-I) or near radial (D) *AS1>>AtHB15-∂miR* petals by scanning electron microscopy. Abaxial (E) and adaxial (I) side of control petal. Proximal (G) and distal (H) epidermis of *AS1>>AtHB15* radialized petal. The scale bar represents 1mm in A-C and 50µm in D-J.

## 2.2 Influence of reduction of class III HD-ZIP transcription factors in preprocambium cells on the development of the vascular system

In the previous sub-chapter I have described the effects of an ectopic presence of class III HD-ZIP transcription factors on plant development. Frequently, the different class III HD-ZIPs triggered the same alterations in development. Increased numbers of differentiated xylem cells in hypocotyl and organ radialization were the most common alterations. However, even when class III HD-ZIP transcription factors were expressed in the pattern of *REV*, no major remodelling of the vascular system occurred, suggesting a possible saturation of this family of transcription factors in the vascular system. In a complementary approach and in order to further characterize the effects of class III HD-ZIP transcription factors on vascular system differentiation, I reduced their expression in preprocambium cells. To do so, I expressed miR165 or KAN1 under the control of the AtHB15 promoter.

### *2.2.1* Expression of MIR165 in the AtHB15 expression pattern

To reduce class III HD-ZIP levels in the vascular system, I expressed the *miR165* pre-miRNA in the *AtHB15* pattern as class III HD-ZIPs are post-transcriptionally regulated by miRNA genes *miR165* and *miR166* (Jones-Rhoades et al., 2003; Tang et al., 2003; Emery et al., 2003; Mallory et al., 2004; Kim et al., 2005; Williams et al., 2005; Alvarez et al., 2006; Jung and Park, 2007) Plants expressing p*AtHB15*-LhG4 were crossed with plants expressing 10Op::miR165 (*AtHB15>>miR165)*.

The *AtHB15* mRNA level in *AtHB15>>miR165* seedlings was slightly reduced (Figure 2.13). Thus the transactivation system was considered to be functional. This was further supported by the similarity of phenotype between multiple null class III HD-ZIP mutants (Prigge et al., 2005) and *AtHB15>>miR165*, suggesting a general reduction of class III HD-ZIP mRNA levels.

Compared to controls (Figure 2.14 A), cotyledons and leaves were epinastic (curved downward); a reduced stature was observed and petals were radialized (Figure 2.14 B,C). To observe the effects of reduced class III HD-

ZIPs in procambium cells, hypocotyl and stem sections were made. *ATHB15>>miR165* seedlings developed an altered vascular system as most vascular cells displayed characteristics of cambium or parenchyma cells in the hypocotyl. Size of the stele and the total number of cells in the stele were increased (Figure 2.14 H) compared to controls (Figure 2.14 D). To ascertain the identity of this altered vascular tissue, xylem and phloem specific markers were monitored. *ATHB8::GUS* signal, used here as a marker of active procambium and protoxylem cells, was localized in the pericycle, cambium and developing xylem elements in controls (Figure 2.14 F). In *AtHB15>>miR165* hypocotyls, the *AtHB8::GUS* reporter highlighted the central region of the stele as procambium and protoxylem (Figure 2.14 I). Thus, *AtHB8* promoter was active in proportionally more cells than controls. Although the intensity of signal should not directly be correlated with promoter activity, it was lower in all control plants (n=5+5) suggesting a stronger activity of the *AtHB8* promoter in *AtHB15>>miR165*. As less mature xylem cells were present in the vascular system but the region with procambium and protoxylem identity was enlarged, diminution of HD-ZIPs in procambium resulted in a multiplication of this tissue. These observations support a model where, class III HD-ZIP trigger xylem differentiation. On the other hand, phloem appeared to be unaffected by diminution of class III HD-ZIPs in the procambium as the activity of the *APL* promoter was similar in controls and *AtHB15>>miR165* plants. In both cases, the *APL::GUS* signal was limited to phloem cells, as well as cambium and pericycle cells flanking the phloem (Figure 2.14 G,J main). In cotyledons, phloem cells also appeared unaltered by the reduced level of class III HD-ZIP as a similar expression pattern of the *APL* promoter was observed in controls and *AtHB15>>miR165* cotyledons (Figure 2.12 G,J insert). However, the xylem organization was disturbed in cotyledons as indicated by the discontinuity of the *AtHB8::GUS* signal (Figure 2.12 F,I insert). This absence of at least one of the actors of protoxylem activity correlated with a discontinuity in xylem elements in cotyledons (data not shown) and in leaves (Figure 2.14 M,N arrowhead). In *ATHB15>>miR165* inflorescence stems, cells with differentiated xylem and phloem characteristics were present, but the bilateral symmetry between phloem and xylem was abolished (Figure 2.14 L) compared to controls (Figure 2.14 K). Cambium centers were multiplied and dispatched in the stele. They

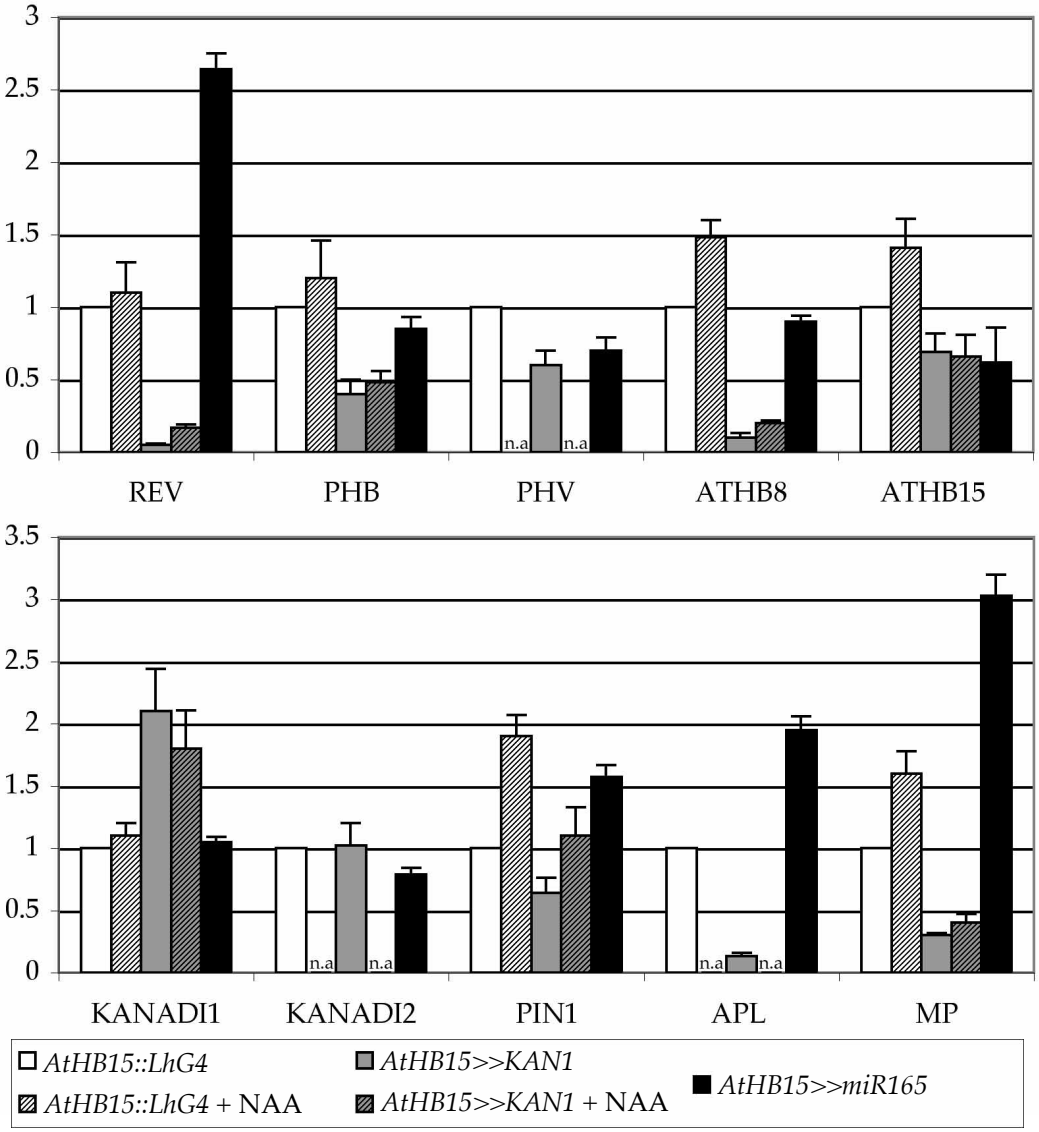


**Figure 2.13: mRNA quantifications of genes involved in vascular tissue differentiation by real-time RT-PCR in *AtHB15>>KAN1* and *AtHB15>>miR165* plants.** Total RNA of seedlings was extracted 15 days after germination. The expression level of each gene in *AtHB15::LhG4* control was set to 1. The ribosomal *S16* gene was used as reference gene. Measurements were performed in triplicates. One representative experiment of 3 to 5 replicates was shown. Where indicated, seedlings were incubated with auxin for 2 hours. NAA treatment, primers and amplification conditions are described in the material and methods section.

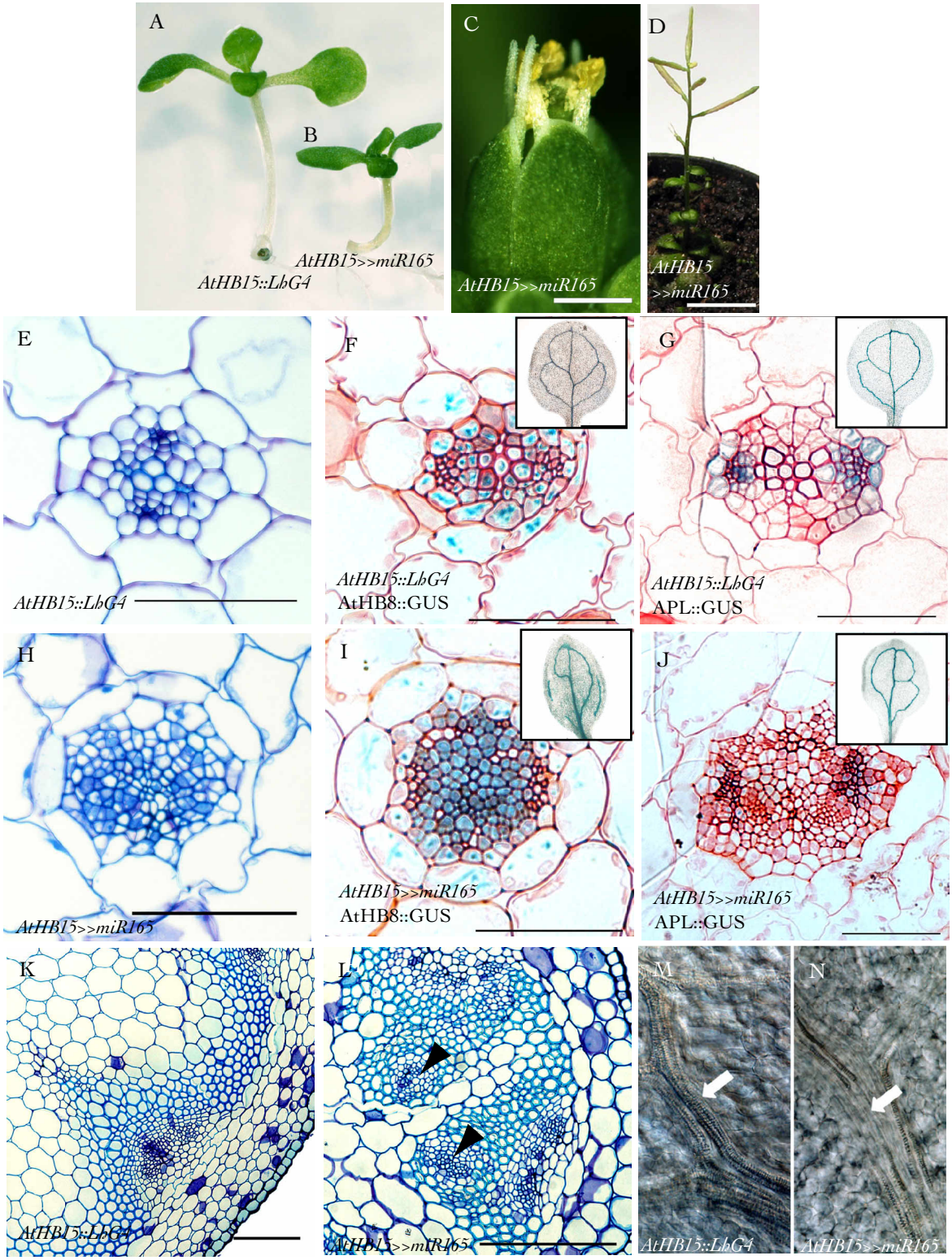


**Figure 2.14: Expression of *miR165* in the *AtHB15* expression pattern.** *miR165* was expressed in the AtHB15 expression pattern using the transactivation system (Moore et al. 1998). Plants expressing *AtHB15>>miR165* (B,C,D,H-K,N) are compared to control plants (A,E-G,K,M). 15DAG seedlings (A,B). Flower (C) and adult phenotype (D) of *AtHB15>>miR165*. In 15 DAG seedlings (E-J), xylem fails to differentiate in *AtHB15>>miR165* (H) compared to control (E). The *AtHB8::GUS* marker was active in procambial cells of control, in the central region of the hypocotyl vascular system (F) and delimited the vascular system of cotyledons (F, insert). In *AtHB15>>miR165* seedlings, *AtHB8::GUS* signal was present in a similar but enlarged zone of the hypocotyl vascular system (I) and was discontinuous in the cotyledon vasculature (I, insert). The *APL::GUS* marker of phloem cells was active in two border of the vascular system of the hypocotyl of controls (G) and *AtHB15>>miR165* (J) seedlings. The *APL::GUS* marker was active in the vascular system of cotyledons of controls (G, insert) and *AtHB15>>miR165* (J, insert). In adult inflorescence stems, organisation of vascular bundles was altered as amphivasal regions (arrowhead) were present near the vascular bundles of *AtHB15>>miR165* (L) compared to controls (K). Xylem strands are discontinuous in *AtHB15>>miR165* leaves (N, arrowhead) compared to controls (M). 5µm transverse sections were stained with safranine orange (F,G,I,J main) or toludine blue (E,H,K,L). Scale bar is 1cm in D, 1mm in C, 100µm in K,L and 50µm in E-J.

formed in some places radialized regions where xylem surrounded companion cells and parenchyma.

To correlate these observations with the ectopic expression of *miR165*, the activity of the *AtHB15* promoter was monitored. This control was also required as altered levels of class III could influence *AtHB15* promoter activity. The use of the *AtHB15>>GFP* construct allowed to observe the activity domains of the *AtHB15* promoter in control (Figure 2.15 A,B,C) and *AtHB15>>miR165* plants (Figure 2.15 D,E,F). In control heart stage embryo, the *AtHB15>>GFP* signal was present in the inner cells of the apical-basal central axis, in the inner cells of the future cotyledons, in the cells surrounding the future shoot apex. Note that signal was fainter in the basal part of the embryo (Figure 2.15 D). In mature embryo, the procambial cells were marked as well as the region of the future hydathodes at the tip of the cotyledons. A faint signal is also present at the site of the shoot apex (Figure 2.15 E). In *AtHB15>>miR165* embryos, the expression pattern of *AtHB15* appeared to be generally enlarged compared to controls (Figure 2.15 A,B). Signal in the central region of the heart stage embryo was brighter. The hypocotyl vasculature, as well as the shoot apex, was strongly marked. In cotyledons, the typical vein pattering was reduced to the central and adjacent veins. No GFP signal was present at the site of the hydathodes. These observations ruled out that an indirect inhibitory effect of *miR165* affected the *AtHB15* promoter activity. However, while in the stele of 15DAG seedlings (Figure 2.15 C,F), the *AtHB15>>GFP* signal was clearly confined to cambium and protoxylem in controls, it was patchy in *AtHB15>>miR165* hypocotyls. In later stages, the *AtHB15* promoter activity, and thus the ectopic presence of *miR165*, differed from the promoter activity of *AtHB8* (Figure 2.14 I).

As the establishment of the vascular system is linked with the presence of auxin, the distribution of auxin was monitored with the DR5::GFP construct. In mature embryo *DR5::GFP* signal is visible in the procambium and at the tip of the cotyledons, root and shoot meristem. In the hypocotyl, two distinct strands are visible (Figure 2.15 H, arrow). In *AtHB15>>mirR165* mature embryo, *DR5::GFP* signal was only different from control in hypocotyl as additional strands were visible (Figure 2.15 K, arrow). In 15DAG control hypocotyls, *DR5::GFP* signal fill an approximate cylinder delimited by the pericycle cells, leaving only the xylem cell without signal (Figure 2.15 I). The

DR5 signal was also visible at the tip of the root and two distinct strands were extending along the entire root length (Figure 2.15 G). In 15DAG *AtHB15>>miR165* seedlings, the wider *DR5::GFP* signal in the vascular system of the hypocotyl was conserved (Figure 2.15 L) and no clear absence of signal in the middle was observed as in developed xylem of control. The auxin presence also lost its clear distribution in two distinct strands in the roots of seedlings (Figure 2.15 G,J). Thus, the reduction of class III HD-ZIP transcription factors in procambium cells correlates with a more diffuse presence of auxin in vascular regions.

As differences between the *AtHB15* and *AtHB8* promoter activity were observed, expression rates of the class III HD-ZIPs and other marker genes of vascular system development were monitored by real-time PCR (Figure 2.13). Quantification of Class III HD-ZIP mRNA levels in 15 DAG seedlings showed that *PHB* and *PHV* levels were reduced in *AtHB15>>miR165* plants. As suggested by the non-superposition of the *AtHB8* and *AtHB15* expression pattern, *AtHB8* mRNA levels remained stable. Expression levels of *REV* were more than doubled. Although activity of the *APL* promoter appeared normal (Figure 2.14 G,J), its expression level was increased in *AtHB15>>miR165* plants. Genes with auxin-dependant expression, *MP* and *PIN1* presented an increased mRNA level. *KAN1* expression was not changed and *KAN2* expression was slightly reduced suggesting a moderate to non-existent alteration of abaxial identity (Figure 2.13).

As it was hypothesized that class III HD-ZIP transcription factors could substitute for one another, 10OP::*AtHB8-∂mir* was used to rescue the phenotype of *AtHB15>>miR165*. Thus, a 10OP::*AtHB8-∂miR* homozygous plant was crossed to an heterozygous *AtHB15>>miR165* plant. No seedling of the F0 generation presented a *AtHB15>>miR165* phenotype (n=300). Seeds issued from the auto fecundation of 30 F0 plants were harvested. No plants of the F1 generation presented offspring with a *AtHB15>>miR165* phenotype. As one quarter of the F1 generation could generate this phenotype, it was improbable not to encounter it ($p<0,05$). The 10OP::*miR165* was suggested to have been lost.

In conclusion, reduced levels of Class III HD-ZIP expression in preprocambium cells favored cambium cell formation and decreased xylem differentiation, whereas arrangement and differentiation of phloem cells were

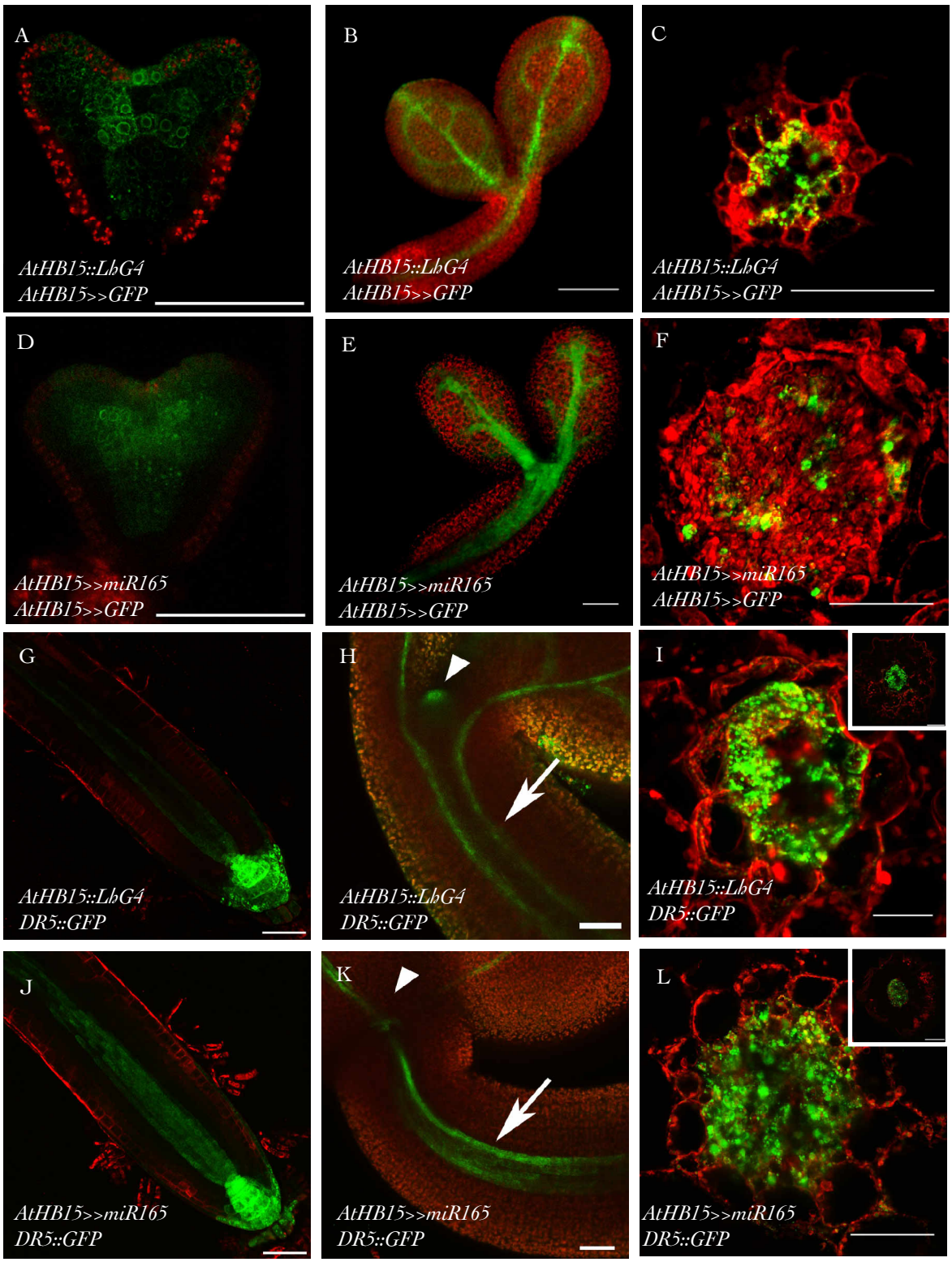


**Figure 2.15: Expression of *miR165* in the *AtHB15* expression pattern (2).** Analysis of the *AtHB15* promoter expression pattern with the *AtHB15>>GFP* construct by confocal microscopy (A-F) in controls (A-C) and *AtHB15>>miR165* (D-F). The *AtHB15* pattern in *AtHB15>>miR165* was enlarged in heart-stage (D) and mature embryo (E) compared to controls (A,B). The *AtHB15>>GFP* signal was patchy in the hypocotyl stem of 15DAG *AtHB15>>miR165* seedlings (F) compared to controls (C). Visualisation of the auxin responsive *DR5::GFP* by confocal microscopy (G-L). 15DAG root tip (J), hypocotyl of mature embryo (K) and 15DAG seedling vascular system of the hypocotyl (L) of *AtHB15>>miR165* presented larger DR5 responsive regions than controls (G,H,I). Arrowhead indicates apical meristem (H,K). Arrows indicated vascular system of the hypocotyl (H,K). Confocal microscopy with GFP signal in green (A-L), chlorophyll autofluorescence in red (A,B,D,E,H,K) and 0,33% (v/v) FM 4-64 dye (C,F,G,I,J,L) in red. Scale bar is 25µm in A-F,H,I,K,L and 50µm in G,J.

not directly influenced. In addition, expanded domains of cambium cells had stimulating effects on promoter activity of Class III HD-ZIP genes.

### 2.2.2 Correct localization of KANADI1 is necessary for the establishment of the vascular system.

The reduction of class III HD-ZIP expression in the vascular system by *miR165* led to the reduction of differentiated xylem cells and the proliferation of procambial tissue. However, the reduction of class III HD-ZIPs provoked by *miR165* was not total as *AtHB15* mRNA was still detectable. In an attempt to have a severe reduction of class III HD-ZIP transcription factors in the procambium, *KAN1* was expressed in the expression pattern of the *AtHB15* promoter. While the function of *miR165* is limited to reduce class III HD-ZIPs, KAN1 has additional functions. Combined with the indications provided by *AtHB15>>miR165* plants, it will allow to gain additional insights on the interplay of *KAN1* and class III HD-ZIPs in the development of the early vascular system.

Ectopic expression of *KAN1* in procambium cells was made using the transactivation system. (Moore et al., 1998). *AtHB15* (*AtHB15::LhG4*) was combined to the cDNA sequence of *KAN1* (*10Op::KAN1*) resulting in *AtHB15>>KAN1*plants. Activity of the system was confirmed by real-time PCR as *KAN1* mRNA levels were more elevated in *AtHB15>>KAN1* seedlings than in controls (Figure 2.13). The *KAN1* expression in the *AtHB15* pattern affected early developmental stages of vascular tissue formation, as seedlings formed no vascular tissue in the hypocotyl (Figure 2.16 C) and root (data not shown). As for *AtHB15>>miR165*, effects of procambial *KAN1* expression were not limited to the vasculature. Meristems were poorly formed as the SAM was nearly absent and no root growth was observed. Seedling phenotype was variable as needle-like, heart-shaped and seedlings with more than two cotyledons were observed (Figure 2.16 A). These observations suggest that KAN1 affects early embryonic development when expressed in the *AtHB15* pattern. The establishment of the SAM in early embryonic development is dependant on a peak in auxin concentration (Hardtke et al., 2004). Thus, the effect of *AtHB15>>KAN1* on embryonic auxin flux was studied by Dr. Pia Stieger (See annexe 1).

### 2.2.3 Auxin and undifferentiated vascular tissue

To determine if precursor cells of cambium, phloem and xylem were formed in *ATHB15>>KAN1* plants, expression patterns of representative genes of precursor cells were monitored with the GUS marker. Where, in control seedlings the *AtHB8::GUS* and *APL::GUS* signal totally overlapped vascular system (Figure 2.16 D,F), in *AtHB15>>KAN1* the *AtHB8* and *APL* promoters were only active in very limited regions of the seedling (Figure 2.16 E,G). In an attempt to evaluate the possible cause of the loss of vascular tissue in *AtHB15>>KAN1* plants, the mRNA levels of several developmental genes were assayed in *AtHB15>>KAN1*. All class III HD-ZIP mRNA levels were reduced in *AtHB15>>KAN1* transformants (Figure 2.13). While in *AtHB15>>miR165* plants, *AtHB8* and *REV* were stable or up regulated, they were the most reduced class III HD ZIPs in *AtHB15>>KAN1* seedlings. To verify that the up regulation of *KAN1* was not due to a secondary effect, but to the ectopic expression driven by the AtHB15 promoter, another member of the *KANADI* family was assayed: *KAN2* expression remained stable. As suggested by the monitoring of *APL::GUS*, *APL* expression was reduced by ectopic *KAN1* expression. To assess the effect of *KAN1* expression on other abaxial genes, *FIL1* expression was tested. It appears that *KAN1* expression in the vascular system does not induce *FIL1* expression ($FIL_{expression}$=0,35 ± 0,03). However, without a localization of *FIL1* mRNA, it is not possible to evaluate if this reduction is due to the reduction of the SAM in *AtHB15>>KAN1*. As *PIN1* and *MP* were also negatively affected in AtHB15>>KAN1 seedlings, this suggests that KAN1 acts negatively on early steps of vasculature differentiation.

It was previously shown that class III HD-ZIP expression level could be up-regulated by the addition of an ectopic source of auxin (Baima et al., 1995; Zhou et al., 2007). To verify if external addition of auxin was sufficient to restore vascular system activity in AtHB15>>KAN1 seedlings, we incubated wt and *AtHB15>>KAN1* 15DAG seedlings for 3h in 50 mM NAA and quantified mRNA levels of class III HD-ZIP genes, *MP*, *PIN1*, *APL* and *KAN* genes (Figure 2.13). In wt seedlings, externally applied NAA moderately increased the expression levels of *ATHB8* and *ATHB15*, whereas *REV* and *PHB* were not influenced by the treatment. *PIN1* and *MP* were induced by NAA, as

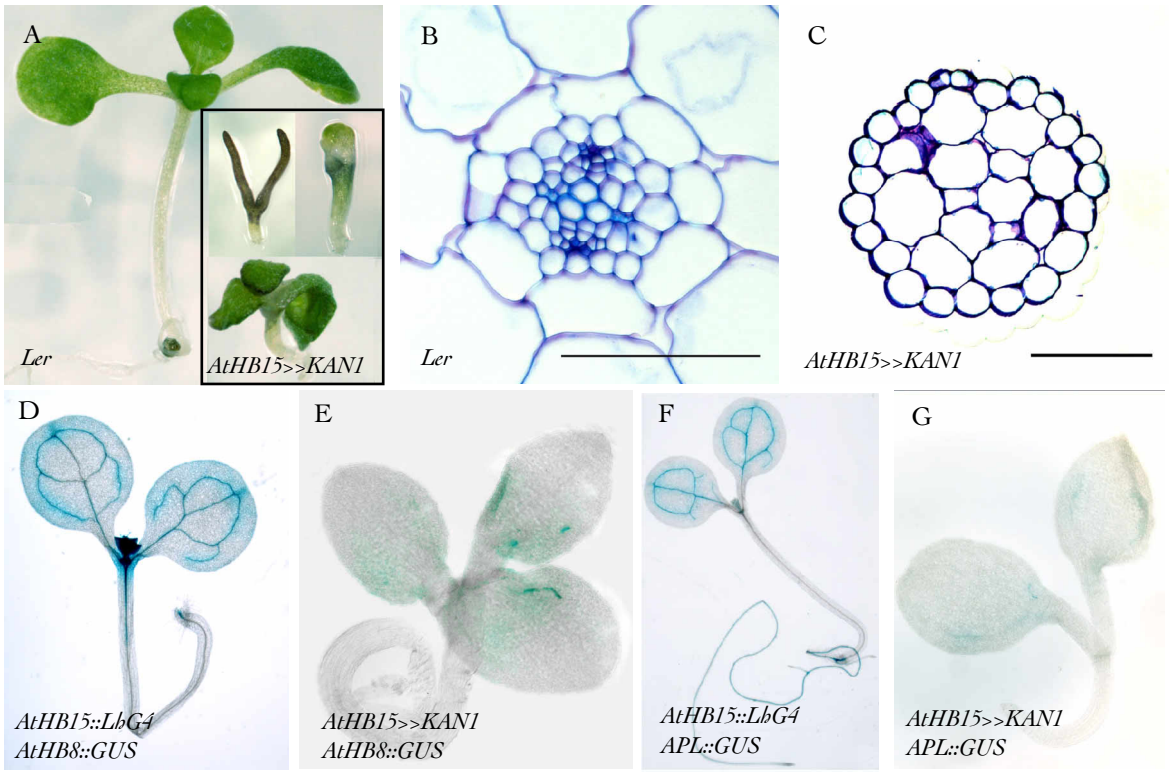


**Figure 2.16: Ectopic expression of *KAN1* in the *AtHB15* expression pattern.** *KAN1* was expressed in the *AtHB15* expression pattern using the transactivation system (Moore et al. 1998). 15DAG seedlings (A-E). (A) Comparison between the Ler (A) and *AtHB15>>KAN1* (A, insert) seedling phenotype. Transversal sections of *Ler* (B) and *AtHB15>>KAN1* (C) hypocotyls. Expression pattern of AtHB8 in *AtHB15::LhG4* (D) and *AtHB15>>KAN1* (E). Expression pattern of *APL* in *AtHB15::LhG4* (D) and *AtHB15>>KAN1* (E). Sections (B,C) were stained with Toludine blue 0,1% (w/v). The scale bar is 100µm in B and C.

previously published (Okada et al., 1991; Przemeck et al., 1996). Although NAA treatments could not restore wt levels of *AtHB8* and *AtHB15* in *AtHB15>>KAN1* seedlings, an increase in mRNA content of the two genes was observed after the treatment with NAA. A similar increase was observed for *PIN1.* Non-significant variations were observed for *PHB* and *MP* expression levels. Given the limited effects that auxin had on class III HD-ZIP promoter activities in *ATHB15>>KAN1* seedlings lacking a vascular system, we conclude that additional factors present in cambium cells might be necessary to maintain Class III HD-ZIP expression levels in addition to auxin.

### 2.2.4 Reduction of class III HD-ZIPs in the *PHV* expression pattern

The ectopic expression of class III HD ZIPs had a minor effect on the development of the vascular system (see chapter 2.1). On the other hand, *miR165* expression in procambium resulted in major alterations of the vasculature. To observe if a reduced level of class III HD-ZIP would also affect leaf development and meristem maintenance, *miR165* was expressed in the regions delimited by the *PHV* promoter.

The *PHV>>miR165* plants were generated by crossing the p*PHV*-LhG4 expressing plant line to the 10Op::*miR165* expressing plant line. The expression of *PHV* is limited to the adaxial side of cotyledons and shoot meristem with a faint expression in the central axis compared to the procambial expression of *AtHB15* (Prigge et al., 2005). Thus, it was not unexpected to observe less severe alteration in *PHV>>miR165* (Figure 2.7 B) at the level of hypocotyl vasculature than in *AtHB15>>miR165* plants (Figure 2.14 H). Differentiated xylem was reduced compared to control (arrowhead) and the area delimited by the endodermis was smaller. Comparably to *AtHB15>>miR165*, cotyledons were epinastic (Figure 2.17 A). Trichomas were scarcer than controls (data not shown). Leaves were partially abaxialized with trumpet morphology (Figure 2.17 A) as in *rev-6 phv-11* mutant (Prigge *et al.* 2005). This comparison support that class III HD-ZIPs were reduced in the *PHV>>miR165* plants. Hand-cut cross section of the inflorescence stem revealed that *PHV>>miR165* adult plants presented amphivasal vascular bundles (Figure 2.17 C, arrow head). Moreover, in the observed stems (n=3), the vast majority of vascular bundles were amphivasal for only a few

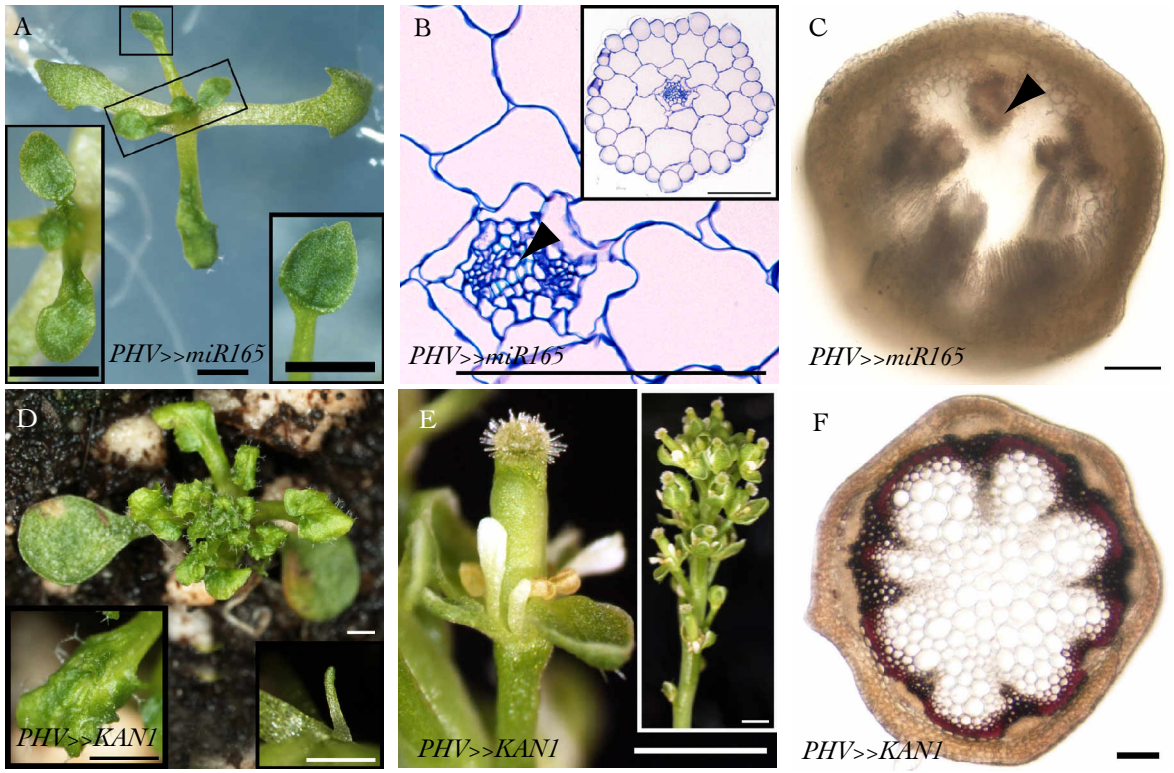


**Figure 2.17: Ectopic expression of *miR165* and *KAN1* in the *PHV* expression pattern.** *miR165* (A,B,C) and *KAN1* (D,E,F) were expressed in the *PHV* expression pattern using the transactivation system (Moore et al. 1998). 15DAG *PHV>>miR165* seedlings presented epinastic cotyledons (A) with partially abaxialized leaves (A, inserts). Hypocotyl cross-section of 15DAG *PHV>>miR165* stained with toludine blue (B). Xylem cells are indicated with arrowheads. *PHV>>miR165* inflorescence stems presented amphivasal vascular bundles (C, arrowhead). 30 DAG *PHV>>KAN1* plants (D) presented radialized first leaves (right insert) and an intermediately radialized leaf phenotype with ectopic growth on the adaxial side (left insert). Flowers of *PHV>>KAN1* plants presented reduced sepals, petals and stamens (E). *PHV>>KAN1* inflorescence stems (F) presented no major alteration compared to controls (Figure 2.4 K). Hand-cut stem sections (C,F) were stained with phloroglucinol. Scale bar is 1mm in A,C,D,E,F and 100µm in B.

presenting a bilateral symmetry. Similar amphivasal structures were observed in *AtHB15>>miR165* (Figure 2.14 L) and *rev-10d* (Figure 2.10 A). To summarize, reduction of class III HD-ZIP in the *PHV* pattern by *miR165* leads to different alterations in the vasculature of seedlings compared to *AtHB15>>miR*. However, in adults, similar alterations are observed in the vasculature.

To further differentiate the *AtHB15* and *PHV* pattern and to determine the interplay of these two pattern on vascular differentiation, *KAN1* was expressed in the *PHV* pattern (*PHV>>KAN1*). Seedlings of *PHV>>KAN1* plants presented a normal cotyledon and development, however the first two leaves were perfectly radialized (Figure 2.17 D). As no trichomes were observed on the first two leaves, an abaxialization of the tissue was suspected (Figure 2.17 D, right insert). The following leaves were not radialized, but abaxial region was extended and leaf surface was irregular (Figure 2.17 D and figure 2.17 D, left insert). Ageing flowers were present on the inflorescence stem instead of maturing siliques suggesting that flowers were not fecunded (Figure 2.17 E). Flowers presented a normal organization, but sepals, petals and carpel were of reduced size. Moreover, stamen stalks did not develop and are thus a possible source of infertility. *PHV>>KAN* plants developed an inflorescence stem vascular system that presented the general features of a control (Figure 2.17 F).

It appears that reduction of class III HD-ZIP in the *PHV* pattern by *miRNAs* induced important alterations at the level of the vascular system. On the other hand, *KAN1* expression in the same pattern was far less deleterious for the vascular system but affected leaf and flower shape.

## 2.3 AtHB8 antibody

In a context where post-transcriptional regulation is common, the ability to monitor the amount of proteins is important. Anti-AtHB8 antibodies were generated using a peptide with a sequence unique to *AtHB8*. However, although only a single band was recognized in a total protein extract of *Arabidopsis* seedlings (data not shown), this protein was also detected in the athb8-11 T-DNA mutant (Prigge et al., 2005) protein extract. *AtHB8* mRNA levels of athb8-11 were quantified by real-time PCR relative to untransformed

*Arabidopsis* ($AtHB8_{expression} = 1.00 \pm 0,08$) and no amplification of AtHB8 mRNA occurred ($AtHB8_{expression} = 0,00 \pm 0,00$). Therefore, antibodies against AtHB8, were not used.

# Chapter 3

# Discussion

## 3.1 Redundant functions of class III HD-ZIP proteins

It is known since 2001 that the transcription factor AtHB8 plays a role in the production of xylem (Baima et al., 2001). Since then, it has been shown that class III HD-ZIP transcription factors are regulated post-transcriptionally by miRNA. Evidence of post-transcriptional regulation derived from studies of dominant mutants with point mutations in the miR165/166 site of *REV*, *PHV*, *PHB* and *AtHB15* (McConnell et al., 2001; Emery et al., 2003; Ochando et al., 2006). In the present work, *AtHB8* with a dominant mutation in the *miR* binding site allowed the analysis of miRNA regulation for this class III HD-ZIP transcription factor. Indeed, *AtHB8::AtHB8-∂miR* plants presented slight alterations in the formation of secondary xylem compared to control plants. This confirmed the involvement of the *AtHB8* transcription factor in the differentiation of the vasculature and suggests post-transcriptional regulation by miRNAs. However, besides those differences, no conspicuous phenotype alteration was observed, in strong contrast to the other class III HD-ZIP gain-of-function mutants (McConnell et al., 2001; Emery et al., 2003; Ochando et al., 2006). As *AtHB8* is the only class III HD-ZIP transcription factor not expressed in globular embryos (Prigge et al., 2005), it can be postulated that a late expression during embryogenesis is responsible for the lack of strong morphological alterations of young seedlings. In adult plants, *AtHB8* expression is confined to the vascular system (Baima et al., 1995), thus there is no change in leaf and shoot morphology. Additionally to a limited expression

in time and space, the number of copies produced by the promoter might be an issue. The lack of phenotypical alterations in *AtHB8>>KAN1* plants also supports a model where *AtHB8* expression is late compared to *AtHB15* or *PHV* (data not shown). Considering that differences in the development of the xylem are observed between *AtHB8::AtHB8* and *AtHB8::AtHB8-∂miR* expressing plants and that products of *AtHB8* mRNA cleavage are detected in *Arabidopsis* (Mallory et al., 2004), one may postulate that *AtHB8* is post-transcriptionally regulated by miRNAs *in planta* and that this regulation allows the maturation of xylem cells. To confirm that the lack of major phenotypical alterations in *AtHB8::AtHB8-∂miR* plants is due to the late and restricted expression pattern of *AtHB8*, two experiments could be done to enhance phenotypical differences between *AtHB8::AtHB8-∂miR* and controls. In a first experiment, exposition of *AtHB8::AtHB8-∂miR* plants to phytohormones such as auxin (Baima et al., 1995) or brassinosteroids (Ohashi-Ito et al., 2002) could induce more severe phenotypes. Alternatively, observations of *AtHB8::AtHB8-∂miR* and control plants grown under short day conditions for a prolonged period might also highlight differences in secondary xylem growth (Chaffey et al., 2002).

In this work, plants constitutively expressing *AtHB8* displayed a similar phenotype as previously described, namely hyponastic leaves, altered xylem differentiation and palisadic parenchyma (Baima et al., 2001). Although *AtHB8* mRNA quantification done in the present work could not be directly compared to the work of Baima and colleagues, a higher mRNA level in the plants analyzed in this study could account for the phenotype of petals specifically observed here. Indeed, this alteration was reduced in lines with lower *AtHB8* expression. In parallel, plants constitutively expressing *AtHB15* were characterized and the mRNA of *AtHB15* was quantified (Figure 2.4). Interestingly, a similar phenotype to 35S::*AtHB8* was observed. However, Kim and coworkers (Kim et al., 2005) observed no noticeable morphological alterations in plants with constitutive expression of *AtHB15.* Thus, constitutive expression of either *AtHB8* or *AtHB15* leads to similar phenotypes, suggesting that both transcription factors have a redundant function. Moreover, plants over-expressing both *AtHB8* and *AtHB15* presented a phenotype comparable to parent plants, further strengthening the hypothesis that AtHB8 and AtHB15 have similar functions and not different functions leading to a similar

phenotype. It can then be postulated that the recent duplication of the ancestor gene of *AtHB8* and *AtHB15* (Floyd *et al.*, 2006; Prigge & Clark, 2006) led to more significant differences in the promoter regions than in the function of their proteic domains.

It was at first surprising that constitutive expression of *AtHB8* and *AtHB15*, two vascular specific genes, resulted in important morphological modifications in leaves, but only limited alterations in the vascular system. Plants with a moderate over-expression of *AtHB15-∂miR* presented reduced primary and secondary xylem in addition to a leaf phenotype (Kim et al., 2005). One can thus suppose that a tightly controlled regulation mechanism of *AtHB8* and *AtHB15* occurs within the vasculature, most likely via miRNAs and little zippers. In contrast, it seems that this regulation is less severe in leaves. Actually, the low levels of *miR165/166* measured within leaves (Jung & Park, 2007) might account for the hyponastic leaves of 35S::*AtHB8* and 35S::*AtHB15* plants. Thus, ectopic presence of *AtHB8* or *AtHB15* in the leaf blade induces the formation of hyponastic leaves. An interesting fact is that the *hyl1* mutant also presents hyponastic rosette leaves (Lu & Fedoroff, 2000). *HYL1* is involved in the miRNA pathway (Han et al., 2004; Vazquez et al., 2004). HYL1 was also shown to be a regulator of *miR165* and to be expressed in the vascular tissues and near leaf margins (Yu et al., 2005). One can suppose that the levels of *AtHB8* and *AtHB15* mRNA are too high in *35S::AtHB8* and *35S::AtHB15* plants for complete post-transcriptional regulation leading to a similar phenotype as the *hyl1* mutant.

A difference in the petals morphology was observed between 35S::*AtHB15* and 35S::*AtHB8* plants, as petals were hyponastic in the later one. The only *miR* targeting class III HD-ZIPs expressed in petals is *miR166g* (Jung & Park, 2007). Thus, petal hyponasty in 35S::*AtHB15* expressing plants could be prevented by *miR166g*, since constitutive expression of *miR166* has been shown to reduce *AtHB15* more efficiently than *AtHB8* due to sequence variations in the miR target site between *AtHB8* and *AtHB15* (Figure 1.4 B) (Kim et al., 2005; Williams et al., 2005; Alvarez et al., 2006; Zhou et al., 2007).

Further analysis of the regulation of *AtHB15* and *AtHB8* by *miRNAs* was performed by constitutively expressing *AtHB8-∂miR* and *AtHB15-∂miR*. Those plants presented major morphological alterations, demonstrating that *AtHB8* and *AtHB15* transcripts of *35S::AtHB8* and *35S::AtHB15* plants are post-

transcriptionaly regulated by miRNAs. The very limited number of transformants obtained suggests that a constitutive expression of class III HD-ZIPs with a point mutation in the miRNA binding site might be lethal for the embryo. However, this affirmation is difficult to demonstrate with the set-up used in this work. A 35S>>*AtHB15/8-∂miR* experiment or the use of an inducible constitutive promoter would allow answering this question.

The radialized leaf phenotype of 35S::*AtHB15-∂miR* and 35S::*AtHB8-∂miR* seedlings was highly similar to the corresponding 35S::*ICU4*-G189D phenotype (Ochando et al., 2006). These data further support the model where both transcription factors elicit the same targets. These observations also suggest that, when expressed in other regions than the vasculature, for instance in the *AS1* pattern, *AtHB8* and *AtHB15* can induce adaxialization of organs like the other class III HD-ZIP transcription factors. Although not as directly comparable as the *PHV>>AtHB8-∂miR* plants, 35S::*AtHB8-∂miR* and 35S::*AtHB15-∂miR* seedlings presented phenotypes highly similar to the *phv-1d* mutant. Furthermore *PHB-∂miR* could also phenocopy *phv-1d,* when expressed in the *PHV* pattern, suggesting a similar proteic function for PHB, PHV, AtHB8 and AtHB15. The fact that the *icu4-1* mutant and *AtHB8::AtHB8-∂miR* plants presented less severe alterations than *phv-1d, phb-1d* or *rev-10d*, is probably due to a more restricted expression pattern. This proposition was confirmed by the expression of *AtHB15>>PHB-∂miR* presenting alterations comparable to *icu4-1*. The expression of *AtHB8* in the *AtHB15* pattern led to similar observations supporting the hypothesis of redundancy between protein functions of some class III HD-ZIPs.

It should be noted that Ochando and coworkers did not observe formation of trumpet-shaped leaves and ectopic tissues on leaves in dominant *athb15* mutant, as it was observed for *AtHB15>>AtHB8-∂miR* and *AtHB15>>PHB-∂miR* (Ochando et al., 2006). Different *Arabidopsis* ecotypes, *En-2* v.s. *Ler*, and the supplementary gene copy induced by ectopic expression might explain these differences. To support this explanation, important variations of phenotypes caused by the constitutive expressions of *AtHB15* with point mutation in the miRNA site were observed in different laboratories (Kim et al., 2005; Ochando et al., 2006). As shown for homo- or heterozygous *icu4-1* (Ochando et al., 2006), the amount of transcription factor influences the degree of leaf adaxialization gradually from slightly upward, to severely up rolled,

from severely up rolled to trumpet-shaped, from trumpet shaped to radialized. Differences were also observed between 10Op::*AtHB8-∂miR* lines inducing light or severe alterations when activated by promoter lines such as *REV::LhG4*.

The experiments carried in this work lead to the conclusion that the class III HD-ZIP transcriptions factors AtHB8, AtHB15, PHB and PHV have roughly the same functions, gradation effects taken into account. It seems, however, that another member of this family, REV, has a different function. Indeed, *REV>>AtHB8-∂mir* could not phenocopy the gain-of-function *rev-10d* mutant. The formation of amphivasal vascular bundles seems to be specific to the ectopic expression of *REV*. In others organs such as flowers and first leaves, it appears that expression of *AtHB8-∂miR* in the *REV* pattern also induces different phenotypical changes than *rev-10d.* The REV loss-of-function mutant, *rev-6*, supports the hypothesis of a difference between REV and other class III HD-ZIP, as *rev-6* is the only class III HD-ZIP mutant that presents alterations (Prigge et al., 2005). However, the absence of a *REV>>REV-∂miR* positive control phenocopying *rev-10d* does not exclude that the unique *REV*::Lhg4 line used here does not exactly reproduce the *REV* pattern. The pattern delimited by the *REV>>GUS* constructs is coherent, however it's not possible to directly compare it to the *REV* pattern due to the lack of a complement to the *miR165* sequence in the *GUS* sequence.

The current observations do not interfere with previous complementation experiments where the expression of *PHB*, *PHV*, *AtHB15* and *AtHB8* in the *rev-6* mutant did not complement the mutant phenotype (Prigge et al., 2005). Moreover, rescue of the *phv-phb-athb15-athb8* quadruple mutant phenotype by constitutive expression of class III HD-ZIPs with the CaMV promoter was the least efficient with the *REV* sequence (Prigge et al., 2005).

On the other hand, phylogenetic comparisons between class III HD-ZIP and their ancestor genes indicated an alternative grouping among this family. From the single gene present in the land plant ancestor, it appeared that two clades are present in *Arabidopsis*: The REV clade including *REV, PHB* and *PHV* and the CNA clade including *AtHB8* and *AtHB15* (Floyd *et al.*, 2006; Prigge & Clark, 2006). These phylogenic alignements of amino acid sequences would suggest a closer relation between functions of members of the same clade. As functional domains are not included in alignment algorithms, it remains

possible that all class III HD-ZIPs have the same general functionality. And that the difference between REV and the other members of the gene family is due to the deletion occurring between the amino acids 143-149. The four additional consecutive amino acids in the MELKHA domain of REV could also be involved in the functional variability of class III HD-ZIPs (Figure 1.5 A). As the moss ancestor of class III HD-ZIP, *PpHB10,* could not complement the *rev* mutant phenotype (Prigge & Clark, 2006), it remains possible that *REV* has functional domains that recently diverged. A similar approach as in the present work, expressing *PpHB10* in the *PHV* pattern could bring answers to this question. In this optic, it was suggested that class III HD-ZIP ancestors regulated vascular tissue differentiation, embryo patterning and meristem size restriction and that *REV* function switched and has now a positive effect on meristem size (Prigge & Clark, 2006). It was also mentioned that *AtHB8* lost his function in meristem size restriction and embryo patterning. In regard of the present result, it could then be postulated that the divergeance of the *REV* function originates from amino acid varations in functional domains of the protein, while the divergeance of the *AtHB8* gene originates from its pattern of expression. Sequence alignments involving precise domains, such as the DNA binding region, could provide additional insights on the question.

Redundant phenotypes were observed between plants expressing *AtHB8* and *AtHB15* constitutively. Constitutive or *AS1* pattern specific expression of *AtHB8-∂miR* and *AtHB15-∂miR* induced similar alterations in the plant. When compared in the *PHV* and *AtHB15* expression pattern, gain-of-function *AtHB8* and *PHB* also induced similar alterations in plant morphology. These alterations were comparable to the dominant *phv* and *athb15* mutant. Altogether these results suggest that the AtHB8 transcription factor regulates similar downstream genes as the other transcription factors tested in the same pattern. Moreover, dominant class III HD-ZIP mutants could be phenocopied. Thus, these several evidences strongly suggest that class III HD-ZIP transcription factors AtHB8, AtHB15, PHV and PHB can be exchanged to substitute each other.

## 3.2 Class III HD-ZIP transcription factors in the vasculature

An increase of metaxylem cells and a change in their size and shape in *AtHB8::AtHB8-∂miR* inflorescence stems suggested that a prolonged exposition to AtHB8 favours the multiplication of secondary xylem. Indeed, an increased number of young secondary xylem cells was observed in the cambium region compared to control plants, confirming that *AtHB8* is a positive regulator of vascular cell differentiation (Baima et al., 2001). It remains however unclear whether secondary xylem is produced more rapidly in the presence of AtHB8, or if AtHB8 retards the differentiation into metaxylem. A double effect is also possible. In the vascular system of *AtHB15>>AtHB8-∂miR* hypocotyl, an increased number of xylem cells were formed. It therefore can be postulated that *AtHB8* induces early steps of xylem differentiation. In parallel to this, 35S::*AtHB8* plants produce more secondary xylem cells than control plants. This has also been observed in the *Columbia* ecotype (Baima et al., 2001). Thus, the presence of *AtHB8-∂miR* in vascular tissue seems to induce similar effects on vascular development as constitutive presence of *AtHB8*. The supplementary amount of *AtHB8* mRNA and proteins in 35S::AtHB8 procambial cells, could saturate the regulators of *AtHB8* activity leading to a similar phenotype as *AtHB8::AtHB8-∂miR* in the vascular system. The hypocotyl sections of *AtHB15>>PHB-∂miR* suggested that PHV may induce a similar effect as *AtHB8* on xylem differentiations. Comparison of inflorescence stem sections of *AtHB8>>PHB-∂miR* and *AtHB8::AtHB8-∂miR* plants should allow to verify this affirmation. On the other hand, the limited differences observed between control and plants with ectopic *AtHB8* expression could originate from another event than saturation. As more *AtHB8* should be present in the cells, it remains possible that the transcription factor was not active. The START domain present in all HD-ZIP proteins could require a binding molecule to activate the transcription factor. This event could also be required to allow translocation to the nucleus. One appealing hypothesis is that auxin or BRs are the binding molecule, implying that one of the plant hormone has to be present to activate the transcription factor.

Secondary wall deposition controlled by *SND1* was shown not to influence *AtHB8* expression (Zhong et al., 2006). It would be interesting to monitor the influence of *AtHB8* on expression levels of *SND1* and other NAC-domain

transcription factors involved in wood formation, in order to assess if *AtHB8* acts upstream of these transcription factors in the process of secondary wall deposition. I have also observed enlarged phloem cap cells in *AtHB8::AtHB8-∂miR* plants. The same phenotype was previously described for plants lacking one or more BR receptors (Cano-Delgado et al., 2004). Thus, AtHB8 could regulate maturation of xylem cells via the brassinosteroid signaling pathway.

It was not possible to assess individual functions of class III HD-ZIPs in the differentiation of the vasculature in *AtHB15>>miR165* plants. Indeed, levels of the different class III HD-ZIPs varied. In these plants, multiplication of cambial tissues correlated with a broader auxin distribution and with high mRNA levels of *REV* and *AtHB8*. Accumulation of auxin was previously shown to generate high cambium activity (Galweiler et al., 1998; Mattsson et al., 1999; Pineau et al., 2005). In *AtHB15>>miR165* plants, the larger distribution of auxin could originate from higher numbers of cambial and parenchymatic cells present in the vascular system in which auxin is transported. Alternatively, early imbalance in auxin localization might result from dis-regulation of *DRN* and *DRNL* proteins. *DRN* and *DRNL* have a negative effect on ARFs and auxin transport during embryogenesis (Chandler et al., 2007; Nag et al., 2007). Thus the reduced interaction of DRN and DRNL with class III HD-ZIP transcription factors might alter their regulating activity.

Interestingly, xylem vascular island in cotyledons of *AtHB15>>miR165* plants resemble strikingly xylem vascular islands in *scarface/van3* (*sfc*) mutants (Koizumi et al., 2005). *SCF/VAN3*, an ADP ribosylation factor GTP-ase activating protein, is involved in auxin-related intracellular membrane trafficking. Thus, we can speculate that the presence of class III HD-ZIPs could be required for proper *SCF/VAN3* signaling in xylem-differentiating cells.

*AtHB15>>miR165* plants displayed an enlarged auxin distribution, increased vascular cambium activities and high levels of *REV* mRNA. In comparison, auxin distribution and *AtHB8* and *REV* mRNA levels were reduced in the *AtHB15>>KAN1* plants, which systematically lack a vascular system. In addition, when auxin was ectopically added to *AtHB15>>KAN1* plants, *REV* were more significantly up regulated than other class III HD-ZIP transcription factors. This suggests that *REV* and *AtHB8* play a major role among class III HD-ZIPs in cambial tissue identity and response to auxin signals.

The exact role of *AtHB15* remains difficult to evaluate in *AtHB15>>miR165* and *AtHB15>>KAN1* plants as *AtHB15* mRNA levels were moderately affected. It is known that *miR166* affects more severely *AtHB15, PHV* and *PHB* than *AtHB8* and *REV* (Kim et al., 2005; Williams et al., 2005). Thus, a complementary experiment with ectopic *miR166* in procambial cells might give further insights on the role of *AtHB15.* It must however not be forgotten that positive or negative feedback regulations between class III HD-ZIPs might affect the interpretation of the results (Prigge et al., 2005; Williams et al., 2005).

It was observed that *AtHB8-∂miR* expression in the *REV* pattern could not phenocopy the amphivasal vascular bundles of the gof *rev-10d* mutant. However, amphivasal vascular bundles were present in the inflorescence stem of *AtHB15>>miR165* plants. It is likely that the amphivasal vascular bundles observed in *AtHB15>>miR165* inflorescence stems are due to the elevated level of *REV* mRNA. The same phenomenon was observed in *PHV>>miR165* (Figure 2.16) and *AS1>>miR165* plants (data not shown). However, *REV* mRNA was not quantified in these last two cases. As class III HD-ZIP transcription factors were suggested to influence one another expression (Prigge et al., 2005), one can postulate that ectopic *miR165* could reduce one of the class III HD-ZIPs more than the others. Without the regulation by the other class III HD-ZIPs and with a different expression pattern *REV* could be up-regulated in *PHV*/*AtHB15>>miR165* plants. Unfortunately, *REV>>miR165* plants were not fully grown up at the present time to confirm this hypothesis. If this hypothesis is correct, *REV>>miR165* plants should not present amphivasal vascular bundles in the inflorescence stem.

*AtHB15>>miR165* plants presented the advantage to affect only genes containing the *miR165* complementary sequence expressed in the procambium, while in *AtHB15>>KAN1* plants the formation of the vascular system was inhibited. The interplay of auxin, *KAN* and class III HD-ZIPs is discussed with supplementary data in the manuscript presented in annexe 1.

To summarize, *AtHB8* appears to promote the differentiation of (pro)cambium into xylem. As the *athb8* mutant presents no visible phenotype (Baima et al., 2001), other signals must act redundantly in this role. Other class III HD-ZIPs, such as *AtHB15,* are potential candidates for this function as their ectopic expression induced similar effects as the ectopic *AtHB8* expression. The fact

that *AtHB15>>miR165* had an important effect on vascular development also support this hypothesis. It should also be taken into account that co-regulators such as ZPRs, or the lack of available downstream targets, will affect the effects of class III HD-ZIP in the vascular system.

## 3.3 Class III HD-ZIPs in radial and proximodistal development

The establishment of a dorsoventral axis of polarity within organ primordia is necessary for a correct development of the lamina. One of the signals defining this polarity, PHB, is present in the SAM and young primordia, and is gradually limited to the adaxial region of young leaves. High PHB concentrations lead to a radial expansion of the tissue, as observed in the dominant *phb-1d* mutants. The presence of PHB, and also PHV, is determinant for adaxial identity of developing leaves. In the present study, we showed that *AtHB8-∂miR*, when expressed in the *PHV* pattern, generates identical adaxial features as the *phv-1d* mutant. Furthermore, *AtHB8-∂miR*, when expressed in the *AS1* or *REV* patterns, generated adaxialisation of the tissues. The effects of the AtHB8 transcription factor are therefore not limited to vascular tissue differentiation but can also influences lateral organ polarity, as *PHV* and *PHB*, when present in the same pattern. AtHB15 might have similar characteristics. Indeed, it induces similar flower phenotype as AtHB8 while expressed in the *AS1* pattern. Petals are also an important organ for abaxial-adaxial interplay. Plants with floral ectopic expression of *KAN2* present cubic epidermal cells in adaxial parts of the petal, normally only found in abaxial parts of petals (Pekker et al., 2005).

When the epidermis of plants with radialized features, such as *PHV>>AtHB8-∂miR*, is compared to the epidermis of control plants, similarities were observed between different organ parts. The epidermis of the petiole, a tissue with near radial features, was comparable to the epidermis at the base of the leaf of *PHV>>AtHB8-∂miR* or *PHV>>PHB-∂miR* plants. The epidermis of the radialized petals of *AS1>>AtHB15-∂miR* flowers is comparable to the epidermis of stamen stalk (Figure 2.12). To develop naturally radialized organs, such as stamens and petioles, plants could rely on class III HD-ZIPs. Supporting this hypothesis, the expression pattern of *PHV* in flowers is accentuated in stamen stalks (Figure 2.5). Very few alterations were observed

in stamens in plants with high class III HD-ZIPs levels, suggesting that this class of transcription factors could already be in saturation within stamens. It is therefore likely that class III HD-ZIPs are involved in the formation of the radial shape of the stamen stalk. The role of *KAN* genes in stamen stalks should also be determined, as microarray data indicates their presence. However, *PHV>>KAN1* plants present no stamen stalk (Figure 2.16) suggesting that class III HD-ZIPs are the genes involved in the regulation of radial stamen stalk formation. A further support for this hypothesis is that the stamens of *kan1kan2kan3kan4* mutants are not altered (Figure 2.10P). However, as the *miR166a* and *miR166g* expression patterns (Jung & Park, 2007) seem to overlap with the *PHV* expression pattern, the stability of class III HD-ZIP mRNA should be assayed. The first leaves of *PHV>>miR165*, have an abaxialized phenotype only in the region adjacent to the SAM, therby suggesting that the *PHV* expression is linked with the petiole region.
Altogether, these data and previous publications on *REV* (Emery et al., 2003) indicate that all class III HD-ZIP transcription factors can determine adaxial identity. Moreover, the present observations suggest that the plant uses class III HD-ZIPs to define organs that are naturally radial such as stamen stalks and petioles.

## 3.4 The *KANADI*-class III HD-ZIP interplay

### 3.4.1 Multiple cotyledons

Beside radialized organs, plants with increased or decreased levels of class III HD-ZIP transcription factors had abnormal numbers of cotyledons. Two to four cotyledons were formed in *REV>>AtHB8-∂miR* plants. One to four cotyledons were present in *AtHB15>>KAN1* plants. In *AtHB15>>miR165* plants, the vast majority of seedlings presented 2 cotyledons, but 3 cotyledons were also sporadically observed. Although *KAN1* and *AtHB8* are known to have antagoniststic functions, a direct link between the *REV>>AtHB8-∂miR* and *AtHB15>>KAN1* cotyledon phenotypes is difficult to establish, as the expression patterns of *REV* and *AtHB15* are not exactly overlapping. The formation of two cotyledons at the end of the globular stage of the embryo requires the establishment of a boundary region adjacent to the SAM. Correct patterning of the *CUC1*, *CUC2* and *STM* genes delimiting this region is

determined by auxin (Aida et al., 1999; Furutani et al., 2004; Heisler et al., 2005; Treml et al., 2005). Concordantly, two mutants of proteins involved in auxin transport, *pin1* and *pid,* were reported to present more than two cotyledons (Okada et al., 1991; Bennett et al., 1995). In *AtHB15>>KAN1* plants, the activity of PIN1 was reduced (Figure 2.13) (data not shown), suggesting a role for *KAN1* in PIN1 expression. As AtHB8 might limit *KAN1* expression at the periphery of the developing SAM of *REV>>AtHB8-∂miR* embryos, PIN1 might be repartitioned in a larger area, leading to disorganized auxin accumulation and, in turn, leading to an unstable number of cotyledons. Alternatively, class III HD-ZIP could have a stimulating effect on auxin transport while present in the developing SAM.

In a third option, the variations in cotyledon numbers might rely on DRN-class III HD-ZIP interactions. Indeed, *drn* mutants also present unstable numbers of cotyledons (Chandler et al. 2007). The interaction of AtHB8 on DRN might have an inactivating effect on DRN, leading to a similar effect on cotyledon separation. However, this option is less likely, as REV also binds to DRN and the dominant mutant *rev-10d* does not present multiple cotyledons.

### 3.4.2 Ectopic laminar growth and altered floral development

Additional evidence of an interaction between *KANADI* and *AtHB8* was given by ectopic expression of *AtHB8-∂miR*. Indeed, the expression of *AtHB8-∂miR* in patterns tested in this work often induced ectopic growth of laminar tissues. Ectopic tissue growth has been reported in several cases, including *kan* mutants like *kan1kan2kan4*, *kan1kan2* or *kan1kan2kan3* (Figure 2.7 K) (Eshed et al., 2001; Eshed et al., 2004), and appears to be linked with the expression of the *YAB* gene family. The stable mRNA quantity of the *YAB* gene, *FIL,* in *AtHB15>>AtHB8-∂miR* plants, does not allow us to conclude that the outgrowth originated from altered *YAB* expression. It should be noted that while the laminar outgrowth in *kan1kan2* were nearly radial and linked with a strong *FIL* expression, outgrowth linked with ectopic class III HD-ZIP expression were rather cabbage-shaped. Thereby, at this point of the experiment, the presence of outgrowths on *AtHB15>>AtHB8-∂miR* leaves cannot be explained by variations in *KAN* or *YAB* levels. Quantification of

*KAN1*, *KAN2* and *FIL* mRNA in isolated *AtHB15>>AtHB8-∂miR* leaf outgrowth would be a first step to determine the tissue origin.

Identically, the inflorescences of *REV>>AtHB8-∂miR* (Figure 2.10 I,J,K) presented a similar, but not perfectly matching, morphology to *kan1kan2kan3kan4* inflorescences (Figure 2.10 N,O,P). The constitutive expression of gain-of-function *AtHB15* also led to flowers with filamentous properties (Ochando et al., 2006). Higher concentrations of class III HD-ZIPs in the floral region, either resulting from ectopic expression of class III HD-ZIPs or reduced presence of their antagonists, leads to an adaxialisation of floral organs. In the case of *REV>>AtHB8-∂miR*, all floral organs are radialized. Due to the special conformation of the floral organs, it is difficult to affirm whether or noteach flower organ is present in these plants. If the *REV>>AtHB8-∂miR* flower had to be entered into the traditional ABC floral model (Bowman *et al.*, 1989; 1991), the best option would be an *AGAMOUS1* (*AG1*) gene repression with an overlapping adaxial component. The *ag1* mutant presents flowers with stamens converted into petals and carpels replaced by a new flower with similar alterations (Bowman et al., 1989). AG1 inhibits stem cell maintenance in flower meristem to induce floral differentiation (Lenhard et al., 2001; Lohmann et al., 2001). As all floral organs acquire a radialized petal morphology in *REV>>AtHB8-∂miR* plants, it is clear that class III HD-ZIPS have to be tightly regulated by by miRNAs in flowers to develop their final shape (Jung & Park, 2007). On the other hand, a reduction of class III HD-ZIPs also lead to flowers with filamentous properties (Alvarez et al., 2006).

The exact interactions between class III HD-ZIPs and KANADIs during laminar growth and flower development are not established here. However, comparison between plants with ectopic *AtHB8-∂miR* expression and *kan* mutants suggest that a tightly controlled presence of class III HD-ZIPs is required for proper floral identity.

## 3.5 Concluding remarks

The results discussed presented new insights on the roles of class III HD-ZIPs in the establishment of the vascular system and in the formation of adaxial tissues in lateral organs. In particular, the expression of a gain-of-function sequence of *AtHB8* allowed identifying post-transcriptional regulation of

AtHB8 by *miR165/166*. This allows the vascular system to have a correct timing of metaxylem differentiation in adult *Arabidopsis*. Moreover, the function of AtHB8 is similar to the function of PHV,PHB and AtHB15, as it was possible to copy their gain-of-function mutant phenotype with ectopic *AtHB8-∂miR* expression. This observation was repeated with the ectopic expression of *AtHB15-∂miR* and *PHB-∂miR* as they induced comparable alterations as *AtHB8-∂miR*. Therefore, it was postulated that these four class III HD-ZIPs genes differ from one another only at the level of expression pattern and post-transcriptional regulation. ,During evolution, the duplication events that generated this family of genes allowed the activation of different sets of downstream pathways by acquiring new expression patterns.

# Chapter 4
# Material and Methods

## 4.1 Materials

### 4.1.1 Biological material

**Arabidopsis**
Wild type (wt) *Arabidopsis* plant always refers to *Arabidopsis thaliana* Landsberg Erecta (*Ler*). Plant transformations for AtHB15 and AtHB8 constructs were made in the *Ler* background. The plants containing the promoter part of the transactivation system, *pAtHB15::LhG4*, *pPHV::LhG4*, *pREV::LhG4* and *pAS1::LhG4*, are gifts from Prof. J. Bowman (Monash University, Melbourne) andProf. Y. Eshed (Weizmann Institute, Israel). Sequences were amplified from *Colombia* DNA and cloned into the binary *pMLBART* vectors to generate p*AtHB15*-LhG4-BJ36, p*PHV*-LhG4-BJ36, p*REV*-LhG4-BJ36 and p*AS1*-LhG4-BJ36 constructs as described by Eshed *et al.* 2001. Plants containing the operator region of the transactivation system, 10Op::*ATHB15-∂miR*-BJ36, 10Op::*PHB-∂miR*-BJ36, 10Op::*ATHB15*-BJ36, 10Op::*KANADI1*-BJ36, 10Op::*miR165*-BJ36, 10Op::*GUS*-BJ36 and 10Op::*GFP*-BJ36 are gifts from Prof. J. Bowman and Prof. Y. Eshed and are described in Eshed *et al.* 2001. *kan1kan2kan4*, *kan1kan2kan3kan4* and *rev-10d* mutants are gift from Prof. J. Bowman (Monash University, Melbourne). 10Op-*ATHB8-∂miR*-BJ36 and 10Op-*ATHB8*-BJ36 lines were generated by Dr. P. Stieger (Université de Neuchâtel, Switzerland). *PIN1:PIN1-GFP* and *DR5rev:GFP* plants (Columbia Background) are a gift from Prof. J. Friml (University of Gent, Belgium). *AtHB8::GUS* plants are a gift from Dr. S. Baima (Unità di Nutrizione

Sperimentale, Rome, Italy). *APL::GUS* plants are a gift from Prof. Y Helariutta (Plant Molecular Biology Laboratory, University of Helsinki, Finland). T-DNA insertion lines N6969 (*athb8-11*) and SALK-017186 (*athb15)* from the SALK collection were obtained from the Nottingham Arabidopsis Stock Centre (Scholl et al., 2000). *Landsberg erecta (Ler) At* transformed with the pMLBART-AtHB8::AtHB8-∂miR or pMLBART-AtHB8::AtHB8 plasmid were obtained from Prof J. Bowman (Monash University, Melbourne). The *AtHB8* promoter used here corresponds to the upstream UTR region of the *AtHB8* gene up to the previous gene coding sequence (~5'000bp). The AtHB8 coding sequence of the construct was cloned from cDNA.

**Micro-organisms**

*Escherichia coli* DH5-α were from Invitrogen and *E. coli* BL21(DE3) cells were from Novagen. *Agrobacterium tumefaciens*, strain C58 was kindly provided by Dr. Roger Kuhn (Institute of Plant Sciences, ETH Zurich, Switzerland).

### 4.1.2 Oligonucleotides

Oligonucleotides were synthesized at Microsynth GmbH. *AtHB15* for real time PCR: 5′- TCC TGC AGG ACT TTT GTC AT –3′ / 5′- CAA TCT GCA ACC TGT A –3′; *AtHB8* for real time PCR: 5′- CTA GTC CTG CTG GAT TAT TG –3′ / 5′-GGA TCT CCG CGA CCC TTG GT –3′; *REV* for real time PCR: 5′-CGA ATA GTC CTG GAT TG-3′ / 5′-GAT CTC TGC AAT CTT CAT AG-3′. *KAN2* for real time PCR: 5′- GCA GCT TCG TCA GGA CAA TC-3′ / 5′- TCT CCGGAA GAA TTG GTC CA –3′. QuantiTect Primer Assay (Qiagen, USA) primers were used for the following real-time PCR reactions: QT00774634 (*S16*); QT00846440 (*REV*); QT00716583 (*PHB*); QT00870877 (*PHV*); QT00879179 (*AtHB15*); QT00830802 (*KANADI1*); QT00723954 (*FIL*); QT00892654 (*PIN1*); QT00744926 (*APL*); QT00861847 (*MP*); QT00774634 (*ACTIN2*).

### 4.1.3 Plasmids

pMLBART AtHB8::AtHB8, pMLBART AtHB8::AtHB8-∂miR, PCR2.1 AtHB15 and PCR2.1 AtHB15-∂miR were kindly provided by Prof. J. Bowman. pMLBART AtHB8 is a pMLBART derivative containing the AtHB8 sequence amplified from cDNA. pMLBART AtHB8-∂miR is identical to pMLBART

AtHB8 except for a point mutation in the putative miRNA binding site (Figure 1.4 B). pCR2.1 AtHB15-∂miR is a pCR2.1 vector derivative (Invitrogen, CA, USA) containing the AtHB15 sequence amplified from cDNA. PCR2.1 AtHB15gof is identical to pCR2.1 AtHB15wt with a point mutation in the miRNA binding site (Figure 1.4 B).

pCAMBIA3300 were obtained from CAMBIA. pCHF5 was kindly provided by Prof. C. Frankhauser (Center for Integrative Genomics, University of Lausanne, Switzerland). pCHF5 is a pCAMBIA3300 derivative with the cauliflower mosaic virus (CaMV) 35S promoter and the RuBisCO small subunit terminator flanking the multiple cloning site. pET21d-H6 was provided by Dr. C. Bréhélin (Laboratoire de physiologie Végétale, Université de Neuchâtel, Switzerland). pET21d-H6 is a pET21d (Novagen) derivative with a six histidin tag flanking the multiple cloning site.

### 4.1.4 Chemicals

Unless stated otherwise, chemicals were purchased from Fluka Chemie GmbH.

### 4.1.5 Antibodies

Antibodies specific to the chlorophyll a/b binding protein (CAB) were kindly provided by Dr. K. Apel (Institute of Plant Sciences, ETH Zurich, Switzerland). Anti-AtHB8 antibodies are described below.

### 4.1.6 Peptides

A 16 amino-acid long peptide $H_2N$-VGS RTA GDS CGS RGN S–$CONH_2$, unique to *AtHB8* was synthetized by Eurogentech.

## 4.2 Methods

### 4.2.1 Physiological methods

#### *A. thaliana* growth conditions

Seeds were surface sterilised by ethanol treatment. Seeds were immerged for 5 min in 70% ethanol under agitation. In sterile conditions, ethanol 70% was

replaced by ethanol 100% for 15 additional min under agitation. Seeds were then dried in sterile conditions on 55mm filter paper circles (Whatman GmbH, Dassel, Germany) and spread on 0.8% (w/v) Phyto Agar (Durchefa) plates containing 0.5x Murashige and Skoog medium (MS; Duchefa) and 0.8% (w/v) sucrose. Germination was synchronized by exposing the seeds for 2 days at 4°C in the dark. Seeds were then grown under short-day conditions (8h light 120 $\mu$mol $m^{-2}/s^{-1}$, 16h dark; 21°C) for 15 days in a CU-36L6D Percival growth chamber (CLF Plant Climatics). Seedlings were then transferred on sandy soil (Top Dressing, Ricoter) in Quickpots (ihort) pots in a PGL-6HID Percival growth chamber (CLF Plant Climatics) in the same condition for an additional 15 days. Plants were then transferred into a long day (16h light 120 $\mu$mol $m^{-2}/s^{-1}$, 8h dark; 21°C) culture room. To facilitate seed collection when needed, AraSystem (BetaTech bvba) was used.

**Selection of herbicide resistant plants**

For selection of phosphinothricin-resistant plants, 30 $\mu$g/ml phosphinothricin (BASTA; Duchefa) was added to the plate media. For selection of kanamycin-resistant plants, 50 $\mu$g/ml kanamycin sulfate (Fluka) was added to the plate media. 15 days after germination, resistant and sensitive plants were counted.

**Plant breeding**

Petals and stamens of flowers, which had not yet released pollen from their anthers were removed and the carpel was pollinated with pollen of interest, using a Nikon SMZ 1000 binocular and marked. Siliques were harvested after 2-3 weeks or opened after 4 (globular embryo) to 10 (mature embryo) days for observation with a confocal microscope, as described in section 4.2.7.

**Count of vascular bundles**

Vascular bundles and protoxylem strands were counted on hand-made transversal sections of the basis of about 10 cm high shoots. Plants were observed between 40 and 45 DAG. Diameter of the stem was measured with a Caliper CCMA 150 (Etalon, Switzerland).

**Auxin treatment**

Two-week-old *Arabidopsis* seedlings grown on Murashige and Skoog medium

were used for auxin treatments as described (Zhou *et al.*, 2007). The seedlings were laid on Murashige and Skoog medium (control), or Murashige and Skoog medium containing 50 $\mu$M naphthylacetic acid for 3 h. After the treatment, RNA was immediately extracted from entire seedlings, as described in section 4.2.12.

### 4.2.2 Methods for Molecular cloning

Standard protocols were used for cloning (Sambrook & Russell, 2001). DNA fragments were amplified using a proof-reading DNA polymerase *pfu* (Promega) and oligonucleotides including appropriate restriction sites in a ThermoHybaid PxE (Thermo) thermal cycler. Pre-existing plasmid-constructs were used as templates for PCR. PCR products and plasmids were digested (restriction enzymes from New England Biolabs or Promega) and purified from agarose gels using the QIAquick kit (Quiagen). Vectors were dephosphorylated using shrimp alkaline phosphatase (Roche) according to the manufacturer's recommendations. T4 DNA ligase (New England Biolabs) was used to ligate vectors and inserts as described (Sambrook & Russell, 2001). Ligation reactions were subsequently transformed by heat shock into competent *E. coli* DH5-$\alpha$ cells (Sambrook & Russell, 2001). Competent *E. coli* cells were prepared as described (Inoue et al., 1990). Selection was done on LB medium [25g/l LB Broth Miller (Becton Dickinson Diagnostic Systems), 1.2% (w/v) Agar Bacteriological Grade (ICN Biomedicals)] supplemented with appropriate antibiotics. Clones were selected by PCR and restriction digestion and DNA sequences were verified by sequencing (Microsynth GmbH).

### 4.2.3 Plasmid isolation and purification

For small-scale plasmid isolation, the GenElute Plasmid Miniprep Kit (Sigma) was used according to the supplier's instructions. The PureYield TM Plasmid Midiprep System (Promega) was used for plasmid isolation from 100 ml culture volume.

### 4.2.4 Stable transformation of Arabidopsis

**Constitutive expression of AtHB8**

The primers: 5′-tga cgg tca tgA TGG GAG GAG GAA GCA AT-3′ (includes BspHI) and 5′-agt act ccc ggg TAT AAA AGA CCA GTT GAG-3′ (includes SmaI) were used to amplify the AtHB8 and AtHB8-∂miR sequence from the pMLBART AtHB8 and pMLBART AtHB8-∂miR plasmids, respectively. The DNA fragment corresponding to AtHB8 was digested with BspHI and SmaI and ligated in the NcoI and SmaI site of pCAMBIA 3300, yielding pCAMBIA3300-AtHB8 and pCAMBIA3300-AtHB8-∂miR respectively. The resulting plasmids (Figure 2.2 A) and the original pCAMBIA 3300 vector were used to transform *Ler At* using the floral dip method.

**Constitutive expression of AtHB15**

The primers 5'- CGG gga tcc ATG GCA ATG TCT- 3' (include BamHI) and 5'-AGA gga tcc TCA CAC AAA GGA-3' (include BamHI) were used to amplify the AtHB15 and AtHB15-∂miR sequences by PCR from the pCR 2.1 AtHB15 and pCR 2.1 AtHB15-∂miR plasmids, respectively. The amplified DNA fragment was digested with BamHI and ligated in the BamHI site of pCHF5, yielding pCHF5-AtHB15 wt and pCHF5-AtHB15 gof respectively. The resulting plasmids (Figure 2.4 A) were used to transform *Ler At* using the floral dip method.

**Transformation of *Agrobacterium tumefaciens* by electroporation**

*A. tumafaciens*, strain C58 were grown in liquid YEB media [0.5% (w/v) Bacto-Trypton, 0.5% (w/v) Bacto-Pepton, 0.1% (w/v) yeast-extract (all from Difco), 2 mM $MgCl_2$] until an optical density (546nm) of 0.8 was achieved. Cells were pelleted (10 min, 4°C, 2'000g) and washed with a 10% glycerol solution. 50 ng plasmid DNA were used for electroporation in a MicroPulser (BioRad Laboratories) device, according to the manufacturer's instructions. Transformants were selected on YEB media supplemented with 1.2% (w/v) agar (bacteriological grade, ICN Biomedicals) and appropriate antibiotics.

**Arabidopsis transformation**

*A. thaliana* plants were transformed using the floral dip method (Bechthold *et al.*, 1993; Clough & Bent, 1998). Transformants were selected on plates containing phosphinothricin.

### 4.2.5 PCR on plant material

**DNA extraction**

DNA was prepared from leaf material using the simple DNA preparation method described on the University of Wisconsin Biotechnology Center Web site: http://www.biotech.wisc.edu. Approximately 20 seedlings or leaf tissue corresponding to 0.5 $cm^2$ was ground in 0.2 M Tris/HCl pH 9, 0.4 M LiCl, 25 mM EDTA, 1% (w/v) SDS. The homogenate was cleared by centrifugation (5 min, 16'000x g, 4°C), supplemented with an equal volume of isopropanol and centrifuged again (45 min, 16'000x g, RT). The supernatant was discarded and the DNA pellet was washed with 80% (v/v) ethanol. Finally, DNA was dried and resuspended in 50 µl TE (10 mM Tris/HCl pH 8, 1 mM EDTA).

**PCR analysis**

PCR reactions contained 2 µl DNA solution, 0.5 U GoTaq DNA polymerase and corresponding buffer (Promega), as well as 0.2 mM dNTPs (Eurobio) in a total volume of 25 µl.

The primer sets HB8 Fw1: 5'-GAA CAA TAC ACA AAA CGG-3' / HB8 Rv1: 5'-TAA GAC CGC GCT AGG CAT A-3' were used to detect wild type and intron-less *AtHB8.* The primer sets HB15 Fw3: 5'-TCC TGC AGG ACT TTT GTC AT-3' / HB15 Rv3: 5'-TCA CAG CTT GTG TCT TTA GCT-3' detect wild type and intron-less *AtHB15.* T-DNA insertions SALK-017186 (*athb15)* was detected using the LBpROK2 primer: 5'-TGG ACT CTT GTT CCA AAC TG-3' in combination HB15 Fw3. The PCR program was as follows: 2 min, 94°C, 37x (30 s, 94°C; 30 s, 50°C; 1 min, 72°C). PCR reactions were analyzed by agarose gel electrophoresis according to standard protocols (Sambrook & Russell, 2001).

### 4.2.6 Photography

Pictures of seedlings were taken with a SMZ 1000 Nikon binocular linked to a Nikon DS-L1-5M CCD camera. Whole plant pictures were taken with a Canon digital IXUS 400 camera.

### 4.2.7 Confocal microscopy

For DR5::GFP, AtHB15>>GFP, and PIN1::PIN1-GFP reporter detections, embryos were prepared out of ovules in 50% glycerol using a plastic pistil in a plastic microtube. An approximate volume of 25$\mu$l was used per preparation, the glycerol solution containing the embryos was distributed on a 76x26mm slide (Menzel-Gläser), and covered with a 24x50mm #1 coverslip (Menzel-Gläser). Hypocotyls of 15 day old seedlings were embedded in 3% agarose and 1-2 mm thick hand sections were made. Roots were mounted on a glass slide under a coverslip. FM 4-64 dye (Invitrogen) in 50% glycerol was added to fresh hypocotyl sections (1/3 v/v), and roots (1/40 v/v).. Samples were observed using a TCS SP5 (DM6000 B microscope, LAS AF software version 1.6.3 build 1163) confocal microscope (Leica). Images were treated in ImageJ.

### 4.2.8 Scanning electron microscopy

Samples were directly observed using a S-3500N Scanning electron microscope (Hitachi) with a Coolstage 20 add-on (Hitachi).

### 4.2.9 Optical microscopy for semi-thin sections

Hypocotyl, leaf and shoot sections were placed in a fixation solution [4% (v/v) formaldehyde (Polysciences Inc), 0,25% (v/v) glutaraldehyde in 50mM phosphate buffer pH7.2] for 2 hours in low vacuum conditions at room temperature and incubated at 4°C O/N. Subsequent dehydration of samples were made in the following conditions: Phosphate buffer (50 mM, pH 7.2) 30 min (2x); dd$H_2O$ 5 min (2x); 25% ethanol 10 min (2x); 50% ethanol 10 min (2x); 75% ethanol 10 min (2x); 85% ethanol 10 min (2x); 95% ethanol 10 min (2x); 100% ethanol 8 min (8x); additionally, this step was used for seedlings: eosin staining solution [0,1%(w/v) Y eosin (Sigma) in ethanol] for 3 hours. Samples were then embedded in Technovit 7100 (Heraeus, Germany) according to the

manufacturer's protocol and oriented in 6x6x14mm molds. 5$\mu$m sections were made with a Ultracut E (Reichert-Jung) microtome and laid in ddH2O on glass slides. 6mm glass (Plano GmbH) knives made with a 7809b knife maker (LKB) were used. Slides were dried O/N at 42°C. For staining, one of the following filtered dyes was used: toludine blue [0,1% (w/v) in 0,18% (v/v) 100mM citric acid, 0,82% (v/v) 100mM Nacitrate dihydrate pH 4.6] for 2 min at 42°C; safranine orange [0,1% (w/v) safranine O (Ciba) in ethanol] for 2 min at room temperature. Astra blue [2,5% (w/v) Astra blue in 50mM $NaPO_4$ pH 4.75] for 2 min at 42°C for safranine orange counter stain. Slides were then washed with ddH2O prior to an additional O/N drying at 42°C. An ethanol pre-wash was applied to samples stained only with safranine orange. Coverlids were mounted on the slides using Merckoglas® (Merck) solution. Sections were observed under a SMZ1000 light microscope (Nikon).
Unless annotated as preliminary, observations and measurements on semi-thin sections were made on 5-10 samples per condition. Observations of semi-thin sections annotated as preliminary include 2-3 different samples.

#### 4.2.10 Phloroglucinol staining

Stems were hand-cut with a razorblade and incubated for 3 min in a phloroglucinol solution [10% (w/v) ethanol]. Samples were then incubated for 1 min in concentrated HCl and transferred to a 50% glycerol solution (AppliChem) on a glass slide and covered with a coverlid. Samples were observed under a SMZ1000 light microscope (Nikon).

#### 4.2.11 GUS reaction

Histochemical 5-Bromo-4-Chloro-3-Indoxyl-β-D glucuronic acid (GUS) (biosynthag) staining of the seedling was performed as described in Koizumi *et al.*, 2000. After the reaction, samples were mounted on glass slides with a 50% glycerol solution (AppliChem) or dehydrated and embedded in Technovit 7100 (Heraeus, Germany) according to the manufacturer's protocol. 5$\mu$m sections of Technovit-embedded hypocotyls were stained with safranine orange solution. Samples were observed under a SMZ1000 light microscope (Nikon).

### 4.2.12 RNA purification

RNA from 15 day old seedlings was purified using the RNAeasy Plant mini kit (Qiagen) according to the manufacturer's protocol.

### 4.2.13 RNA migration

RNA quality was tested by RNA migration on electrophoresis gels. The RNA migration protocol follows the same procedure as described in 4.2.5 except that migration tank, combs and additional containers were treated for 20 min in a NaOH solution and reagents were autoclaved for 120 min. 0.5$\mu$g of sample were loaded per lane and migrated at 90-100mV.

### 4.2.14 Reverse transcription of RNA

Secondary RNA structures were denatured by incubating 1$\mu$g total RNA for 10 min at 65°C and reverse transcription was performed in the presence of 5$\mu$g oligo(dT)15-mers (Promega), 0.5 mM dNTPs, 200u moloney murine leukemia virus Reverse Transcriptase (Promega) according to the supplier's recommendations in a total volume of 25$\mu$l. All steps were carried out in the presence of RNasin RNase inhibitors (Promega). cDNA was subsequently diluted in a total volume of 477$\mu$l RNAse free dd$H_2O$ and 7,2 $\mu$l were used per PCR reaction.

### 4.2.15 Semi-quantitative RT-PCR

Standard PCR conditions (section 4.2.5) were used for semi-quantitative RT-PCR. The *ACTIN2* gene was used as control with the following set of primers: 5'-CAG CAG CAA TCG TGA TGA CTT GCC C-3' / 5'-GTT AGC AAC TGG GAT GAT ATG G-3'. The AtHB8-Fw1 and AtHB8-Rv1 primers were used for *AtHB8* quantification. The AtHB15-Fw3 and AtHB15-Rv3 primers were used for *AtHB15* quantification.

### 4.2.16 Real-time quantitative RT-PCR

Absolute SYBR Fluoroscein 1219 (ABgene) Solutions were transferred using MulTIGuard Barrier Tips (Sorenson) and appropriate pipettes (Gilson). 12x8 PCR plates (ABgene) and QPCR seal (ABgene) were used.

Real-time quantitative RT-PCR was performed with a iCycler iQ Real-Time PCR detection system (Bio-rad, Hercules, CA, USA), using Absolute SYBR Fluoroscein 1219 Green (ABgene, Epsom, Surrey, UK). The ribosomal *S16* gene was used as a standard control. Reactions were in triplicate in a 20 $\mu$L volume using 100 ng cDNA and 0.4 mM MgCl per reaction. Negative controls were in duplicate. QuantiTect Primer Assay (Qiagen) primers (section 4.1.2) were used according to manufacturer's protocol. Additionally, oligonucleotide probes (section 4.1.2) were used at a concentration of 0.5 $\mu$M. Sets of oligonucleotides were tested *in silico* (section 4.2.20), by melt-curve and dilution analysis. Solutions were transferred using MulTIGuard Barrier Tips (Sorenson) and appropriate pipettes (Gilson). 12x8 PCR plates (ABgene) and QPCR seal (ABgene) were used. Thermal cycling parameters were 95°C for 15 minutes, followed by 45 cycles at 95°C for 30 seconds, 59.7°C for 30 seconds and 45°C for 45 seconds. RT-PCR specificity was tested with melt-curve analysis and electrophoresis. Experiments were repeated 3 times.

### 4.2.17 Preparation of an anti-AtHB8 antibody

Two regions unique to *AtHB8* were amplified from pMLBART-AtHB8wt plasmid by PCR using 5' and 3' primers including NcoI sites. AtHB8-597 : 5'-GAG ATA TAC CAT GGC ATC AA-3' / 5'-TGG TGA CCC ATG GCC ATC AC-3'; AtHB8-680: 5'-GAT ATA CCA TGG GGT CTT ATC-3' / 5'-TGG TGA CCC ATG GCA AGA TT-3'. The digested PCR products were ligated into the NcoI restriction site of the pET21d-H6 vector. The two His6-tagged proteins were expressed in *E Coli* BL21 (DE3) (Novagen) and purified under denaturing conditions by Ni-NTA affinity chromatography (Qiagen), according to the manufacturer's recommendations. Protein sequence was verified by tandem mass spectrometry. Eight aliquots of purified AtHB8-597 (100 $\mu$g recombinant protein in [10 mM $Na_2PO_4$, 10 mM Tris/HCL pH 8.0, 0.8 M urea, 10\% glycerol]) in combination with the AtHB8 peptide described in

the materials section were used to produce rabbit polyclonal antibodies (Eurogentec, Belgium).
Antibodies were affinity purified using synthethic AtHB8 peptide coupled to Affi-Gel10 (Bio-Rad Laboratories) according to the supplier's instructions. Serum from the immunised rabbit was incubated with the Affi-Gel slurry for 2 h on a rolling shaker at 4°C. Affi-Gel beads were washed extensively with PBS (140 mM NaCl, 2.7 mM KCl, 10 mM $Na_2PO_4$, 1.8 mM $KH_2PO_4$ pH 7.4). Bound antibodies were eluted with 0.2 M glycine (pH 2.2). Tris/HCl pH 9.0 was added to affinity-purified antibodies to adjust the pH to 7.

### 4.2.18 Tandem mass spectrometry

**In-gel protein digestion**
50$\mu$g purified HIS-tagged fragment of AtHB8 protein was separated by SDS-PAGE and the corresponding band was cut out of the gel. The band was cut in several pieces and washed twice with water. The following washes and incubation were made: acetonitrile (Scharlau) 1min, 50mM $NH_4HCO_3$ 5min, acetonitrile 1min, 50mM $NH_4HCO_3$ 5min, acetonitile 1min twice, DTT [10mM DTT in 50mM $NH_4HCO_3$] 30min at 45°C, acetonitile 1min twice, 50mM $NH_4HCO_3$ 5min, acetonitrile 1min, 50mM $NH_4HCO_3$ 5min, acetonitile 1min twice. Gel pieces were dried at room temperature for 15 min. Gel pieces were incubated over night at room temperature in digestion buffer [0,2 $\mu$g trypsin (promega) in 25mM $NH_4HCO_3$]. All the following washing solutions and the digestion buffer were collected together: acetonitrile 5min twice, 2% (w/v) formic acid 10min, acetonitrile 5min, 2% (w/v) formic acid 10min, acetonitrile 5min twice. The collected solutions were centrifuged 10min at 12'000 RMP and the supernatant was collected. The supernatant was evaporated in speed vac for 3 hours. The remaining pellet was sent for identification.

**Protein identification by LC-MSMS**
Digested proteins were analyzed by the Protein Analysis Group (Functional Genomics Center, Zurich, Switzerland).

### 4.2.19 Protein extraction and Western blot analysis

Total proteins were isolated from Arabidopsis leaves or seedlings according to Rensink *et al.* (1998). To avoid proteolytic degradation, 0.5% (v/v) protease inhibitor cocktail for plant cell extracts (Sigma P9599) was added to the extraction buffer. Proteins were concentrated by chloroform - methanol precipitation (Wessel & Flügge, 1984) and resuspended in sample buffer [50 mM Tris/HCl pH 6.8, 0.1 M DTT, 2% (w/v) SDS, 0.1% (w/v) bromophenol blue, 10% (v/v) glycerol]. Proteins were separated by SDS-PAGE and blotted onto Protran® nitrocellulose membrane (Schleicher & Schuell) using the Mini-PROTEAN System (BioRad Laboratories). Western blot membranes were stained with Amido Black (= Naphthol Blue Black) as described (Sambrook & Russell, 2001) and scanned. To block unspecific binding of antibodies, membranes were incubated in blocking buffer [PBS (150 mM NaCl, 7.5 mM $Na_2HPO_4$, 1.5 mM $NaH_2PO_4$), containing 5% (w/v) skim milk powder] for 90 min. Membranes were then incubated for 90 min with a 1'000x dilution of AtHB8 antibody or 3'000x dilution of LHCP antibody in blocking buffer and washed extensively with PBS buffer.

To reveal primary antibodies, membranes were incubated 30 min with a 3'000x dilution of horseradish peroxidase-coupled goat anti-rabbit IgG (Bio-Rad Laboratories) in blocking buffer.

After washing with PBS buffer, signals were detected by enhanced chemiluminescence. The membranes were incubated 1 min in [0.1 M Tris/HCl pH 8.5, 1.25 mM 3-aminophthalhydrazide (=luminol), 0.2 mM p-coumaric acid, 0.009% (v/v) $H_2O_2$] and exposed to high performance chemiluminescence films (Amersham Biosciences).

### 4.2.20 Bioinformatics

Lasergene suite software 7.0.0 (DNASTAR, Inc, Madison, USA) was used for cloning design and sequence alignment. Additional sequence alignment was made with Blast2Sequence at (http://www.ncbi.nlm.nih.gov/blast/blast.cgi). The ClustalW software (http://www.ch.embnet.org\software\ClustalW.html) was used to generate multiple sequence alignments. Gene sequences were retrieved from the NCBI website (http://www.ncbi.nlm.nih.gov/).

DNA microarray data were retrieved from public databases and analyzed using the Geenevestigaror toolbox (Zimmermann et al., 2004); (https://www.genevestigator.ethz.ch/). Oligonucleotides properties were verified at http://www.basic.northwestern.edu/biotools/oligocalc.html and possible primer dimmers were checked at https://www.operon.com/oligos/toolkit.php

### 4.2.21 Data processing

Data was processed using Excel (Microsoft). Graphics, plots and statistics were made with Excel (Microsoft, Redmond, WA, USA) and R (R_Development_Core_Team, 2005); (http://www.R-project.org.). All real-time PCR calculations were performed with the Gene Expression Macro 1.1 (Bio-Rad) macros for Excel (Microsoft, Redmond, WA, USA). Scale and color balance of images was made with Photoshop 7.0 (Adobe) and Image J 1.38. Schemas and picture notations were made with Illustrator 10.0 (Adobe).

# Chapter 5

# Bibliography


Aida, M., Ishida, T., Fukaki, H., Fujisawa, H. & Tasaka, M. (1997) Genes involved in organ separation in Arabidopsis: an analysis of the cup-shaped cotyledon mutant. *Plant Cell*, **9**, 841-857.

Aida, M., Ishida, T. & Tasaka, M. (1999) Shoot apical meristem and cotyledon formation during Arabidopsis embryogenesis: interaction among the CUP-SHAPED COTYLEDON and SHOOT MERISTEMLESS genes. *Development*, **126**, 1563-1570.

Aida, M., Vernoux, T., Furutani, M., Traas, J. & Tasaka, M. (2002) Roles of PIN-FORMED1 and MONOPTEROS in pattern formation of the apical region of the Arabidopsis embryo. *Development*, **129**, 3965-3974.

Allen, E., Xie, Z., Gustafson, A.M. & Carrington, J.C. (2005) microRNA-directed phasing during trans-acting siRNA biogenesis in plants. *Cell*, **121**, 207-221.

Alvarez, J.P., Pekker, I., Goldshmidt, A., Blum, E., Amsellem, Z. & Y., E. (2006) Endogenous and Synthetic MicroRNAs Stimulate Simultaneous, Efficient, and Localized Regulation of Multiple Targets in Diverse Species. *Plant Cell*.

Baima, S., Nobili, F., Sessa, G., Lucchetti, S., Ruberti, I. & Morelli, G. (1995) The expression of the Athb-8 homeobox gene is restricted to provascular cells in Arabidopsis thaliana. *Development*, **121**, 4171-4182.

Baima, S., Possenti, M., Matteucci, A., Wisman, E., Altamura, M.M., Ruberti, I. & Morelli, G. (2001) The arabidopsis ATHB-8 HD-zip protein acts as a differentiation-promoting transcription factor of the vascular meristems. *Plant Physiol*, **126**, 643-655.

Bao, N., Lye, K.-W. & Barton, M.K. (2004) MicroRNA Binding Sites in Arabidopsis Class III HD-ZIP mRNAs Are Required for Methylation of the Template Chromosome. *Developmental Cell*, **7**, 653-662.

Bartel, B. (2005) MicroRNAs directing siRNA biogenesis. *Nat Struct Mol Biol*, **12**, 569-571.

Bartel, D.P. (2004) MicroRNAs: genomics, biogenesis, mechanism, and function. *Cell*, **116**, 281–297.

Baulcombe, D. (2004) RNA silencing in plants. *Nature*, **431**, 356-363.

Bechthold, N., Ellis, J. & Pelletier, G. (1993) in planta Agrobacterium-mediated gene transfert by infiltration of Arabidopsis thaliana plants. *CR Acad Sci Ser III SCi Vie*, **316**, 1194-1199.

Benjamins, R. & Scheres, B. (2008) Auxin: The Looping Star in Plant Development. *Annu. Rev. Plant Biol.*, **59**, 443-465.

Bennett, M.J., Marchant, A., Green, H.G., May, S.T., Ward, S.P., Millner, P.A., Walker, A.R., Schulz, B. & Feldmann, K.A. (1996) Arabidopsis AUX1 gene: a permease-like regulator of root gravitropism. *Science*, **273**, 948-950.

Bennett, S.R.M., Alvarez, J., Bossinger, G. & Smyth, D.R. (1995) Morphogenesis in pinoid mutants of Arabidopsis thaliana. *Plant J*, **8**, 505-520.

Berleth, T. & Jurgens, G. (1993) The role of the monopteros gene in organising the basal body region of the Arabidopsis embryo. *Development*, **118**, 575-587.

Berleth, T. & Sachs, T. (2001) Plant morphogenesis: Long-distance coordination and local patterning. *Curr. Opin. Plant Biol.*, 57–62

Blakeslee, J.J., Peer, W.A. & Murphy, A.S. (2005) Auxin transport. *Curr Opin Plant Biol*, **8**, 494-500.

Blilou, I., Xu, J., Wildwater, M., Willemsen, V., Paponov, I., Friml, J., Heidstra, R., Aida, M., Palme, K. & Scheres, B. (2005) The PIN auxin efflux facilitator network controls growth and patterning in Arabidopsis roots. *Nature*, **433**, 39-44.

Boerjan, W., Cervera, M.T., Delarue, M., Beeckman, T., Dewitte, W., Bellini, C., Caboche, M., Van Onckelen, H., Van Montagu, M. & Inze, D. (1995) Superroot, a recessive mutation in Arabidopsis, confers auxin overproduction. *Plant Cell*, **7**, 1405-1419.

Bonke, M., Thitamadee, S., Mahonen, A.P., Hauser, M.T. & Helariutta, Y. (2003) APL regulates vascular tissue identity in Arabidopsis. *Nature*, **426**, 181-186.

Bowman, J.L. & Eshed, Y. (2000) Formation and maintenance of the shoot apical meristem. *Trends Plant Sci*, **5**, 110-115.

Bowman, J.L., Eshed, Y. & Baum, S.F. (2002) Establishment of polarity in angiosperm lateral organs. *Trends Genet*, **18**, 134-141.

Bowman, J.L., Smyth, D.R. & Meyerowitz, E.M. (1989) Genes Directing Flower Development in Arabidopsis *Plant Cell*, **1**, 37-52.

Bowman, J.L., Smyth, D.R. & Meyerowitz, E.M. (1991) Genetic interactions among floral homeotic genes of Arabidopsis. *Development*, **112**, 1-20.

Brown, D.E., Rashotte, A.M., Murphy, A.S., Normanly, J., Tague, B.W., Peer, W.A., Taiz, L. & Muday, G.K. (2001) Flavonoids act as negative regulators of auxin transport in vivo in arabidopsis. *Plant Physiol*, **126**, 524-535.

Byrne, M.E. (2005) Networks in leaf development. *Curr Opin Plant Biol*, **8**, 59-66.

Byrne, M.E., Barley, R., Curtis, M., Arroyo, J.M., Dunham, M., Hudson, A. & Martienssen, R.A. (2000) Asymmetric leaves1 mediates leaf patterning and stem cell function in Arabidopsis. *Nature*, **408**, 967-971.

Cano-Delgado, A., Yin, Y., Yu, C., Vafeados, D., Mora-Garcia, S., Cheng, J.C., Nam, K.H., Li, J. & Chory, J. (2004) BRL1 and BRL3 are novel brassinosteroid receptors that function in vascular differentiation in Arabidopsis. *Development*, **131**, 5341-5351.

Caplin, S.M. & Steward, F.C. (1948) Effects of coconut milk on the growth of the explant from carrot root. *Science*, **108**.

Carlsbecker, A. & Helariutta, Y. (2005) Phloem and xylem specification: pieces of the puzzle emerge. *Curr Opin Plant Biol*, **8**, 512-517.

Chaffey, N., Cholewa, E., Regan, S. & Sundberg, B. (2002) Secondary xylem development in Arabidopsis: a model for wood formation. *Physiol. Plant.*, **114**, 594-600.

Chandler, J.W., Cole, M., Flier, A., Grewe, B. & Werr, W. (2007) The AP2 transcription factors DORNRO_SCHEN and DORNRO_SCHEN-LIKE redundantly control Arabidopsis embryo patterning via interaction with PHAVOLUTA *Development*, **134**, 1-10.

Chapman, E.J. & Carrington, J.C. (2007) Specialization and evolution of endogenous small RNA pathways. *Nat Rev Genet*, **8**, 884-896.

Cheng, Y., Dai, X. & Zhao, Y. (2006) Auxin biosynthesis by the YUCCA flavin monooxygenases controls the formation of floral organs and vascular tissues in Arabidopsis. *Genes Dev*, **20**, 1790-1799.

Cheng, Y., Dai, X. & Zhao, Y. (2007) Auxin synthesized by the YUCCA flavin monooxygenases is essential for embryogenesis and leaf formation in Arabidopsis. *Plant Cell*, **19**, 2430-2439.

Clark, S.E. (2001) Cell signalling at the shoot meristem. *Nat Rev Mol Cell Biol*, **2**, 276-284.

Clough, S.J. & Bent, A.F. (1998) Floral dip: a simplified method for Agrobacterium-mediated transformation of Arabidopsis thaliana. *Plant J*, **16**, 735-743.

Clouse, S.D. & Sasse, J.M. (1998) BRASSINOSTEROIDS: Essential Regulators of Plant Growth and Development. *Annu Rev Plant Physiol Plant Mol Biol*, **49**, 427-451.

Darwin, F. & Darwin, C. (1881) The Power of Movement in Plants.

Demura, T. & Fukuda, H. (2007) Transcriptional regulation in wood formation. *Trends Plant Sci*, **12**, 64-70.

Dharmasiri, N., Dharmasiri, S. & Estelle, M. (2005a) The F-box protein TIR1 is an auxin receptor. *Nature*, **435**, 441-445.

Dharmasiri, N., Dharmasiri, S., Weijers, D., Lechner, E., Yamada, M., Hobbie, L., Ehrismann, J.S., Jurgens, G. & Estelle, M. (2005b) Plant development is regulated by a family of auxin receptor F box proteins. *Dev Cell*, **9**, 109-119.

Emery, J.F., Floyd, S.K., Alvarez, J., Eshed, Y., Hawker, N.P., Izhaki, A., Baum, S.F. & Bowman, J.L. (2003) Radial patterning of Arabidopsis shoots by class III HD-ZIP and KANADI genes. *Curr Biol*, **13**, 1768-1774.

Eshed, Y., Baum, S.F. & Bowman, J.L. (1999) Distinct mechanisms promote polarity establishment in carpels of Arabidopsis. *Cell*, **99**, 199-209.

Eshed, Y., Baum, S.F., Perea, J.V. & Bowman, J.L. (2001) Establishment of polarity in lateral organs of plants. *Current Biology*, **11**, 1251-1260.

Eshed, Y., Izhaki, A., Baum, S.F., Floyd, S.K. & Bowman, J.L. (2004) Asymmetric leaf development and blade expansion in Arabidopsis are mediated by KANADI and YABBY activities. *Development*, **131**, 2997-3006.

Fahlgren, N., Montgomery, T.A., Howell, M.D., Allen, E., Dvorak, S.K., Alexander, A.L. & Carrington, J.C. (2006) Regulation of AUXIN RESPONSE FACTOR3 by TAS3 ta-siRNA affects developmental timing and patterning in Arabidopsis. *Curr Biol*, **16**, 939-944.

Fiers, M., Ku, K.L. & Liu, C.-M. (2007) CLE peptide ligands and their roles in establishing meristems. *Curr Opin Plant Biol*, **10**, 39-43.

Fisher, K. & Turner, S. (2007) PXY, a receptor-like kinase essential for maintaining polarity during plant vascular-tissue development. *Curr Biol*, **17**, 1061-1066.

Floyd, S.K. & Bowman, J.L. (2004) Gene regulation: ancient microRNA target sequences in plants. *Nature*, **428**, 485-486.

Floyd, S.K., Zalewski, C.S. & Bowman, J.L. (2006) Evolution of class III homeodomain-leucine zipper genes in streptophytes. *Genetics*, **173**, 373-388.

Friml, J., Vieten, A., Sauer, M., Weijers, D., Schwarz, H., Hamann, T., Offringa, R. & Jurgens, G. (2003) Efflux-dependent auxin gradients establish the apical-basal axis of Arabidopsis. *Nature*, **426**, 147-153.

Fukuda, H. (2004) Signals that control plant vascular cell differentiation. *Nat Rev Mol Cell Biol*, **5**, 379-391.

Furutani, M., Vernoux, T., Traas, J., Kato, T., Tasaka, M. & Aida, M. (2004) PIN-FORMED1 and PINOID regulate boundary formation and cotyledon development in Arabidopsis embryogenesis. *Development*, **131**, 5021-5030.

Galweiler, L., Guan, C., Muller, A., Wisman, E., Mendgen, K., Yephremov, A. & Palme, K. (1998) Regulation of polar auxin transport by AtPIN1 in Arabidopsis vascular tissue. *Science*, **282**, 2226-2230.

Garbers, C., DeLong, A., Deruere, J., Bernasconi, P. & Soll, D. (1996) A mutation in protein phosphatase 2A regulatory subunit A affects auxin transport in Arabidopsis. *EMBO J*, **15**, 2115-2124.

Gil, P., Dewey, E., Friml, J., Zhao, Y., Snowden, K.C., Putterill, J., Palme, K., Estelle, M. & Chory, J. (2001) BIG: a calossin-like protein required for polar auxin transport in Arabidopsis. *Genes Dev*, **15**, 1985-1997.

Gilles-Gonzalez, M.A. & Gonzalez, G. (2004) Signal transduction by heme-containing PAS-domain proteins. *J Appl Physiol*, **96**, 774-783.

Haecker, A. & Laux, T. (2001) Cell-cell signaling in the shoot meristem. *Curr Opin Plant Biol*, **4**, 441-446.

Hagen, G. & Guilfoyle, T. (2002) Auxin-responsive gene expression: genes, promoters and regulatory factors. *Plant Mol Biol*, **49**, 373-385.

Hamann, T., Benkova, E., Baurle, I., Kientz, M. & Jurgens, G. (2002) The Arabidopsis BODENLOS gene encodes an auxin response protein inhibiting MONOPTEROS-mediated embryo patterning. *Genes Dev*, **16**, 1610-1615.

Han, M.H., Goud, S., Song, L. & Fedoroff, N. (2004) The Arabidopsis double-stranded RNA-binding protein HYL1 plays a role in microRNA-mediated gene regulation. *Proc Natl Acad Sci U S A*, **101**, 1093-1098.

Hannon, G.J. (2002) RNA interference. *Nature*, **418**, 244-251.

Hardtke, C.S., Ckurshumova, W., Vidaurre, D.P., Singh, S.A., Stamatiou, G., Tiwari, S.B., Hagen, G., Guilfoyle, T.J. & Berleth, T. (2004) Overlapping and non-redundant functions of the Arabidopsis auxin response factors MONOPTEROS and NONPHOTOTROPIC HYPOCOTYL 4. *Development*, **131**, 1089-1100.

Heisler, M.G., Ohno, C., Das, P., Sieber, P., Reddy, G.V., Long, J.A. & Meyerowitz, E.M. (2005) Patterns of auxin transport and gene expression during primordium development revealed by live imaging of the Arabidopsis inflorescence meristem. *Curr Biol*, **15**, 1899-1911.

Hellmann, H., Hobbie, L., Chapman, A., Dharmasiri, S., Dharmasiri, N., del Pozo, C., Reinhardt, D. & Estelle, M. (2003) Arabidopsis AXR6 encodes CUL1 implicating SCF E3 ligases in auxin regulation of embryogenesis. *EMBO J*, **22**, 3314-3325.

Henderson, I.R. & Jacobsen, S.E. (2007) Epigenetic inheritance in plants. *Nature*, **447**, 418-424.

Hutvagner, G. & Zamore, P.D. (2002) A microRNA in a multiple-turnover RNAi enzyme complex. *Science*, **297**, 2056-2060.

Hwang, I. & Sheen, J. (2001) Two-component circuitry in Arabidopsis cytokinin signal transduction. *Nature*, **413**, 383–389.

Inoue, H., Nojima, H. & Okayama, H. (1990) High efficiency transformation of escherichia coli with plasmids. *Gene*, **96**, 23-28.

Inoue, T., Higuchi, M., Hashimoto, Y., Seki, M., Kobayashi, M., Kato, T., Tabata, S., Shinozaki, K. & Kakimoto, T. (2001) Identification of CRE1 as a cytokinin receptor from Arabidopsis. *Nature*, **409**, 1060–1063.

Ito, Y., Nakanomyo, I., Motose, H., Iwamoto, K., Sawa, S., Dohmae, N. & Fukuda, H. (2006) Dodeca-CLE peptides as suppressors of plant stem cell differentiation. *Science*, **313**, 842-845.

Iyer, L., Koonin, E.V. & Aravind, L. (2001) Adaptations of the helix-grip fold or ligand binding and catalysis in the START domain superfamily. *Proteins*, **43**, 134-144.

Iyer, L.M., Koonin, E.V. & Aravind, L. (2003) Evolutionary connection between the catalytic subunits of DNA-dependent RNA polymerases and eukaryotic RNA-dependent RNA polymerases and the origin of RNA polymerases. *BMC Struct Biol*, **3**, 1.

Izhaki, A. & Bowman, J.L. (2007) KANADI and class III HD-Zip gene families regulate embryo patterning and modulate auxin flow during embryogenesis in Arabidopsis. *Plant Cell*, **19**, 495-508.

Jenik, P.D. & Barton, M.K. (2005) Surge and destroy: the role of auxin in plant embryogenesis. *Development*, **132**, 3577-3585.

Jung, J.H. & Park, C.M. (2007) MIR166/165 genes exhibit dynamic expression patterns in regulating shoot apical meristem and floral development in Arabidopsis. *Planta*, **225**, 1327-1338.

Kakimoto, T. (2003) Perception and signal transduction of cytokinins. *Annu. Rev. Plant Biol.*, **54**, 605–627.

Kepinski, S. & Leyser, O. (2005) The Arabidopsis F-box protein TIR1 is an auxin receptor. *Nature*, **435**, 446-451.

Kerstetter, R.A., Bollman, K., Taylor, R.A., Bomblies, K. & Poethig, R.S. (2001) KANADI regulates organ polarity in Arabidopsis. *Nature*, **411**, 706-709.

Kerstetter, R.A., Laudencia-Chingcuanco, D., Smith, L.G. & Hake, S. (1997) Loss-of-function mutations in the maize homeobox gene knotted1 are defective in shoot meristem maintenance. *Development*, **124**, 3045–3054.

Kidner, C.A. & Martienssen, R.A. (2003) Macro effects of microRNAs in plants. *Trends Genet*, **19**, 13-16.

Kidner, C.A. & Martienssen, R.A. (2005) The developmental role of microRNA in plants. *Curr Opin Plant Biol*, **8**, 38-44.

Kim, J., Jung, J.H., Reyes, J.L., Kim, Y.S., Kim, S.Y., Chung, K.S., Kim, J.A., Lee, M., Lee, Y., Narry Kim, V., Chua, N.H. & Park, C.M. (2005) microRNA-directed cleavage of ATHB15 mRNA regulates vascular development in Arabidopsis inflorescence stems. *Plant J*, **42**, 84-94.

Kim, Y.S., Kim, S.G., Lee, M., Lee, I., Park, H.Y., Seo, P.J., Jung, J.H., Kwon, E.J., Suh, S.W., Paek, K.H. & Park, C.M. (2008) HD-ZIP III Activity Is Modulated by Competitive Inhibitors via a Feedback Loop in Arabidopsis Shoot Apical Meristem Development. *Plant Cell*.

Koizumi, K., Naramoto, S., Sawa, S., Yahara, N., Ueda, T., Nakano, A., Sugiyama, M. & Fukuda, H. (2005) VAN3 ARF-GAP-mediated vesicle transport is involved in leaf vascular network formation. *Development*, **132**, 1699-1711.

Kubo, M., Udagawa, M., Nishikubo, N., Horiguchi, G., Yamaguchi, M., Ito, J., Mimura, T., Fukuda, H. & Demura, T. (2005) Transcription switches for protoxylem and metaxylem vessel formation. *Genes Dev*, **19**, 1855-1860.

Kumaran, M.K., Bowman, J.L. & Sundaresan, V. (2002) YABBY polarity genes mediate the repression of KNOX homeobox genes in Arabidopsis. *Plant Cell*, **14**, 2761-2770.

Laudet, V. & Gronemeyer, H. (2002) *The Nuclear Receptors FactsBook*, London.

Lenhard, M., Bohnert, A., Jurgens, G. & Laux, T. (2001) Termination of stem cell maintenance in Arabidopsis floral meristems by interactions between WUSCHEL and AGAMOUS. *Cell*, **105**, 805-814.

Lin, W.C., Shuai, B. & Springer, P.S. (2003) The Arabidopsis LATERAL ORGAN BOUNDARIES-domain gene ASYMMETRIC LEAVES2

functions in the repression of KNOX gene expression and in adaxial-abaxial patterning. *Plant Cell*, **15**, 2241-2252.

Ljung, K., Hull, A.K., Celenza, J., Yamada, M., Estelle, M., Normanly, J. & Sandberg, G. (2005) Sites and regulation of auxin biosynthesis in Arabidopsis roots. *Plant Cell*, **17**, 1090-1104.

Lohmann, J.U., Hong, R.L., Hobe, M., Busch, M.A., Parcy, F., Simon, R. & Weigel, D. (2001) A molecular link between stem cell regulation and floral patterning in Arabidopsis. *Cell*, **105**, 793-803.

Long, J.A. & Barton, M.K. (1998) The development of apical embryonic pattern in Arabidopsis. *Development*, **125**, 3027-3035.

Long, J.A., Moan, E.I., Medford, J.I. & Barton, M.K. (1996) A member of the KNOTTED class of homeodomain proteins encoded by the STM gene of Arabidopsis. *Nature*, **379**, 66-69.

Lu, C. & Fedoroff, N. (2000) A mutation in the Arabidopsis HYL1 gene encoding a dsRNA binding protein affects responses to abscisic acid, auxin, and cytokinin. *Plant Cell*, **12**, 2351-2366.

Mahonen, A.P., Bonke, M., Kauppinen, L., Riikonen, M., Benfey, P.N. & Helariutta, Y. (2000) A novel two-component hybrid molecule regulates vascular morphogenesis of the Arabidopsis root. *Genes Dev*, **14**, 2938-2943.

Mahonen, A.P., Higuchi, M., Tormakangas, K., Miyawaki, K., Pischke, M.S., Sussman, M.R., Helariutta, Y. & Kakimoto, T. (2006) Cytokinins regulate a bidirectional phosphorelay network in Arabidopsis. *Curr Biol*, **16**, 1116-1122.

Mallory, A.C., Reinhart, B.J., Jones-Rhoades, M.W., Tang, G., Zamore, P.D., Barton, M.K. & Bartel, D.P. (2004) MicroRNA control of PHABULOSA in leaf development: importance of pairing to the microRNA 5' region. *EMBO J*, **23**, 3356-3364.

Mattsson, J., Sung, Z.R. & Berleth, T. (1999) Responses of plant vascular systems to auxin transport inhibition. *Development*, **126**, 2979-2991.

McAbee, J.M., Hill, T.A., Skinner, D.J., Izhaki, A., Hauser, B.A., Meister, R.J., Venugopala Reddy, G., Meyerowitz, E.M., Bowman, J.L. & Gasser, C.S. (2006) ABERRANT TESTA SHAPE encodes a KANADI family member, linking polarity determination to separation and growth of Arabidopsis ovule integuments. *Plant J*, **46**, 522-531.

McConnell, J.R., Emery, J., Eshed, Y., Bao, N., Bowman, J. & Barton, M.K. (2001) Role of PHABULOSA and PHAVOLUTA in determining radial patterning in shoots. *Nature*, **411**, 709-713.

Michniewicz, M., Zago, M.K., Abas, L., Weijers, D., Schweighofer, A., Meskiene, I., Heisler, M.G., Ohno, C., Zhang, J., Huang, F., Schwab, R., Weigel, D., Meyerowitz, E.M., Luschnig, C., Offringa, R. & Friml, J. (2007) Antagonistic regulation of PIN phosphorylation by PP2A and PINOID directs auxin flux. *Cell*, **130**, 1044-1056.

Miller, C.O., Skoog, F., Von Saltza, M.H. & Strong, F. (1955) Kinetin, a cell division factor from deoxyribonucleic acid. *J. Am. Chem. Soc.*, **77**, 1392-1393.

Mitsuda, N., Iwase, A., Yamamoto, H., Yoshida, M., Seki, M., Shinozaki, K. & Ohme-Takagi, M. (2007) NAC transcription factors, NST1 and NST3, are key regulators of the formation of secondary walls in woody tissues of Arabidopsis. *Plant Cell*, **19**, 270-280.

Mitsuda, N., Seki, M., Shinozaki, K. & Ohme-Takagi, M. (2005) The NAC transcription factors NST1 and NST2 of Arabidopsis regulate secondary wall thickening and are required for anther dehiscence. *Plant Cell*, **17**, 2993–3006.

Moissiard, G. & Voinnet, O. (2006) RNA silencing of host transcripts by cauliflower mosaic virus requires coordinated action of the four Arabidopsis Dicer-like proteins. *Proc. Natl Acad. Sci.*, **103**, 19593–19598.

Montoya, T., Nomura, T., Yokota, T., Farrar, K., Harrison, K., Jones, J.D., Kaneta, T., Kamiya, Y., Szekeres, M. & Bishop, G.J. (2005) Patterns of Dwarf expression and brassinosteroid accumulation in tomato reveal the importance of brassinosteroid synthesis during fruit development. *Plant J*, **42**, 262-269.

Moore, I., Galweiler, L., Grosskopf, D., Schell, J. & Palme, K. (1998) A transcription activation system for regulated gene expression in transgenic plants. *Proc Natl Acad Sci U S A*, **95**, 376-381.

Mukherjee, K. & Burglin, T.R. (2006) MEKHLA, a novel domain with similarity to PAS domains, is fused to plant homeodomain-leucine zipper III proteins. *Plant Physiol*, **140**, 1142-1150.

Murphy, A., Peer, W.A. & Taiz, L. (2000) Regulation of auxin transport by aminopeptidases and endogenous flavonoids. *Planta*, **211**, 315-324.

Murphy, A.S. (Year) Auxin Function – Six part lecture series, University of Bern. City.

Murphy, A.S., Hoogner, K.R., Peer, W.A. & Taiz, L. (2002) Identification, purification, and molecular cloning of N-1-naphthylphthalmic acid-binding plasma membrane-associated aminopeptidases from Arabidopsis. *Plant Physiol*, **128**, 935-950.

Nag, A., Yang, Y. & Jack, T. (2007) DORNROSCHEN-LIKE, an AP2 gene, is necessary for stamen emergence in Arabidopsis. *Plant Mol Biol*, **65**, 219-232.

Nagata, N., Asami, T. & Yoshida, S. (2001) Brassinazole, an inhibitor of brassinosteroid biosynthesis, inhibits development of secondary xylem in cress plants (Lepidium sativum). *Plant Cell Physiol*, **42**, 1006-1011.

Nagawa, S., Sawa, S., Sato, S., Kato, T., Tabata, S. & Fukuda, H. (2006) Gene trapping in Arabidopsis reveals genes involved in vascular development. *Plant Cell Physiol*, **47**, 1394-1405.

Nakajima, K. & Benfey, P.N. (2002) Signaling in and out: control of cell division and differentiation in the shoot and root. *Plant Cell*, **14 Suppl**, S265-276.

Nelson, T. & Dengler, N. (1997) Leaf Vascular Pattern Formation. *Plant Cell*, **9**, 1121-1135.

Noh, B., Bandyopadhyay, A., Peer, W.A., Spalding, E.P. & Murphy, A.S. (2003) Enhanced gravi- and phototropism in plant mdr mutants mislocalizing the auxin efflux protein PIN1. *Nature*, **423**, 999-1002.

Noh, B., Murphy, A.S. & Spalding, E.P. (2001) Multidrug resistance-like genes of Arabidopsis required for auxin transport and auxin-mediated development. *Plant Cell*, **13**, 2441-2454.

Ochando, I., Jover-Gil, S., Ripoll, J.J., Candela, H., Vera, A., Ponce, M.R., Martinez-Laborda, A. & Micol, J.L. (2006) Mutations in the microRNA complementarity site of the INCURVATA4 gene perturb meristem function and adaxialize lateral organs in arabidopsis. *Plant Physiol*, **141**, 607-619.

Ohashi-Ito, K., Demura, T. & Fukuda, H. (2002) Promotion of transcript accumulation of novel Zinnia immature xylem-specific HD-Zip III homeobox genes by brassinosteroids. *Plant Cell Physiol*, **43**, 1146-1153.

Ohashi-Ito, K. & Fukuda, H. (2003) HD-zip III homeobox genes that include a novel member, ZeHB-13 (Zinnia)/ATHB-15 (Arabidopsis), are involved in procambium and xylem cell differentiation. *Plant Cell Physiol*, **44**, 1350-1358.

Ohashi-Ito, K., Kubo, M., Demura, T. & Fukuda, H. (2005) Class III homeodomain leucine-zipper proteins regulate xylem cell differentiation. *Plant Cell Physiol*, **46**, 1646-1656.

Okada, K., Ueda, J., Komaki, M.K., Bell, C.J. & Shimura, Y. (1991) Requirement of the Auxin Polar Transport System in Early Stages of Arabidopsis Floral Bud Formation. *Plant Cell*, **3**, 677-684.

Otsuga, D., DeGuzman, B., Prigge, M.J., Drews, G.N. & Clark, S.E. (2001) REVOLUTA regulates meristem initiation at lateral positions. *Plant J*, **25**, 223-236.

Papp, I., Mette, M.F., Aufsatz, W., Daxinger, L., Schauer, S.E., Ray, A., van der Winden, J., Matzke, M. & Matzke, A.J. (2003) Evidence for nuclear processing of plant micro RNA and short interfering RNA precursors. *Plant Physiol*, **132**, 1382-1390.

Park, M.Y., Wu, G., Gonzalez-Sulser, A., Vaucheret, H. & Poethig, R.S. (2005) Nuclear processing and export of microRNAs in Arabidopsis. *Proc Natl Acad Sci U S A*, **102**, 3691-3696.

Park, W.J., Schafer, A., Prinsen, E., van Onckelen, H., Kang, B.G. & Hertel, R. (2001) Auxin-induced elongation of short maize coleoptile segments is supported by 2,4-dihydroxy-7-methoxy-1,4-benzoxazin-3-one. *Planta*, **213**, 92-100.

Pekker, I., Alvarez, J.P. & Eshed, Y. (2005) Auxin response factors mediate Arabidopsis organ asymmetry via modulation of KANADI activity. *Plant Cell*, **17**, 2899-2910.

Peragine, A., Yoshikawa, M., Wu, G., Albrecht, H.L. & Poethig, R.S. (2004) SGS3 and SGS2/SDE1/RDR6 are required for juvenile development and the production of trans-acting siRNAs in Arabidopsis. *Genes Dev*, **18**, 2368-2379.

Petrasek, J., Mravec, J., Bouchard, R., Blakeslee, J.J., Abas, M., Seifertova, D., Wisniewska, J., Tadele, Z., Kubes, M., Covanova, M., Dhonukshe, P., Skupa, P., Benkova, E., Perry, L., Krecek, P., Lee, O.R., Fink, G.R., Geisler, M., Murphy, A.S., Luschnig, C., Zazimalova, E. & Friml, J. (2006) PIN proteins perform a rate-limiting function in cellular auxin efflux. *Science*, **312**, 914-918.

Pineau, C., Freydier, A., Ranocha, P., Jauneau, A., Turner, S., Lemonnier, G., Renou, J.P., Tarkowski, P., Sandberg, G., Jouanin, L., Sundberg, B., Boudet, A.M., Goffner, D. & Pichon, M. (2005) hca: an Arabidopsis mutant exhibiting unusual cambial activity and altered vascular patterning. *Plant J*, **44**, 271-289.

Plomion, C., Leprovost, G. & Stokes, A. (2001) Wood formation in trees. *Plant Physiol*, **127**, 1513–1523.

Ponting, C.P. & Aravind, L. (1999) START: a lipid-binding domain in StAR, HD-ZIP and signalling proteins. *Trends Biochem Sci*, **24**, 130-132.

Prigge, M.J. & Clark, S.E. (2006) Evolution of the class III HD-Zip gene family in land plants. *Evol Dev*, **8**, 350-361.

Prigge, M.J., Otsuga, D., Alonso, J.M., Ecker, J.R., Drews, G.N. & Clark, S.E. (2005) Class III homeodomain-leucine zipper gene family members have overlapping, antagonistic, and distinct roles in Arabidopsis development. *Plant Cell*, **17**, 61-76.

Przemeck, G.K., Mattsson, J., Hardtke, C.S., Sung, Z.R. & Berleth, T. (1996) Studies on the role of the Arabidopsis gene MONOPTEROS in vascular development and plant cell axialization. *Planta*, **200**, 229-237.

R_Development_Core_Team (2005) *R: A language and environment for statistical computing*. R Foundation for Statistical Computing, Vienna, Austria.

Raven, J.A. (1975) Transport of indoleacetic acid in plant cells in relation to pH and electrical potential gradients, and its significance for polar IAA transport. *New Phytol.* , **74**, 163–172

Reinhardt, D., Pesce, E.R., Stieger, P., Mandel, T., Baltensperger, K., Bennett, M., Traas, J., Friml, J. & Kuhlemeier, C. (2003) Regulation of phyllotaxis by polar auxin transport. *Nature*, **426**, 255-260.

Reinhart, B.J., Weinstein, E.G., Rhoades, M.W., Bartel, B. & Bartel, D.P. (2002) MicroRNAs in plants. *Genes Dev*, **16**, 1616-1626.

Rhoades, M.W., Reinhart, B.J., Lim, L.P., Burge, C.B., Bartel, B. & Bartel, D.P. (2002) Prediction of plant microRNA targets. *Cell*, **110**, 513-520.

Rubery, P.H. & Sheldrake, A.R. (1974) Carrier-mediated auxin transport *Planta*, **118**, 101–121.

Sachs, T. (1981) The control of the patterned differentiation of vascular tissues. *Adv. Bot. Res*, **9**, 151-262.

Sachs, T. (1991) Cell polarity and tissue patterning in plants. *Development Suppl.* , **1**, 83 -93.

Sakamoto, T., Kamiya, N., Ueguchi-Tanaka, M., Iwahori, S. & Matsuoka, M. (2001) KNOX homeodomain protein directly suppresses the expression of a gibberellin biosynthetic gene in the tobacco shoot apical meristem. *Genes Dev*, **15**, 581-590.

Sambrook, J. & Russell, D.W. (2001) *Molecular cloning: a laboratory manual*. Cold Spring Harbor Laboratory Press, Cold Spring Harbor, New York.

Sauer, M., Balla, J., Luschnig, C., Wisniewska, J., Reinohl, V., Friml, J. & Benkova, E. (2006) Canalization of auxin flow by Aux/IAA-ARF-dependent feedback regulation of PIN polarity. *Genes Dev*, **20**, 2902-2911.

Sawa, S., Kinoshita, A., Nakanomyo, I. & Fukuda, H. (2006) CLV3/ESR-related (CLE) peptides as intercellular signaling molecules in plants. *Chem Rec*, **6**, 303-310.

Scarpella, E., Francis, P. & Berleth, T. (2004) Stage-specific markers define early steps of procambium development in Arabidopsis leaves and correlate termination of vein formation with mesophyll differentiation. *Development*, **131**, 3445-3455.

Scarpella, E. & Meijer, A. (2004) Pattern formation in the vascular system of monocot and dicot plant species. *New Phytol*, **164**, 209-242.

Scholl, R.L., May, S.T. & Ware, D.H. (2000) Seed and molecular resources for Arabidopsis. *Plant Physiol*, **124**, 1477-1480.

Schrick, K., Nguyen, D., Karlowski, W.M. & Mayer, K.F. (2004) START lipid/sterol-binding domains are amplified in plants and are predominantly associated with homeodomain transcription factors. *Genome Biol.*, **5**.

Seo, M., Akaba, S., Oritani, T., Delarue, M., Bellini, C., Caboche, M. & Koshiba, T. (1998) Higher activity of an aldehyde oxidase in the auxin-overproducing superroot1 mutant of Arabidopsis thaliana. *Plant Physiol*, **116**, 687-693.

Sessa, G., Steindler, C., Morelli, G. & Ruberti, I. (1998) The Arabidopsis Athb-8, -9 and -14 genes are members of a small gene family coding for highly related HD-ZIP proteins. *Plant Mol Biol*, **38**, 609-622.

Shimada, Y., Goda, H., Nakamura, A., Takatsuto, S., Fujioka, S. & Yoshida, S. (2003) Organ-specific expression of brassinosteroid-biosynthetic genes and distribution of endogenous brassinosteroids in Arabidopsis. *Plant Physiol*, **131**, 287-297.

Sieburth, L.E. & Deyholos, M.K. (2006) Vascular development: the long and winding road. *Curr Opin Plant Biol*, **9**, 48-54.

Siegfried, K.R., Eshed, Y., Baum, S.F., Otsuga, D., Drews, G.N. & Bowman, J.L. (1999) Members of the YABBY gene family specify abaxial cell fate in Arabidopsis. *Development*, **126**, 4117-4128.

Stieger, P.A., Reinhardt, D. & Kuhlemeier, C. (2002) The auxin influx carrier is essential for correct leaf positioning. *Plant J*, **32**, 509-517.

Swarup, R., Friml, J., Marchant, A., Ljung, K., Sandberg, G., Palme, K. & Bennett, M. (2001) Localization of the auxin permease AUX1 suggests two functionally distinct hormone transport pathways operate in the Arabidopsis root apex. *Genes Dev*, **15**, 2648-2653.

Symons, G.M. & Reid, J.B. (2004) Brassinosteroids do not undergo long-distance transport in pea. Implications for the regulation of endogenous brassinosteroid levels. *Plant Physiol*, **135**, 2196-2206.

Szemenyei, H., Hannon, M. & Long, J.A. (2008) TOPLESS Mediates Auxin-Dependent Transcriptional Repression During Arabidopsis Embryogenesis. *Science*, **319**, 1384-1386.

Taiz, L. & Zeiger, E. (2006) *Plant Physiology, Fourth Edition*. Sinauer Associates, Inc., Sunderland, MA, USA.

Talbert, P.B., Adler, H.T., Parks, D.W. & Comai, L. (1995) The REVOLUTA gene is necessary for apical meristem development and for limiting cell divisions in the leaves and stems of Arabidopsis thaliana. *Development*, **121**, 2723-2735.

Tang, G., Reinhart, B.J., Bartel, D.P. & Zamore, P.D. (2003) A biochemical framework for RNA silencing in plants. *Genes Dev*, **17**, 49-63.

Thimann, K.V. (1935) Growth Substances in Plants. *Annual Review of Biochemistry*, **4**, 545-568.

Tiwari, S.B., Hagen, G. & Guilfoyle, T. (2003) The roles of auxin response factor domains in auxin-responsive transcription. *Plant Cell*, **15**, 533-543.

Treml, B.S., Winderl, S., Radykewicz, R., Herz, M., Schweizer, G., Hutzler, P., Glawischnig, E. & Ruiz, R.A. (2005) The gene ENHANCER OF PINOID controls cotyledon development in the Arabidopsis embryo. *Development*, **132**, 4063-4074.

Truernit, E. & Sauer, N. (1995) The promoter of the Arabidopsis thaliana SUC2 sucrose-H+ symporter gene directs expression of beta-glucuronidase to the phloem: evidence for phloem loading and unloading by SUC2. *Planta*, **196**, 564-570.

Tsiantis, M., Schneeberger, R., Golz, J.F., Freeling, M. & Langdale, J.A. (1999) The maize rough sheath2 gene and leaf development programs in monocot and dicot plants. *Science*, **284**, 154-156.

Ulmasov, T., Murfett, J., Hagen, G. & Guilfoyle, T.J. (1997) Aux/IAA proteins repress expression of reporter genes containing natural and highly active synthetic auxin response elements. *Plant Cell*, **9**, 1963-1971.

Vazquez, F., Gasciolli, V., Crete, P. & Vaucheret, H. (2004) The nuclear dsRNA binding protein HYL1 is required for microRNA accumulation and plant development, but not posttranscriptional transgene silencing. *Curr Biol*, **14**, 346-351.

Voinnet, O. (2005) Induction and suppression of RNA silencing: insights from viral infections. *Nat Rev Genet*, **6**, 206-220.

Vollbrecht, E., Reiser, L. & Hake, S. (2000) Shoot meristem size is dependent on inbred background and presence of the maize homeobox gene, knotted1. *Development*, **127**, 3161–3172.

Vroemen, C.W., Mordhorst, A.P., Albrecht, C., Kwaaitaal, M.A. & de Vries, S.C. (2003) The CUP-SHAPED COTYLEDON3 gene is required for boundary and shoot meristem formation in Arabidopsis. *Plant Cell*, **15**, 1563-1577.

Waites, R. & Hudson, A. (1995) phantastica: a gene required for dorsoventrality of leaves in Antirrhinum majus. *development*, **121**, 2143-2153.

Wang, X.J., Reyes, J.L., Chua, N.H. & Gaasterland, T. (2004) Prediction and identification of Arabidopsis thaliana microRNAs and their mRNA targets. *Genome Biol*, **5**, R65.

Watanabe, K. & Okada, K. (2003) Two discrete cis elements control the abaxial side-specific expression of the FILAMENTOUS FLOWER gene in Arabidopsis. *Plant Cell*, **15**, 2592-2602.

Wenkel, S., Emery, J., Hou, B.H., Evans, M.M. & Barton, M.K. (2007) A feedback regulatory module formed by LITTLE ZIPPER and HD-ZIPIII genes. *Plant Cell*, **19**, 3379-3390.

Went, F.W. (1928) *Receuil des Travaux Botaniques Neerlandais*.

Wessel, D. & Flügge, U.I. (1984) A method for the quantitative recovery of protein in dilute solution in the presence of detergents and lipids. *Anal Biochem*, **138**, 141-143.

Williams, L., Grigg, S.P., Xie, M., Christensen, S. & Fletcher, J.C. (2005) Regulation of Arabidopsis shoot apical meristem and lateral organ formation by microRNA miR166g and its AtHD-ZIP target genes. *Development*, **132**, 3657-3668.

Xie, Z., Johansen, L.K., Gustafson, A.M., Kasschau, K.D., Lellis, A.D., Zilberman, D., Jacobsen, S.E. & Carrington, J.C. (2004) Genetic and functional diversification of small RNA pathways in plants. *PLoS Biol*, **2**, E104.

Yamamoto, R., Fujioka, S., Demura, T., Takatsuto, S., Yoshida, S. & Fukuda, H. (2001) Brassinosteroid levels increase drastically prior to morphogenesis of tracheary elements. *Plant Physiol*, **125**, 556-563.

Ye, Z.H., Freshour, G., Hahn, M.G., Burk, D.H. & Zhong, R. (2002) Vascular development in Arabidopsis. *Int Rev Cytol*, **220**, 225-256.

Yu, L., Yu, X., Shen, R. & He, Y. (2005) HYL1 gene maintains venation and polarity of leaves. *Planta*, **221**, 231-242.

Zhang, Y. (2005) miRU: an automated plant miRNA target prediction server. *Nucleic Acids Res*, **33**, W701-704.

Zhao, C., Craig, J.C., Petzold, H.E., Dickerman, A.W. & Beers, E.P. (2005) The xylem and phloem transcriptomes from secondary tissues of the Arabidopsis root-hypocotyl. *Plant Physiol*, **138**, 803-818.

Zhong, R., Demura, T. & Yea, Z. (2006) SND1, a NAC domain transcription factor, is a key regulator of secondary wall synthesis in fibers of Arabidopsis. *Plant Cell*, **18**, 3158–3170.

Zhong, R., Taylor, J.J. & Ye, Z.H. (1997) Disruption of interfascicular fiber differentiation in an Arabidopsis mutant. *Plant Cell*, **9**, 2159-2170.

Zhong, R. & Ye, Z.H. (2001) Alteration of auxin polar transport in the Arabidopsis ifl1 mutants. *Plant Physiol*, **126**, 549-563.

Zhou, G.K., Kubo, M., Zhong, R., Demura, T. & Ye, Z.H. (2007) Overexpression of miR165 affects apical meristem formation, organ polarity establishment and vascular development in Arabidopsis. *Plant Cell Physiol*, **48**, 391-404.

Zimmermann, P., Hirsch-Homann, M., Hennig, L. & Gruissem, W. (2004) Genevestigator. Arabidopsis microarray database and analysis toolbox. *Plant Physiol*, **136**, 2621-2632.

# Acknowledgements

To my thesis director, Dr. Pia Stieger, for giving me opportunity to work in her team and to carry this work in the best possible conditions. I thank you for your patience, trust and your sense to anticipate experiments. I also thank you for always having quick answers to my requests, on technicals concerns or on plant development literature.

To my thesis co-director, Felix Kessler, for welcoming me in the Laboratory of Plant Physiology in Neuchâtel. I really appreciated to always have an office door open for discussion and thank you for all the suggestions and advices.

To the members of my thesis committee, Prof. John Bowman and Dr. Philippe Reymond. I thank you for the advices and expertise you provided during all this PhD and for the carefull reading of my manuscript.

To Marlyse Meylan who helped me every time I needed it. I thank you for all the support and kindness during my presence in the laboratory. Without your help I would probably still be collecting seeds at the present time.

To Dr. Claire Bréhélin. I thank you for being always available to my numerous and almost daily questions on molecular biology, biochemistry and on the exact location of the cookies in the laboratory.

To Dr. Birgit Agne for her precious help with protein concerns, your expertise was really appreciated.

To Veronique Douet and Dany Arsic for the discussions on real-time PCR fine tunning and other subjects. I also would like to acknowledge Guillaume Gouzerh and Michèle Vlimant for their help on microscopy and sample preparation.

To Saul Rusconi for his help and sense of humor.

To all the current and previous members of the lpv laboratory and particularly to Sibylle Infanger, Joanne Schwaar, Pierre-Alexandre Vidi, Gwendoline Rahim, Jennifer Cadby, Sylvain Bischof, Meryl Martin, Astrid Willi, Christelle

Joss, Didier Lochmatter and Jana Smutny for the discussions and contributions to this work. The helpful and friendly atmosphere you established in this lab greatly contributed to make me work with pleasure .
To all the members of Prof. John Bowman's laboratory and especially to Yuval Eshed for providing a significant ratio of the biological material that was used during this PhD.
To the members of the Development laboratory in the Plant Sciences departement of the University of Bern, for the help with scanning electron microscopy.
To the Swiss National Science Fundation for providing the funding of this work. I also thank the University of Neuchâtel and NCCR Plant Survival doctoral school for the financial and logistical support.
To my parents for their kindness, continuous support and love. I am really gratefull.
Last but not least, to Clémentine Perrier for her support on molecular biology for one part but mostly for her patience and love.

# Annexe 1

# Interplay of auxin, KANADI and Class III HD-ZIP transcription factors in vascular tissue formation

Michael Ilegems[1], Marlyse Meylan-Bettex[1], John L. Bowman[2] and Pia A. Stieger[1*]

[1] Institute of Biology, University of Neuchâtel, Rue Emile Argand 11, Case Postale 158, 2009 Neuchâtel, Switzerland

[2] School of Biological Sciences, Monash University, Melbourne, Victoria 3800, Australia

*To whom correspondence should be addressed.

pia.stieger@unine.ch

**Running title: Regulators of vascular development**

**Key words: vasculature, auxin, KANADI, Class III HD-ZIP, cambium, xylem, pattern formation**

**Summary**

Differentiation of the vascular system starts with the recruitment of procambium cells. Precursors of xylem and phloem derive from procambium cells and are arranged in a collateral pattern in *Arabidpsis thaliana* with phloem at the periphery or abaxially and xylem in the center or adaxially, separated by procambium cells that are stabilised in their undifferentiated state. The conducting functions of vascular tissues require perfect cell alignment and tissue patterning. Class III HD-ZIP and KANADI gene family members have complementary expression patterns in the vasculature and their gain-of-function and loss-of-function mutants have complementary vascular phenotypes. This suggests that the two gene family members are regulators of a dorsiventral gradient system to regulate transversal arrangement of phloem, cambium and xylem. We have analysed the vasculature of plants with altered expression levels of Class III HD-ZIP and KANADI transcription factors in provascular cells. Removal of either KANADI or Class III HD-ZIP expression in procambium cells led to a wider distribution of auxin in internal tissues, to an excess of procambium cell recruitment and to increased cambium activity. Ectopic expression of KANADI1 in provascular cells inhibited procambium cell recruitment due to negative effects of KANADI1 on expression and polar localization of the auxin efflux-associated protein PINFORMED. Ectopic expression of Class III HD-ZIPs promoted xylem differentiation. We propose that Class III HD-ZIP and KANADI transcription factors control cambium activity, KANADI proteins by acting on auxin transport and Class III HD-ZIP proteins by promoting xylem differentiation.

## Introduction

The vascular system connects all parts of the plant body and serves as the transport system for nutrients, hormones and water, as well as in physical stabilization. It is composed of the meristematic tissue cambium and the differentiated units phloem and xylem and intervening parenchymous cells. In *Arabidopsis thaliana* the vascular system is organized in the parallel placement of xylem and phloem, called collateral pattern, which is found in many but not all seed plant species (Fig. 1A,B). The conducting functions of vascular tissues require perfect cell alignment and tissue continuity, transverse patterning within veins, proper integration within the non-vascular tissues, as well as coordinated maturation of the different vascular cell types.

Vascular differentiation is initiated from defined cells that are recruited within a growing organ to form continuous files – the procambium. Precursors of xylem and phloem differentiate from procambium cells. During this process, some procambial cells remain stabilized in their undifferentiated state and function as cambium cells (Busse and Evert, 1999a; Busse and Evert, 1999b; Eseau, 1965; Sachs, 1981; Steeves and Sussex, 1989).

Early physiological experiments and recent molecular studies have revealed hormonal regulators and several transcription factors that may govern the network of regulation in vascular tissue differentiation. The location of procambial strands is defined by the directional transport of the plant hormone auxin in a self-reinforcing canalization process from source to sink (Sachs, 1981; Sachs, 1991). This model is based on a feedback effect that auxin exerts on the polarity of its transport (Paciorek et al., 2005; Sauer et al., 2007). Indeed, basal localization of the auxin efflux associated protein PIN-FORMED1 (PIN1) in cell files is the earliest event that has been observed in developing procambium cells (Reinhardt et al., 2003; Scarpella et al., 2004; Scarpella et al., 2006). Along with the spatial restriction of PIN proteins to single cell files, the expression pattern of the auxin response factor *MONOPTEROS* (*MP/ARF5*) is restricted to procambim and developing xylem cells (Hardke and Berleth, 1998; Wenzel et al., 2007). The discontinous vasculature formed in *mp* loss-of-function mutants suggests MP functions in auxin-signal transduction during vascular development (Hardke and Berleth, 1998, Mattson et al., 2003).

Some procambium cells differentiate into protoxylem and protophloem precursors providing the vascular bundles with a specific transversal pattern. This pattern is likely formed and maintained

by dorsiventral gradients of antagonistically acting regulators. For example, the cytokinin class of plant hormones negatively regulates protoxylem specification and promotes cambium cell division rates and phloem differentiation. In protoxylem cells *ARABIDOPSIS HISTIDINE PHOSPHOTRANSFER PROTEIN 6* (*AHP6*) counteracts cytokinin signaling (Mähönen et al., 2000; Mähönen et al., 2006).

Phloem identity is specified by *ALTERED PHLOEM DEVELOPMENT* (*APL*), a MYB coiled-coil-type transcription factor that is expressed in phloem precursor cells and negatively influences xylem specification (Bonke et al., 2003). In *apl* mutants cells with xylem characteristics differentiate in the positions normally occupied by phloem. Factors that specify xylem identity have not been identified so far. However, Class III HD-ZIP transcription factors are candidates, since the 5 members encoded in the genome of *Arabidopsis thaliana*, namely *PHABULOSA* (*PHB*), *PHAVOLUTA* (*PHV*), *REVOLUTA* (*REV*), *ATHB15/CORONA* and *ATHB8* are expressed in the cambium, xylem precursors and developing xylem cells (Baima et al., 1995; McConnell et al., 2001; Ohashi-Ito and Fukuda, 2003; Ohashi-Ito et al., 2005; Otsuga et al., 2001; Prigge et al., 2005). *PHB, PHV* and *REV* are also expressed in the adaxial part of lateral organs and in meristems and act antagonistically on abaxially expressed transcription factors of the GARP family, the KANADI genes (Emery et al., 2003; Eshed et al., 2001; Eshed et al., 2004; Izhaki and Bowman; 2007; Kerstetter et al., 2001; McConnell and Barton, 1998; McConnell et al., 2001). KANADI genes (*KAN1, KAN2, KAN3*) are expressed in phloem precursor cells (Emery et al., 2003). Multiple KANADI loss-of-function mutants develop phloem cells, indicating that KANADI genes are not required for phloem identity. However, the arrangement of xylem and phloem changes to amphivasal with xylem surrounding the phloem in inflorescence stems of KANADI double, triple and quadruple loss-of-function mutants (Emery et al., 2003; Izhaki and Bowman, 2007). This phenotype is also found in the stem of *REV* and in lateral organs of *PHB* and *PHV* gain-of-function mutants, whereas multiple Class III HD-ZIP loss-of-function mutants have amphicribal vascular bundles with phloem surrounding the xylem (Emery et al, 2003, McConnell and Barton, 1998; McConnell et al., 2001; Zhong and Ye, 2004). Based on these phenotypes, Emery et al. (2003) proposed KANADI and Class III HD-ZIP transcription factors to be components of a dorsiventral gradient system for cell patterning in the vasculature.

Several observations suggest an association of KANADI and Class III HD-ZIP genes with auxin. Atypical expression patterns of the auxin efflux associated protein PIN1 were observed in KANADI and Class III HD-ZIP multiple mutants (Izhaki and Bowman, 2007). Class III HD-ZIP gene expression patterns are similar to auxin distribution patterns (Floyd et al., 2006; Floyd and Bowman 2006; Heisler et al., 2005). Mainly expression of *ATHB8*, but also of *REV*, *PHV* and *ATHB15* are induced by auxin (Baima et al., 1995; Zhou et al., 2007). *ETTIN* (*ARF3*) and *AUXIN RESPONSE FACTOR 4* (*ARF4*) mediate the KANADI abaxial pathway in lateral organ development and *kan1 kan2* phenotypes are strikingly similar to those of the *ettin arf4* double mutants (Pekker et al., 2005).

The aim of this study was to uncover the regulatory mechanisms of Class III HD-ZIP and KANADI transcription factors in transversal vascular patterning. In particular we were interested in early effects of antagonistic actions of these two classes of transcription factors on cell differentiation, gene expression and auxin distribution in procambium strands. In addition to studies of the vasculature in Class III HD-ZIP and KANADI mutants, we analysed vascular development in plants with manipulated Class III HD-ZIP and KANADI expression levels in procambium cells.

**Materials and methods**

*Plant material and growth conditions*

Plants were grown at 8 hours light / 16 hours dark for 25 days and transferred to 16 hours light /8 hours dark. To generate *pATHB15::LhG4* , five thousand base pairs of the 5' upstream sequence of *ATHB15* were amplified by PCR, and cloned in front of the *LhG4* sequence (pATHB15-LhG4-BJ36) and cloned into the binary pMLBART vector (Eshed et al., 2001). The plasmid was introduced into *Agrobacterium* strain ASE by electroporation and transformed into *Arabidopsis thaliana* (Ler) wild-type plants. To generate the *10Op::ATHB8δmiR* construct, a non-silent, single point mutation was introduced in the miR165/166 complementary site of an *ATHB8* cDNA and the cDNA was cloned behind the *10Op* sequence (10Op-ATHB8δmiR-BJ36) and transferred into the binary pMLBART vector (Eshed et al., 2001). The plasmid was introduced into *Agrobacterium* strain C58 by electroporation and transformed into *Arabidopsis* (Ler) wild type plants. Plants homozygous for the transactivation driver line *pATHB15::LhG4* were crossed to plants homozygous for the various reporter constructs *6Op::KAN1* (Eshed et al., 2001),

*10Op::miR165*, *10Op::ATHB8δmiR* and *10Op::GFP* (Alvarez et al., 2005). *APL::GUS* (Bonke et al., 2003) and *ATHB8::GUS* (Baima et al., 1995) plants were crossed with the *pATHB15::LhG4* driver line and plants homozygous for *pATHB15::LhG4* and either *APL::GUS* or *ATHB8::GUS* were crossed with homozygous reporter lines. Similarly, *PIN1::GFP* (Benkova et al., 2003) and *DR5rev::GFP* (Friml et al., 2003) were introduced in the *pATHB15::LhG4* line.

*RNA extraction and real time quantitative RT-PCR*

RNA was extracted from 15 day old plant seedlings grown on MS medium using the RNeasy® Plant mini Kit (Qiagen, Valencia, CA, USA). 1 µg of purified RNA was treated with DNAse RQ1 (Promega, Madison, WI, USA) and reverse transcribed using MMLV enzyme (Promega). Real-time quantitative RT-PCR was performed with a iCycler iQ Real-Time PCR detection system (Bio-rad, Hercules, CA, USA), using Absolute SYBR Green Fluorescein (ABgene, Epsom, Surrey, UK). The ribosomal *S16* gene was used as a standard control. Reactions were in triplicate in a 20 µL volume using 100 ng cDNA and 0.4 mM MgCl per reaction. Negative controls were in duplicate. The following QuantiTect Primer Assay (Qiagen) primers were used: QT00774634 (*S16*); QT00716583 (*PHB*); QT00870877 (*PHV*); QT00830802 (*KAN1*); QT00892654 (*PIN1*); QT00744926 (*APL*); QT00861847 (*MP*). Additionally, the following oligonucleotide probes (Microsynth, Balgach, Sg, Switzerland) were used at a concentration of 0.5 µM: for *REV* (5'-CGA ATA GTC CTG CTG GAT TG-3' and 5'-GAT CTC TGC AAT CTT CAT AG-3' ); for *ATHB15* (5'-AGT CCT GCA GGA CTT TTG TC-3' and 5'-CAA TCT CTG CAA CCC TTG TA-3' ); for *ATHB8* (5'-AAG CAG AGG AAA CTC AA G-3' and 5'-AAA TGT GAA TAC CGG AGA T-3'); for *KAN2* (5'-GCA GCT TCG TCA GGA CAA TC-3' and 5'-TCT CCG GAA GAA TTG GTC CA-3'). Thermal cycling parameters were 95°C for 15 minutes, followed by 45 cycles at 95°C for 30 seconds, 59.7°C for 30 seconds and 45°C for 45 seconds. RT-PCR specificity was tested with melt-curve analysis and electrophoresis. Experiments were repeated 3 times. All calculations were performed with the Gene Expression Macro 1.1 (Bio-Rad) macros for Excel (Microsoft, Redmond, WA, USA).

*Histology and in situ hybridizations*

Plant material was fixed in 50 mM Na-phosphate buffer (pH 7.2) containing formaldehyde (4%), gluteraldehyde (0.25%) at room temperature applying a low vacuum for 2 to 4 hours followed at

4°C over night, dehydrated (25%, 50%, 75%, 85%, 95%, 100% ethanol, 2x10 min each) and stained over night with eosin (0.1% in ethanol). To perform plastic sections, plant samples were embedded in Technovit 7100 (Heraeus, Hanau, Hesse, Germany) and 5 µm sections were made with a microtome (Leica Microsystems GmbH, Wetzlar, Hesse, Germany) and a glass knife and stained with 0.1% toluidine blue. For in situ hybridisations, plant samples were embedded in paraffin (Leica), 7 µm sections were made with metal blades. Sections were hybridized with digoxigenin-labelled riboprobes according to Vernoux et al. (2000).

*GUS assay and microscopy*

Histochemical GUS staining of seedlings was performed as described in Koizumi et al. (2000). After the reaction, samples were mounted in a 50% glycerol solution or dehydrated and embedded in Technovit 7100 (Heraeus). 5µm hypocotyl sections were stained with 0.1% safranine orange. For detection of GFP signals in *DR5::GFP*, *ATHB15>>GFP*, and *PIN1::PIN1-GFP* reporter lines, embryos were prepared in 50% glycerol and mounted under a coverslip. FM 4-64 dye at a concentration from 1 µM to 10 µM (Invitrogen, Carlsbad, CA, USA) in 50% glycerol was added to hypocotyl hand-sections. Samples were observed using a TCS SP5 DM6000 B confocal microscope (Leica). Images were treated in ImageJ.

**Results**

*KAN1 negatively acts on cambium activity*

To evaluate the role of *KANADI* genes in vascular tissue patterning, we studied the vascular anatomy in hypocotyls of *kan1 kan2 kan3 kan4* loss-of-function seedlings, and in seedlings with ectopic expression of *KAN1* in developing procambium cells. In wild type hypocotyls of 15 day old seedlings, the vasculature is composed of a central xylem plate, two peripheral phloem poles and cambium cells between xylem and phloem cells. This structure is encircled by a layer of pericycle cells and the endodermis (Fig. 1B,C). In *kan1 kan2 kan3 kan4* hypocotyls, the arrangement of xylem, cambium and phloem was not changed, but pericycle cells were composed of more than one cell layer and the number of cambium cells was increased (Fig. 1D,E). Extra cell divisions of pericycle and cambium cells were observed in the basal part of the hypocotyl (Fig. 1D) and were more frequent in the apical part of the hypocotyl, where the transition to the collateral vascular arrangement found in cotyledons occurs (Fig. 1E). Ectopic

expression of *KAN1* in procambium cells was accomplished by using the *ATHB15* promoter in the pOp/LhG4 transcription factor system (Moore et al., 1998). *ATHB15>>KAN1* seedlings formed no vascular tissue in the hypocotyl (Fig. 1F), shoot (Fig. 1I) or root (Fig. 1M). Effects of ectopic *KAN1* expression were not limited to the vasculature, since seedlings manifested reduced shoot and root growth and a variable number of cotyledons that varied from needle-like to heart-shaped (Fig. 1G). The shoot apical meristem (SAM) was reduced to a few cells or was lacking and primary leaves very rarely formed (Fig. 1H,I). Similarly, the root meristem was missing and cells at the tip of the root were differentiated (Fig. 1M). These observations suggest that KAN1 negatively controls meristematic activity of cells.

To determine if precursor cells of cambium, phloem and xylem were formed in *ATHB15>>KAN1* plants, we introduced the β-glucuronidase gene (GUS) controlled either by the promoter of *ATHB8* or of *APL* into *ATHB15>>KAN1* plants (Fig. 1K,L). *ATHB8::GUS* and *APL::GUS* expression were detected in primary and secondary veins of cotyledons in control plants, but in *ATHB15>>KAN1* seedlings only faint blue staining was observed after a prolonged incubation in the reaction medium in a pattern resembling fragmented developing vasculature. We quantified expression levels of genes involved in early steps of vasculature differentiation in *ATHB15>>KAN1* seedlings. Ectopic *KAN1* expression reduced the amount of Class III HD-ZIP transcription factors *REV*, *PHB*, *PHV*, *ATHB15* and *ATHB8* (Table 1). Most affected were *ATHB8* and *REV*, whereas expression of *ATHB15*, *PHB* and *PHV* were less reduced. Since ectopic expression of *KAN1* is driven by the *ATHB15* promoter, we quantified *KAN1* expression. *KAN1* expression was high in *ATHB15>>KAN1* seedlings compared to controls, whereas expression of *KAN2* was not changed, indicating that the transgene was active. Expression of *PIN1*, *MP* and *APL* was also reduced by ectopic *KAN1* expression. These results suggest that KAN1 acts negatively on early steps of vasculature differentiation.

*KAN1 expressed in preprocambium cells does not influence ATHB15 and MP expression, but negatively affects PIN1 activity during embryogenesis.*

To identify the stage of procambium differentiation that ectopic *KAN1* activity inhibits, we analysed expression patterns of *ATHB15*, *PIN1* and *MP* during embryogenesis. We followed activity domains of the *ATHB15* promoter using distribution patterns of the green fluorescent protein (GFP) in developing embryos and young seedlings of *ATHB15>>GFP* plants. In

globular stage embryos, GFP accumulated evenly throughout the subepidermal cells and was predominantly in the apical part of the embryo during the transition phase (Fig. 2A). By the heart stage, GFP was observed in vascular precursor cells and the SAM (Fig. 2B,C). In mature embryos, *ATHB15* expression was restricted to the SAM and procambium cells throughout the embryo, but was absent from the root meristem. In cotyledons, GFP accumulated in primary and secondary veins and also at the tip in hydathodes (Fig. 2D). This pattern corresponds to *ATHB15* expression patterns described earlier (Prigge et al., 2005; Ohashi-Ito et al., 2003).

In globular to heart stage embryos of *ATHB15>>KAN1;GFP* plants, GFP accumulated in a similar way as in controls (Fig. 2A,B), indicating that initial activity of the *ATHB15* promoter was not influenced by *KAN1*. However, in torpedo stage and mature embryos the GFP signal remained bright in the SAM, but was weaker in vascular precursors (Fig. 2C,D). In conclusion, expression of *KAN1* in the *ATHB15* domain had a minor influence on the activity of the *ATHB15* promoter in developing embryos until heart stage. However, the activity of the promoter was reduced in vascular precursor cells in embryos after heart stage and severely affected in young seedlings.

In parallel with *ATHB15* expression, we analyzed the localization of PIN1 with a *PIN1::PIN1-GFP* marker line and monitored auxin distribution using the auxin-inducible synthetic promoter *DR5rev* driving GFP expression (Benkova et al., 2003; Friml et al., 2003). In wild-type embryos, PIN1-GFP was detected in the epidermis in the apical regions of globular embryos. At transition stage, PIN1-GFP accumulated in the epidermis at convergence points marking future cotyledons and in internal tissues (Fig. 2E). At heart stage, PIN1-GFP was localized to epidermal cells in the distal regions of cotyledons and epidermal cells between cotyledons and the forming shoot apical meristem. During the heart stage, PIN1-GFP was detected at basal ends of procambium cells (Fig. 2F) and by torpedo stage, PIN1-GFP was detected in one continuous file of cells in cotyledons and in three cell files of the stele, predominantly localized to the basal end of cells (Fig. 2G). In the mature embryo, PIN1-GFP was detected in procambium cells throughout the plant body (Fig. 2H).

In *ATHB15>>KAN1* embryos, PIN1-GFP was detected in the epidermis of upper regions of the embryo at the transition stage, but no convergence points formed and the GFP signal was not detected in presumptive procambium cells (Fig. 2E). At heart stage, the GFP signal was localized to epidermal cells in the distal regions of developing cotyledons and randomly in a few cells of

internal tissue near cotyledon tips (Fig. 2F). In torpedo stage embryos, several files of cells in the cotyledons accumulated PIN1-GFP (Fig. 2G). The GFP signal was frequently located at the distal sides of these cells, suggesting auxin transport being directed towards the cotyledon tips (arrows in Fig. 2G). In mature embryos, either no GFP signal was detected, or patches of cells accumulated GFP in a non-polar manner (Fig. 2H).

Distribution of *DR5rev::GFP* in *ATHB15>>KAN1* embryos was comparable to the distribution in wild-type embryos until heart stage. In both genotypes, *DR5rev::GFP* was detected in the hypophysis and the uppermost suspensor cell, the place of root meristem formation (data not shown). At heart stage, GFP signals appeared in the tips of the developing cotyledons and in a single cell file of procambium precursor cells in wild-type embryos, but the corresponding GFP signal was variable, ranging from normal, to weak, to not detectable in the tips of developing cotyledons and was not narrowed down to a single file of procambium precursor cells in *ATHB15>>KAN1* embryos (Fig. 2I). In fully developed embryos, the GFP signal accumulated in hydathodes of cotyledons, in provasculature throughout the seedling and in the root apical meristem in wild-type plants, but was only occasionally detected in tips of cotyledons and rarely in the root meristem in *ATHB15>>KAN1* seedlings (Fig. 2K).

*MP* was present in all subepidermal cells in globular embryos and was confined to more central domains along the midlines of the cotyledons and the embryo axis at heart stage in a similar way as *ATHB15* in wild-type embryos (Fig. 2L,M, Hardke and Berleth 1998). Ectopic *KAN1* expression in procambium precursor cells had no influence on *MP* distribution during embryogenesis. *MP* mRNA accumulated in the subepidermal cells of globular embryos in a similar manner as in controls and in torpedo stage embryos was confined to vascular precursor cells in the cotyledons and the stele (Fig. 2L,M).

In summary, *KAN1* expression in domains of *ATHB15* activity negatively affected *PIN1* expression and distribution starting in transition stage embryos. In contrast, expression levels of *ATHB15* decreased after torpedo stage and *MP* was not affected during embryogenesis. Therefore we conclude that reductions of *ATHB15* and *MP* expression in *ATHB15>>KAN1* seedlings were not directly caused by KAN1. Ectopic *KAN1* expression in procambium cells exerted inhibitory effects on cambium cell formation and activity, whereas a lack of *KAN1* expression had stimulating effects on cambium activity. Inhibitory effects of ectopic *KAN1*

expression on the activity of PIN1 early during embryogenesis suggest that the influence of *KAN1* expression on cambium activity is mediated by auxin.

*Class III HD-ZIPs promote xylem differentiation and control cambium activity*

We examined the function of Class III HD-ZIPs in vascular tissue differentiation and patterning by analyzing vascular anatomy in hypocotyls with ectopic or inhibited Class III HD-ZIP expression. This transcription factor family is post-transcriptionally regulated by *miR165* and *miR166* (Emery et al., 2003; Jones-Rhoades et al., 2003; Jung and Park, 2007; Kim et al., 2005; Mallory et al., 2004; Tang et al., 2003; Williams et al., 2005). To study effects of ectopic Class III HD-ZIP expression during vascular development, we used *rev-10d* (Emery et al., 2003), as well as *ATHB15>>ATHB8-δmiR* plants, both containing one nucleotide substitution in the region complementary to *MIR165/166.* Expression of microRNA resistant *REV* coding sequence under the control of its endogenous promoter had only a slight influence on hypocotyl vascular anatomy, in that the stele contained an increased number of differentiated xylem cells (Fig. 3A,B). The same result was obtained when the microRNA resistant *ATHB8* coding sequence was expressed under the control of the *ATHB15* promoter (Fig. 3C).

It has been shown that multiple related genes can be quantitatively regulated by the expression of their miRNA (Alvarez et al., 2006). In order to reduce Class III HD-ZIP mRNA in preprocambium cells, we expressed *miR165* under the control of the *ATHB15* promoter. *ATHB15>>miR165* seedlings developed a defective vascular system. In the hypocotyl, most vascular cells displayed characteristics of cambium or parenchyma and the size of the stele and cell number within the stele were increased. The stele was surrounded by one cell layer of pericycle and one cell layer of endodermis (Fig. 3D). In *ATHB15>>miR165* inflorescence stems, differentiated xylem and phloem was present, but the transversal arrangement of cambium flanked by phloem abaxially and xylem adaxially was abolished (Fig. 3E). Islands of cambium cells flanked by phloem sieve elements, companion cells and parenchymea were surrounded by xylem (Fig. 3E, arrowheads). Furthermore, xylem elements in leaves and stems were partially disconnected (Fig. 3F). Expression of the procambium and protoxylem marker *ATHB8::GUS* and the protophloem marker *APL::GUS* was confined to vascular tissues in cotyledons of *ATHB15>>miR165* plants in a similar way as in control plants, but expression of *ATHB8::GUS* was often lacking in parts of the vasculature, indicating that a lack of Class III HD-ZIP activity

in provascular cells interfered with the proper formation of xylem cells (Fig. 3G,H). These results suggest that Class III HD-ZIP genes promote xylem differentiation and control cambium activity by negatively influencing cell proliferation.

Although bilateral symmetry was maintained in *ATHB15>>miR165* seedlings, they exhibited typical features of abaxialisation, found in Class III HD-ZIP multiple loss of function mutants. Cotyledons and leaves curled downwards, expansion of leaf lamina was inhibited, and petals were radialised (Fig. 3I-N), indicating that expression levels of Class III HD-ZIPs were reduced (Prigge et al., 2005). In addition, plant stature was dwarfed, growth was reduced and flowering was retarded. Quantification of Class III HD-ZIP expression levels in seedlings 15 days after germination showed that *ATHB15*, *PHB* and *PHV* expression levels were reduced in *ATHB15>>miR165* plants, but *ATHB8* remained stable and expression levels of *REV* were more than doubled (Table 1). Expression levels of *MP*, *APL* and *PIN1* increased, whereas *KAN1* expression was not changed and *KAN2* expression was slightly reduced.

Increased numbers of cambium cells and reduced or retarded differentiation of xylem and phloem cells in *ATHB15>>miR165* plants may be due to expanded expression domains of genes involved in cambium formation and maintenance. To test this hypothesis, we analysed auxin distribution and expression patterns of *ATHB15*, *ATHB8* and *APL* in hypocotyls of seedlings 15 days after germination. Since *ATHB8::GUS* and *ATHB15>>GFP* are not susceptible to microRNA degradation, their expression patterns show promoter activity domains of these genes. In wild-type hypocotyls, the procambium marker gene *ATHB8::GUS* was expressed in the pericycle, cambium and developing xylem elements and in the endodermis, but was absent from the phloem and fully differentiated xylem. In *ATHB15>>miR165* hypocotyls, *ATHB8::GUS* expression was strong in all stelar cells with the exception of phloem cells and a few cells that had initiated secondary cell wall formation (Fig. 4A). *APL::GUS* expression was confined to phloem cells, cambium and pericycle cells flanking the phloem in both control and *ATHB15>>mir165* hypocotyls (Fig. 4B). *ATHB15>>GFP* expression was found in cambium and protoxylem cells and was absent from the pericycle, phloem and differentiated xylem in hypocotyls of control plants (Fig. 4C). In *ATHB15>>miR165* plants, *ATHB15>>GFP* expression was found in patches throughout the stele (Fig. 4C). *DR5::GFP* was detected in pericycle, cambium and phloem cells in control plants, whereas in *ATHB15>>miR165* hypocotyls, the GFP signal was detected throughout the stele (Fig. 4D). The broader expression

pattern of *DR5::GFP* as well as of *ATHB15>>GFP* in vascular cells was already visible during embryogenesis in *ATHB15>>miR165* plants (Fig. 4E,F).

Thus, ectopic expression of *miR165* in preprocambium cells enlarged the expression patterns of *DR5::GFP*, *ATHB8::GUS* and *ATHB15>>GFP* in the stele, whereas expression of *APL::GUS* remained confined to phloem cells. Promoter activity of Class III HD-ZIPs might be regulated by auxin, since in *ATHB15>>miR165* seedlings, wider expression patterns of *ATHB8::GUS* and *ATHB15>>GFP* correlated with *DR5rev::GFP* distribution and in *ATHB15>>KAN1* embryos, the decrease of *ATHB15>>GFP* expression followed a decrease of the *DR5::GFP* signal. To test this hypothesis we incubated wild-type and *ATHB15>>KAN1* seedlings for 3 hours in 50 μM 1-naphthaleneacetic acid (NAA) and quantified mRNA levels of Class III HD-ZIP genes, *MP*, *PIN1*, *APL* and *KAN* genes (Table 1). In wild-type seedlings, externally applied NAA moderately increased the expression levels of *ATHB8* and *ATHB15*, whereas *REV* and *PHB* were not influenced by the treatment. Also induced by NAA were *PIN1* and *MP*. NAA treatments of *ATHB15>>KAN1* seedlings had minor effects on expression levels of Class III HD-ZIP genes and *MP*, but expression levels of *PIN1* were nearly doubled. Given the minor effects that auxin had on Class III HD-ZIP promoter activities in *ATHB15>>KAN1* seedlings, we conclude that additional factors of cambium cells might be necessary to maintain Class III HD-ZIP expression levels.

In conclusion, reduced levels of Class III HD-ZIP expression in preprocambium cells favored cambium cell formation and decreased xylem differentiation, whereas arrangement and differentiation of phloem cells were not directly influenced. In addition, expanded domains of cambium cells had stimulating effects on promoter activity of Class III HD-ZIP genes.

**Discussion**

A key role for Class III HD-ZIP and KANADI transcription factors in transversal patterning of vascular tissues is inferred from complementary vascular phenotypes of mutants of the two families. Here we show that KANADI and Class III HD-ZIP genes regulate spatial distributions of phloem, cambium and xylem by influencing cambium proliferation and auxin distribution and that vascular phenotypes in KANADI and Class III HD-ZIP mutants are due to altered activity domains of cambium cells.

*Cambium cell activity is controlled by auxin*

Vascular bundle formation in leaves is initiated by events in epidermal cells, where a peak of auxin accumulates, with auxin subsequently flowing into subepidermal layers in spatially restricted single cell files (Scarpella et al., 2006). *MP* expression accompanies the dynamic process of gradual refinement of *PIN1* expression in the ground tissue of leaf primordia, suggesting a regulatory feedback loop between auxin, *PIN1* and *MP* that regulates restriction of auxin transport to single cell files initiating procambium formation (Hardke and Berleth, 1998; Wenzel et al., 2007). A similar mechanism of initial vascular bundle formation may be proposed for embryogenesis, since *PIN1* and *MP* expression patterns in developing cotyledons are comparable to those in leaf primordia (Fig. 2; Benkova et al., 2003). Our investigations show that auxin transport is instructive for procambium cell differentiation and activity, but not for the establishment of a prepattern for vascular tissue formation. Procambium cell recruitment was inhibited when auxin was lacking in preprocambium cells of *ATHB15>>KAN1* plants, and conversely, was enhanced when auxin occurred in a wider spatial distribution in *ATHB15>>miR165* embryos. A prepattern for procambium cell development was evident in the initial expression of *MP* and *ATHB15*, but was not maintained after torpedo stage embryos that lack auxin transport into internal tissues. Thus auxin and procambial cell formation are required to maintain expression levels of genes directing early vascular tissue differentiation and cambium cell proliferation, but not for the establishment of a vascular prepattern.

The hypothesis of auxin being a trigger of cambium activity was already formulated in earlier studies. Enlarged veins and increased cambial activities were observed in plants with inhibited auxin transport and in *pin1* mutants (Gälweiler et al., 1998; Mattsson et al., 1999) and the high cambial activity mutant (*hca*) has altered cytokinin and auxin responses (Pineau et al., 2005). In pine trees the width of a radial concentration gradient of indole-3-acetic acid across the cambium and its differentiating derivatives regulates cambium activity (Uggla et al., 1998; Uggla et al., 2001).

*Cambium activity domains are controlled by KANADI and Class III HD-ZIPs*

*KAN1* exerts negative effects on cambium formation and activity. In *kan1 kan2 kan3 kan4* hypocotyls, cambium and pericycle cell divisions are increased (Fig. 1) and in inflorescence stems, phloem cells are encircled by cambium and xylem cells, probably due to cambium activity

on the abaxial side of phloem cells (Inzhaki and Bowman, 2007). In plants with ectopic vascular *KAN1* expression the development of the vascular system is inhibited (Eshed et al, 2001; Kerstetter et al., 2001, Fig. 1). Restriction of cambium activity by *KAN1* may be mediated by auxin, since recent and the present studies on KANADI genes propose a function of this family of transcription factors in regulating auxin action. KANADI multiple loss-of-function mutants exhibit ectopic *PIN1* expression in cells that normally express KANADI (Izhaki and Bowman, 2007). Ectopic expression of *KAN1* in presumptive procambium cells severely affects the local arrangement of PIN1 in procambium precursor cells (Fig. 2). This observation implies a negative action of KAN1 on procambium cell formation either due to a general effect of *KAN1* expression on meristematic cell activity, or due to inhibition of *PIN1* expression or polar localization and thus a lack of auxin. Since *MP* and *AtHB15* were not directly affected by *KAN1* we favor the hypothesis of KAN1 exerting inhibitory effects via auxin efflux proteins.

The effects of ectopic *KAN1* expression in *ATHB15>>KAN1* seedlings on embryo polarity and root and shoot development further strengthen the idea that KAN1 negatively regulates, directly or indirectly, the activity of PIN proteins. Establishment of cotyledons from the shoot apical meristem in late globular embryos involves boundary genes as well as regulated auxin transport and signaling (Aida et al., 1999; Furutani et al., 2004; Treml et al., 2005). Activation of boundary gene expression such as *CUP-SHAPED COTYLEDON1* (*CUC1*), *CUC2* and *STM* is closely associated with auxin flow, suggesting expression domains of boundary genes being patterned by the cycles of PIN1 focus or an upstream action of boundary genes on PIN1 behavior (Furutani et al., 2004; Heisler et al., 2005). Subcellular polar localization of PIN1 is controlled by the antagonistic regulation of PIN1 phosphorylation by the Ser-Thr protein kinase PINOID and PP2A phosphatase (Benjamins et al., 2001; Friml et al., 2004; Lee and Cho, 2006; Michniewicz et al., 2007). Root meristem formation from the hypophysis and the uppermost suspensor cell depends on auxin accumulation in these cells (Aida et al., 2004; Blilou et al., 2005; Sabatini et al., 1999). Unstable numbers and partial fusions of cotyledons may reflect disorganized auxin transport in the epidermis of globular to heart stage embryos and disappearance of the auxin maximum in the root meristem suggests loss of auxin transport into the root in *ATHB15>>KAN1* seedlings.

Class III HD-ZIPs may be seen as differentiation promoting factors that temporally and spatially coordinate differentiation of xylem cells in vascular tissues. Seedlings with ectopic Class III HD-

ZIP expression developed more xylem cells in the hypocotyl vasculature, whereas seedlings with reduced Class III HD-ZIP activity in preprocambium cells developed a vascular system with fewer xylem cells that were sometimes disconnected. Broader auxin distribution and increased stele cambium cell proliferation in *ATHB15>>miR165* plants might be due to a reduction in xylem differentiation with a concomitant increase of cambium and parenchymous cells, in which auxin can be transported. In SAMs it has been shown that the AP2-domain proteins DORNROESCHEN (DRN) and DRN-like (DRNL) control SAM development by promoting differentiation in the peripheral zone (Kirch et al., 2003), and also negatively acting on auxin response factors and influencing auxin transport during embryogenesis (Chandler et al. 2007; Nag et al., 2007). Class III HD-ZIP proteins interact with DRN and DRNL (Chandler et al., 2007). It is therefore tempting to speculate that Class III HD-ZIP proteins, in concert with DRN/DRNL, balance cell proliferation and differentiation in meristematic tissues via interactions with auxin signaling and perception.

Class III HD-ZIP gene expression, in particular *ATHB8*, but also of *REV, PHV* and *ATHB15* is induced by auxin (Table 1, Baima et al., 1995, Zhou et al., 2007). We found enlarged activity domains of the promoters *ATHB8* and *ATHB15* in the vasculature of *ATHB15>>miR165* seedlings and reduced activity of the *ATHB15* promoter in *ATHB15>>KAN1* seedlings. Class III HD-ZIP promoter activity positively correlated with the presence of auxin. However, addition of exogenous auxin to *ATHB15>>KAN1* seedlings increased Class III HD-ZIP transcription levels only slightly compared to the large increase in *PIN1* mRNA, indicating that additional factors probably contained in cambial cells are necessary to regulate Class III HD ZIP gene expression. For instance, *ATHB8* is likely regulated by the auxin response factor *MP*, since *mp* mutants express all members of the Class III HD-ZIP gene family except *ATHB8* (data not shown). In *ATHB15>>miR165* seedlings, mRNA levels of *ATHB8* were not affected and *REV* mRNA levels were increased (Table 2). We propose that during embryogenesis, Class III HD-ZIP mRNAs were reduced in preprocambium cells of *ATHB15>>miR165* plants. Consequently, transversal auxin gradients broadened and more procambium cells were recruited, resulting in higher Class III HD-ZIP transcription levels.

A feed-back mechanism between PIN proteins and the auxin inducible AP2-domain transcription factor *PLETHORA* (*PLT*) regulates root meristem patterning by focusing the auxin maximum, which in turn restricts the expression domain of *PLT* genes (Blilou et al., 2005). A similar

regulatory mechanism between auxin, PIN proteins and Class III HD-ZIP transcription factors may restrict auxin transport domains as well as Class III HD-ZIP expression domains in the differentiating vasculature.

*A model for interactions of auxin, Class III HD-ZIP and KANADI in vascular tissue patterning*

Integrating our research observations with results obtained in other research groups, we draw the following model for procambium cell recruitment and vascular tissue differentiation. Embryonic vascular tissue formation begins with opposing epidermal subcellular polarity of PIN1 converging towards a central point (convergence point) at the tips of future cotyledons where it is associated with a subepidermal basal orientation of PIN1. During cotyledon initiation, PIN1 is basally located in cells along the entire incipient midvein. Auxin flow in cell files of internal tissues from the cotyledon tips towards the root meristem induces the formation and maintenance of procambium cells (Fig. 5A). The formation of convergence points and subepidermal expression of *PIN1* is preceded by a reduction of *PIN1* expression at the basal abaxial domain of the embryo. This correlates with the expression of *KAN* genes and a reversal at the central apical region of the embryo mediated in part by the expression of boundary genes such as *PID* and the *CUC* transcription factors. Coincident Class III HD-ZIP and *MP* gene expression is restricted to an internal corridor of future cotyledons, hypocotyl and root. This overlaps with accumulation of PIN1 at the basal ends of preprocambium cells, but the two events are independent and separable (Fig. 5B). Class III HD-ZIP transcription factors induce differentiation of xylem cells, whereas phloem cell differentiation is confined to cells with *APL* expression. The number and activity of cambium cells is adjusted by a feedback-regulation between auxin transport proteins and Class III HD-ZIP transcription factors at sites of xylem differentiation, and by KANADI gene expression at sites of phloem formation (Fig. 5C).

**Acknowledgments**

We thank Sandra Floyd and Jan Traas for stimulating discussions, Yuval Eshed for sharing unpublished plant material, Therese Mandel for technical help with in situ hybridizations, Saul Rusconi and Astrid Willi for help in the laboratory. This research was supported by the Swiss National Foundation (P. S.), research projects 3100AO-105364/1 and PIOIA-117064/1 and the Australian Research Council (J. L. B.; DP0771232, FF0561326)

## References


**Aida, M., Ishida, T., and Tasaka, M.** (1999). Shoot apical meristem and cotyledon formation during Arabidopsis embryogenesis: interaction among the CUP-SHAPED COTYLEDON and SHOOT MERISTEMLESS genes. Development **126,** 1563-1570.

**Aida, M., Beis, D., Heidstra, R., Willemsen, V., Blilou, I., Galinha, C., Nussaume, L., Noh, Y.S., Amasino, R., and Scheres, B.** (2004). The PLETHORA genes mediate patterning of the Arabidopsis root stem cell niche. Cell **119,** 109-120.

**Alvarez J.P., Pekker I., Goldshmidt A., Blum E., Amsellem Z., Eshed Y.** (2005). Endogenous and synthetic MicroRNAs stimulate simultaneous, efficient, and localized regulation of multiple targets in diverse species. Plant Cell **18,** 1134-1151.

**Baima, S., Nobili, F., Sessa, G., Lucchetti, S., Ruberti, I., and Morelli, G.** (1995). The expression of the Athb-8 homeobox gene is restricted to provascular cells in Arabidopsis thaliana. Development **121,** 4171-4182.

**Benjamins, R., Quint, A., Weijers, D., Hooykaas, P., and Offringa, R.** (2001). The PINOID protein kinase regulates organ development in Arabidopsis by enhancing polar auxin transport. Development **128,** 4057-4067.

**Benkova, E., Michniewicz, M., Sauer, M., Teichmann, T., Seifertova, D., Jurgens, G., and Friml, J.** (2003). Local, efflux-dependent auxin gradients as a common module for plant organ formation. Cell **115,** 591-602.

**Blilou, I., Xu, J., Wildwater, M., Willemsen, V., Paponov, I., Friml, J., Heidstra, R., Aida, M., Palme, K., and Scheres, B.** (2005). The PIN auxin efflux facilitator network controls growth and patterning in Arabidopsis roots. Nature **433,** 39-44.

**Bonke, M., Thitamadee, S., Mahonen, A.P., Hauser, M.T., and Helariutta, Y.** (2003). APL regulates vascular tissue identity in Arabidopsis. Nature **426,** 181-186.

**Busse J.S., Evert R.F.** (1999a). Pattern of differentiation of the first vascular elements in the embryo and seedling of Arabidopsis thaliana. Int. J. Plant Sci. **160**, 1-13.

**Busse, J.S., and Evert, R.F.** (1999b). Vascular Differentiation and Transition in the Seedling of Arabidopsis thaliana (Brassicaceae). International Journal of Plant Sciences **160,** 241-251.

**Chandler, J.W., Cole, M., Flier, A., Grewe, B., and Werr, W.** (2007). The AP2-type transcription factors DORNROSCHEN and DORNROSCHEN-LIKE redundantly control Arabidopsis embryo patterning via interaction with PHAVOLUTA. Development **134**, 1653-1662.

**Emery, J.F., Floyd, S.K., Alvarez, J., Eshed, Y., Hawker, N.P., Izhaki, A., Baum, S.F., and Bowman, J.L.** (2003). Radial patterning of Arabidopsis shoots by class III HD-ZIP and KANADI genes. Curr Biol **13,** 1768-1774.

**Eseau K.** (1965). Vascular differentiation in plants. Holt, Rinehart, Winston, New York.

**Eshed Y., Baum S.F., Perea J.V., Bowman J.L.** (2001). Establishment of polarity in lateral organs of plants. Curr. Biol. **11**, 1251-1260.

**Eshed, Y., Izhaki, A., Baum, S.F., Floyd, S.K., and Bowman, J.L.** (2004). Asymmetric leaf development and blade expansion in Arabidopsis are mediated by KANADI and YABBY activities. Development **131,** 2997-3006.

**Floyd, S.K., and Bowman, J.L.** (2006). Distinct developmental mechanisms reflect the independent origins of leaves in vascular plants. Curr Biol **16,** 1911-1917.

**Floyd, S.K., Zalewski, C.S., and Bowman, J.L.** (2006). Evolution of class III homeodomain-leucine zipper genes in streptophytes. Genetics **173,** 373-388.

**Friml, J., Vieten, A., Sauer, M., Weijers, D., Schwarz, H., Hamann, T., Offringa, R., and Jurgens, G.** (2003). Efflux-dependent auxin gradients establish the apical-basal axis of Arabidopsis. Nature **426,** 147-153.

**Friml, J., Yang, X., Michniewicz, M., Weijers, D., Quint, A., Tietz, O., Benjamins, R., Ouwerkerk, P.B., Ljung, K., Sandberg, G., Hooykaas, P.J., Palme, K., and Offringa, R.** (2004). A PINOID-dependent binary switch in apical-basal PIN polar targeting directs auxin efflux. Science **306,** 862-865.

**Furutani, M., Vernoux, T., Traas, J., Kato, T., Tasaka, M., and Aida, M.** (2004). PIN-FORMED1 and PINOID regulate boundary formation and cotyledon development in Arabidopsis embryogenesis. Development **131,** 5021-5030.

**Galweiler, L., Guan, C., Muller, A., Wisman, E., Mendgen, K., Yephremov, A., and Palme, K.** (1998). Regulation of polar auxin transport by AtPIN1 in Arabidopsis vascular tissue. Science **282,** 2226-2230.

**Hardtke, C.S., and Berleth, T.** (1998). The Arabidopsis gene MONOPTEROS encodes a transcription factor mediating embryo axis formation and vascular development. Embo J **17,** 1405-1411.

**Hawker, N.P., and Bowman, J.L.** (2004). Roles for Class III HD-Zip and KANADI genes in Arabidopsis root development. Plant Physiol **135,** 2261-2270.

**Heisler, M.G., Ohno, C., Das, P., Sieber, P., Reddy, G.V., Long, J.A., and Meyerowitz, E.M.** (2005). Patterns of auxin transport and gene expression during primordium development revealed by live imaging of the Arabidopsis inflorescence meristem. Curr Biol **15,** 1899-1911.

**Izhaki, A., and Bowman, J.L.** (2007). KANADI and class III HD-Zip gene families regulate embryo patterning and modulate auxin flow during embryogenesis in Arabidopsis. Plant Cell **19,** 495-508.

**Jung J.H. and Park C.M.** (2007). MIR166/165 genes exhibit dynamic expression patterns in regulating shoot apical meristem and floral development in Arabidopsis. Planta **225**, 1327-1338.

**Kerstetter, R.A., Bollman, K., Taylor, R.A., Bomblies, K., and Poethig, R.S.** (2001). KANADI regulates organ polarity in Arabidopsis. Nature **411,** 706-709.

**Kim, J., Jung, J.H., Reyes, J.L., Kim, Y.S., Kim, S.Y., Chung, K.S., Kim, J.A., Lee, M., Lee, Y., Narry Kim, V., Chua, N.H., and Park, C.M.** (2005). microRNA-directed cleavage of ATHB15 mRNA regulates vascular development in Arabidopsis inflorescence stems. Plant J **42,** 84-94.

**Kirch, T., Simon, R., Grunewald, M., and Werr, W.** (2003). The DORNROSCHEN/ENHANCER OF SHOOT REGENERATION1 gene of Arabidopsis acts in the control of meristem ccll fate and lateral organ development. Plant Cell **15,** 694-705.

**Koizumi K., Sugiyama M., Fukuda H.** (2000). A series of novel mutants of Arabidopsis thaliana are defective in the formation of continuous vascular networks: calling the auxin signal flow canalization hypothesis into question. Development **127**, 3197-3204

**Lee, S.H., and Cho, H.T.** (2006). PINOID positively regulates auxin efflux in Arabidopsis root hair cells and tobacco cells. Plant Cell **18,** 1604-1616.

**Mähönen, A.P., Higuchi, M., Tormakangas, K., Miyawaki, K., Pischke, M.S., Sussman, M.R., Helariutta, Y., and Kakimoto, T.** (2006). Cytokinins regulate a bidirectional phosphorelay network in Arabidopsis. Curr Biol **16,** 1116-1122.

**Mähönen A.P., Bonke M., Kauppinen L., Riikonen M., Benfey P., Helariutta Y.** (2000). A novel two-component hybrid molecule regulates vascular morphogenesis of the Arabidopsis root. Genes Dev. **14**, 2938-2943.

**Mallory A.C., Reinhart B.J., Jones-Rhoades M.W., Tang G., Zamore P.D., Barton M.K. and Bartel D.P.** (2004). MicroRNA control of PHABULOSA in leaf development: importance of pairing to the microRNA 5′ region. EMBO J. **23,** 3356–3364.

**Mattsson, J., Sung, Z.R., and Berleth, T.** (1999). Responses of plant vascular systems to auxin transport inhibition. Development **126,** 2979-2991.

**Mattsson, J., Ckurshumova, W., and Berleth, T.** (2003). Auxin signaling in Arabidopsis leaf vascular development. Plant Physiol **131,** 1327-1339.

**Michniewicz, M., Zago, M.K., Abas, L., Weijers, D., Schweighofer, A., Meskiene, I., Heisler, M.G., Ohno, C., Zhang, J., Huang, F., Schwab, R., Weigel, D., Meyerowitz, E.M., Luschnig, C., Offringa, R., and Friml, J.** (2007). Antagonistic regulation of PIN phosphorylation by PP2A and PINOID directs auxin flux. Cell **130,** 1044-1056.

**McConnell JR., Barton MK.** (1998) Leaf polarity and meristem formation in Arabidopsis. Development **125**, 2935-2942.

**McConnell JR., Emery J., Eshed, Y, Bao, N., Bowman J., Barton MK.** (2001) Role of PHABULOSA and PHAVOLUTA in determining radial patterning in shoots. Nature **411**, 709-713.

**Moore, I., Galweiler, L., Grosskopf, D., Schell, J., and Palme, K.** (1998). A transcription activation system for regulated gene expression in transgenic plants. Proc Natl Acad Sci U S A **95,** 376-381.

**Nag, A., Yang, Y., and Jack, T.** (2007). DORNROSCHEN-LIKE, an AP2 gene, is necessary for stamen emergence in Arabidopsis. Plant Mol Biol **65,** 219-232.

**Ohashi-Ito K. and Fukuda H.** (2003). HD-Zip III homeobox genes that include a novel member, ZeHB-13 (Zinnia)/ATHB-15 (Arabidopsis), are involved in procambium and xylem cell differentiation. Plant Cell Physiol **44**, 1350-1358.

**Ohashi-Ito K., Kubo M., Demura T. and Fukuda H.** (2005). Class III homeodomain leucine-zipper proteins regulate xylem cell differentiation. Plant Cell Physiol. **46**, 1646-1656.

**Otsuga D., DeGuzman B., Prigge M.J., Drews G.N., Clark S.E.** (2001). REVOLUTA regulates meristem initiation at lateral positions. Plant J **25**, 223-236.

**Paciorek, T., Zazimalova, E., Ruthardt, N., Petrasek, J., Stierhof, Y.D., Kleine-Vehn, J., Morris, D.A., Emans, N., Jurgens, G., Geldner, N., and Friml, J.** (2005). Auxin inhibits endocytosis and promotes its own efflux from cells. Nature **435,** 1251-1256.

**Pekker, I., Alvarez, J.P., and Eshed, Y.** (2005). Auxin response factors mediate Arabidopsis organ asymmetry via modulation of KANADI activity. Plant Cell **17,** 2899-2910.

**Pineau, C., Freydier, A., Ranocha, P., Jauneau, A., Turner, S., Lemonnier, G., Renou, J.P., Tarkowski, P., Sandberg, G., Jouanin, L., Sundberg, B., Boudet, A.M., Goffner, D., and Pichon, M.** (2005). hca: an Arabidopsis mutant exhibiting unusual cambial activity and altered vascular patterning. Plant J **44,** 271-289.

**Prigge, M.J., Otsuga, D., Alonso, J.M., Ecker, J.R., Drews, G.N., and Clark, S.E.** (2005). Class III homeodomain-leucine zipper gene family members have overlapping, antagonistic, and distinct roles in Arabidopsis development. Plant Cell **17,** 61-76.

**Reinhardt, D., Pesce, E.R., Stieger, P., Mandel, T., Baltensperger, K., Bennett, M., Traas, J., Friml, J. and Kuhlemeier, C.** (2003). Regulation of phyllotaxis by polar auxin transport. Nature **426,** 255-260.

**Sabatini, S., Beis, D., Wolkenfelt, H., Murfett, J., Guilfoyle, T., Malamy, J., Benfey, P., Leyser, O., Bechtold, N., Weisbeek, P., and Scheres, B.** (1999). An auxin-dependent distal organizer of pattern and polarity in the Arabidopsis root. Cell **99,** 463-472.

**Sachs T.** (1981). The control of vascular development. Annu. Rev. Plant Physiol. **30**, 313-337.

**Sachs, T.** (1991). Cell polarity and tissue patterning in plants. Development Suppl. **1,** 83 -93.

**Sauer, M., Balla, J., Luschnig, C., Wisniewska, J., Reinohl, V., Friml, J., and Benkova, E.** (2006). Canalization of auxin flow by Aux/IAA-ARF-dependent feedback regulation of PIN polarity. Genes Dev **20,** 2902-2911.

**Scarpella, E., Francis, P., and Berleth, T.** (2004). Stage-specific markers define early steps of procambium development in Arabidopsis leaves and correlate termination of vein formation with mesophyll differentiation. Development **131,** 3445-3455.

**Scarpella, E., Marcos, D., Friml, J., and Berleth, T.** (2006). Control of leaf vascular patterning by polar auxin transport. Genes Dev **20,** 1015-1027.

**Steeves T.A. and Sussex I.M.** (1989). Patterns in plant development, 2nd ed. (New York: Cambridge University Press).

**Tang, G., Reinhart, B.J., Bartel D.P. and Zamore P.D.** (2003). A biochemical framework for RNA silencing in plants. Genes & Development **17**, 49–63.

**Treml, B.S., Winderl, S., Radykewicz, R., Herz, M., Schweizer, G., Hutzler, P., Glawischnig, E., and Ruiz, R.A.** (2005). The gene ENHANCER OF PINOID controls cotyledon development in the Arabidopsis embryo. Development **132,** 4063-4074.

**Uggla, C., Mellerowicz, E.J., and Sundberg, B.** (1998). Indole-3-acetic acid controls cambial growth in scots pine by positional signaling. Plant Physiol **117,** 113-121.

**Uggla, C., Magel E., Moritz T. and Sundberg, B.** (2001). Function and Dynamics of Auxin and Carbohydrates during Earlywood/Latewood Transition in Scots Pine. Plant Physiol **125**, 2029–2039.

**Vernoux T.**, **Kronenberger J, Grandjean O, Laufs P, Traas J** (2000) PIN-FORMED 1 regulates cell fate at the periphery of the shoot apical meristem. Development **127,** 5157-5165

**Wenzel, C.L., Schuetz, M., Yu, Q., and Mattsson, J.** (2007). Dynamics of MONOPTEROS and PIN-FORMED1 expression during leaf vein pattern formation in Arabidopsis thaliana. Plant J **49,** 387-398.

**Williams, L., Grigg, S.P., Xie, M., Christensen, S., and Fletcher, J.C.** (2005). Regulation of Arabidopsis shoot apical meristem and lateral organ formation by microRNA miR166g and its AtHD-ZIP target genes. Development **132,** 3657-3668.

**Zhou, G.K., Kubo, M., Zhong, R., Demura, T., and Ye, Z.H.** (2007). Overexpression of miR165 affects apical meristem formation, organ polarity establishment and vascular development in Arabidopsis. Plant Cell Physiol **48,** 391-404.

**Zhong, R.Q. and Ye, Z.H.** (2004). Amphivasal vascular bundle 1, a gain-of-function mutation of the IFL1/REV gene, is associated with alterations in the polarity of leaves, stems and carpels. Plant Cell Physiol **45**: 369-385.

**Legends to figures**

**Figure 1.** *Effects of altered KANADI expression in vascular bundles.* (A) Schematic drawing of collateral vascular arrangement and the corresponding distribution of factors involved in the regulation of vascular tissue differentiation in *Arabidopsis thaliana*. (B) Schematic drawing of vascular arrangement in the hypocotyl. (C) Transverse section through the hypocotyl of wild type, (D,E) *kan1 kan2 kan3 kan4* and (F) *ATHB15>>KAN1* seedlings. Extra cell divisions in the cambium and pericycle in *kan1 kan2 kan3 kan4* hypocotyls are indicated (arrowhead). (G) Phenotype of *ATHB15>>KAN1* seedlings with different penetrance levels of the transgene. Shoot and root growth are reduced and the establishment of bilateral symmetry is affected. (H) Longitudinal sections (5 μm) through the shoot apex of a wild type and (I) an *ATHB15>>KAN1* seedling. Expression of the *ATHB8::GUS* and the *APL::GUS* genes observed in the vasculature of wild type seedlings (K) are absent in *ATHB15>>KAN1* (L) seedlings. (M) longitudinal section through the root of a *ATHB15>>KAN1* seedling. Scale bars C-E=50 μm, F-M= 100 μm; p=pericycle, e=endodermis.

**Figure 2.** *Expression patterns of ATHB15, PIN1, DR5rev and MP in ATHB15>>KAN1 embryos.* (A-D) Activity domains of the *ATHB15* promoter during embryogenesis are visualized by expressing *ATHB15>>GFP* in wild-type or *ATHB15>>KAN1* embryos. (A) transition stage, (B) heart stage, (C) torpedo stage, (D) mature embryo. (E-H) Localisation of *PIN1::PIN1-GFP* in wild-type and *ATHB15>>KAN1* embryos. PIN1-GFP accumulates in the epidermis at convergence points marking the cotyledon tips (arrows) and in internal tissues in transition (E) and heart stage (F) embryos and accumulates at the basal ends of cells arranged in single cell files (arrows) in internal tissues in torpedo stage (G) in wild-type embryos. In *ATHB15>>KAN1* embryos, expression of *PIN1::PIN1-GFP* is reduced in the epidermis and internal tissues in transition (E) and heart stage embryos (F) and accumulates preferentially at the apical sides of cells (arrows) in the internal tissues, and is not in single cell files during torpedo stage (G). (H) In mature embryos *PIN1-GFP* is localized to provascular cells throughout wild-type embryos, but a faint signal of *PIN1-GFP* expression is observed in multiple cells in internal tissues in *ATHB15>>KAN1* embryos. (I) *DR5rev::GFP* accumulates in single cell files of preprocambium

cells in developing cotyledons in wild-type torpedo stage embryos, but is reduced and not restricted to single cell files in *ATHB15>>KAN1* cotyledon tips. (K) In mature wild-type embryos, *DR5rev::GFP* is detected in cotyledon tips, the procambium and the root meristem, but is reduced in cotyledon tips, the procambium and the root meristem of *ATHB15>>KAN1* plants. (L,M) mRNA expression pattern of *MP* in wild-type and *ATHB15>>KAN1* torpedo embryos. (L) Longitudinal view, (M) transverse section of torpedo cotyledons. Scale bars = 50 μm.

**Figure 3.** *Effects of altered Class III HD-ZIP expression in vascular bundles.* (A) Transverse section through hypocotyls of wild type, (B) *rev-10d* (C) *ATHB15>>ATHB8δmiR* and (D) *ATHB15>>miR165* seedlings. Xylem cell number is increased in *rev-10d* and *ATHB15>>ATHB8δmiR* hypocotyls (asterisks in B,C) and cambium cell number is increased in *ATHB15>>miR165* hypocotyls. (E) Vasculature of inflorescence stems. In wild type, vascular bundles are composed of phloem towards the outside, cambium in the middle and xylem towards the inside of the stem and are separated by interfascicular spaces, but in *ATHB15>>miR165* inflorescence stems, the arrangement of phloem, xylem and cambium is changed. (F) Xylem strands in leaves are disconnected in *ATHB15>>miR165* plants (arrows). (G) Expression of the *ATHB8::GUS* and the *APL::GUS* genes is observed in the vasculature in cotyledons of wild-type seedlings. (H) In *ATHB15>>miR165* cotyledons, *APL::GUS* expression is contiguous throughout the entire vascular system, whereas *ATHB8::GUS* expression is fragmented. (I) SAMs of *ATHB15>>miR165* seedlings are missing or reduced in size. (K) *ATHB15>>miR165* seedlings have reduced growth, (L) cotyledons are epinastic, (M) leaf expansion is reduced and (N) flowers have radialised petals. Scale bars A-D=50 μm, E,I=100 μm.

**Figure 4.** *Influence of miR165 on expression patterns of ATHB8::GUS, APL::GUS, ATHB15>>GFP and DR5rev::GUS.* The distribution of GUS in vascular cells of the hypocotyl of wild-type and *ATHB15>>miR165* seedlings was analysed 15 days after germination: (A) *ATHB8::GUS,* (B) *APL::GUS*. Expression patterns of *ATHB15>>GFP* were analysed in (C) the hypocotyl 15 days after germination and (E) in mature embryos of wild-type and *ATHB15>>miR165* plants. Expression patterns of *DR5rev::GFP* were analysed in (D) the hypocotyl 15 days after germination and (F) in mature embryos of wild-type and *ATHB15>>miR165* plants. Scale bars 50 μm.

**Figure 5.** *A theoretical model of vascular tissue differentiation.* (A) At transition state, auxin is transported in the epidermis from lower parts of the embryo and from the SAM towards developing cotyledon tips, where auxin accumulates in a convergence point and is directed towards the root meristem in cell files of internal tissues. (B) Expression patterns of *KANADI*, *Class III HD-ZIP*, *MP*, *PID* and *CUC* genes during heart stage. Expression of *KANADI* in lower parts of the embryo restricts *PIN1* activity and *PID*, *CUC1* and *CUC2* induce reversal polarity of PIN1 in the epidermis to direct auxin transport towards the cotyledon tips. (C) Transversal arrangement of phloem, cambium and xylem. Cambium activity is maintained in cells with auxin transport. Canlisation of auxin is controlled by a positive feedback effect of auxin on *PIN1* expression and polarity, by a negative action of *KANADI* on *PIN1* activity and by the promoting effect of *Class III HD-ZIPs* on xylem differentiation. Equilibrium between cambium proliferation and xylem differentiation is established through stimulation by auxin on cambium proliferation and *Class III HD-ZIP* transcription and a negative feedback effect of Class III HD-ZIP activity on cambium proliferation. Expression levels of *Class III HD-ZIPs* are modulated by miR165/166.

**Table 1**. *mRNA quantifications of genes involved in vascular tissue differentiation by real-time RT-PCR.*

| | *ATHB15::LhG4* | | *ATHB15>>KAN1* | | *ATHB15>>miR165* |
|---|---|---|---|---|---|
| Gene | - NAA | +NAA | -NAA | +NAA | -NAA |
| *REVOLUTA* | 1 | 1.1 ± 0.21 | 0.05 ±0.01 | 0.17 ± 0.02 | 2.64 ± 0.11 |
| *PHABULOSA* | 1 | 1.2 ± 0.26 | 0.4 ± 0.1 | 0.48 ± 0.08 | 0.85 ± 0.08 |
| *PHAVOLUTA* | 1 | n.a | 0.6 ± 0.1 | n.a | 0.7 ± 0.09 |
| *ATHB8* | 1 | 1.48 ± 0.12 | 0.1 ± 0.03 | 0.2 ± 0.02 | 0.9 ± 0.04 |
| *ATHB15* | 1 | 1.41 ± 0.20 | 0.69 ± 0.13 | 0.66 ± 0.15 | 0.62 ± 0.24 |
| *KANADI1* | 1 | 1.1 ± 0.10 | 2.1 ± 0.34 | 1.8 ± 0.31 | 1.05 ± 0.04 |
| *KANADI2* | 1 | n.a | 1.02 ± 0.18 | n.a | 0.79 ± 0.05 |
| *PIN1* | 1 | 1.9±0.17 | 0.64 ± 0.12 | 1.1 ± 0.23 | 1.57 ± 0.1 |
| *APL* | 1 | n.a | 0.13 ± 0.03 | n.a | 1.95± 0.11 |
| *MP* | 1 | 1.6±0.18 | 0.3 ± 0.02 | 0.4 ± 0.07 | 3.03 ± 0.17 |

Total RNA of seedlings was extracted 15 days after germination. Relative expression levels of the genes indicated were normalized to the expression level of *S16* . Expression levels were set to 1 in *AtHB15::LhG4* (control) plants. Measurements were performed in triplicates.

Fig. A1

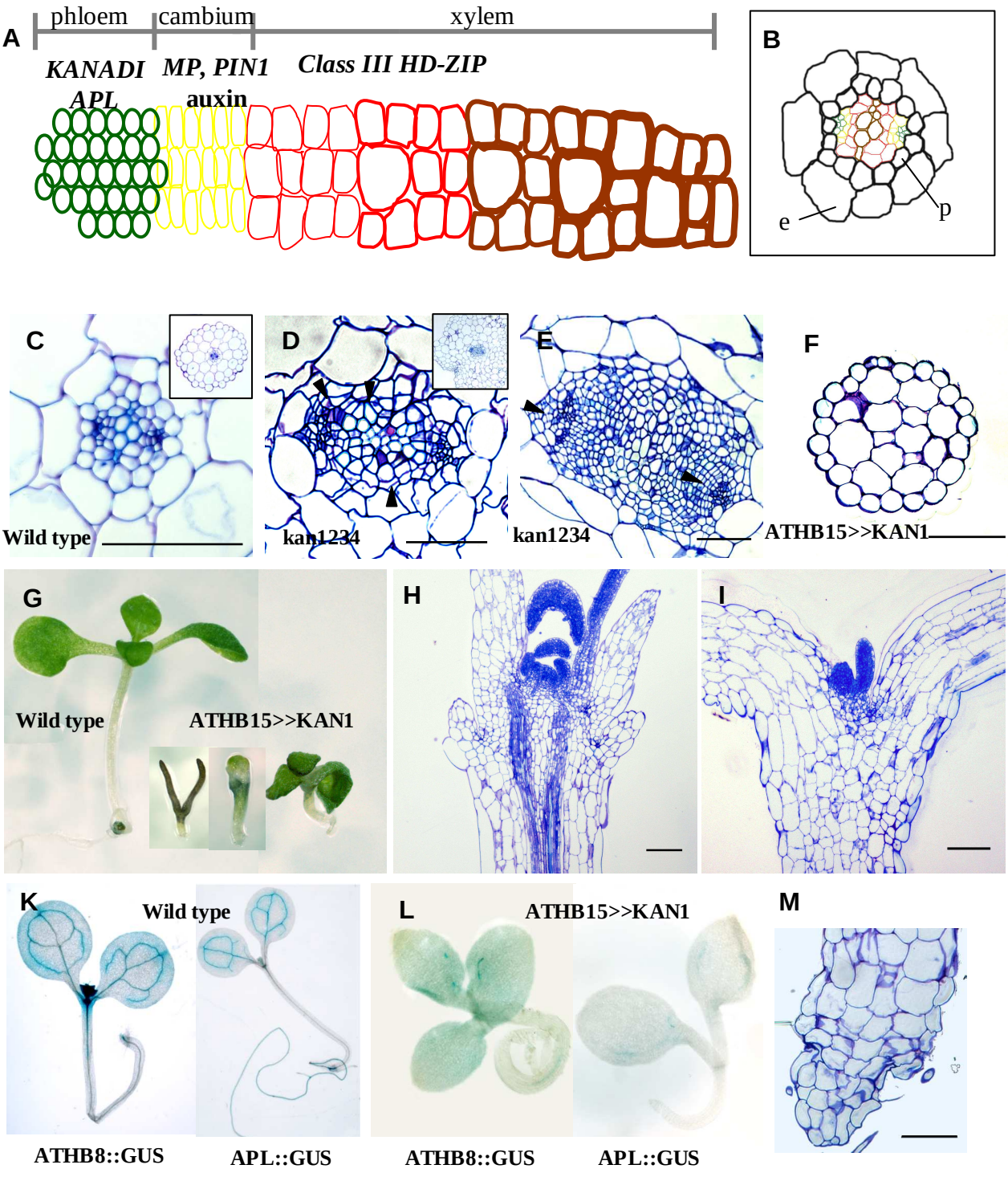
A
phloem
cambium
xylem
KANADI
APL
MP, PIN1
auxin
Class III HD-ZIP
B
e
p
C
Wild type
D
kan1234
E
kan1234
F
ATHB15>>KAN1
G
Wild type
ATHB15>>KAN1
H
I
K
Wild type
ATHB8::GUS
APL::GUS
L
ATHB15>>KAN1
ATHB8::GUS
APL::GUS
M

Fig. A2

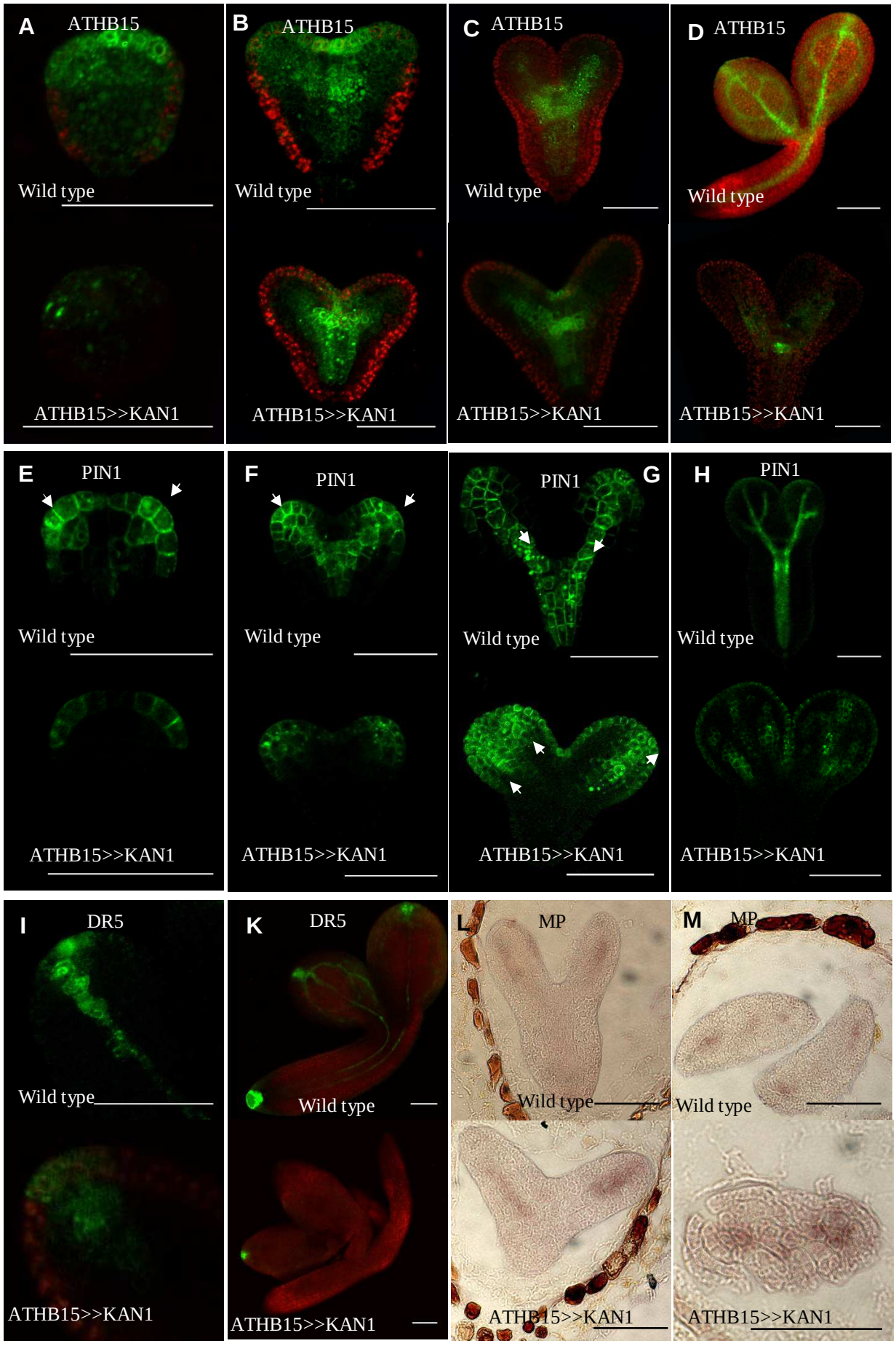
A
ATHB15
Wild type
ATHB15>>KAN1
B
ATHB15
Wild type
ATHB15>>KAN1
C
ATHB15
Wild type
ATHB15>>KAN1
D
ATHB15
Wild type
ATHB15>>KAN1
E
PIN1
Wild type
ATHB15>>KAN1
F
PIN1
Wild type
ATHB15>>KAN1
G
PIN1
Wild type
ATHB15>>KAN1
H
PIN1
Wild type
ATHB15>>KAN1
I
DR5
Wild type
ATHB15>>KAN1
K
DR5
Wild type
ATHB15>>KAN1
L
MP
Wild type
ATHB15>>KAN1
M
MP
Wild type
ATHB15>>KAN1

Fig. A3

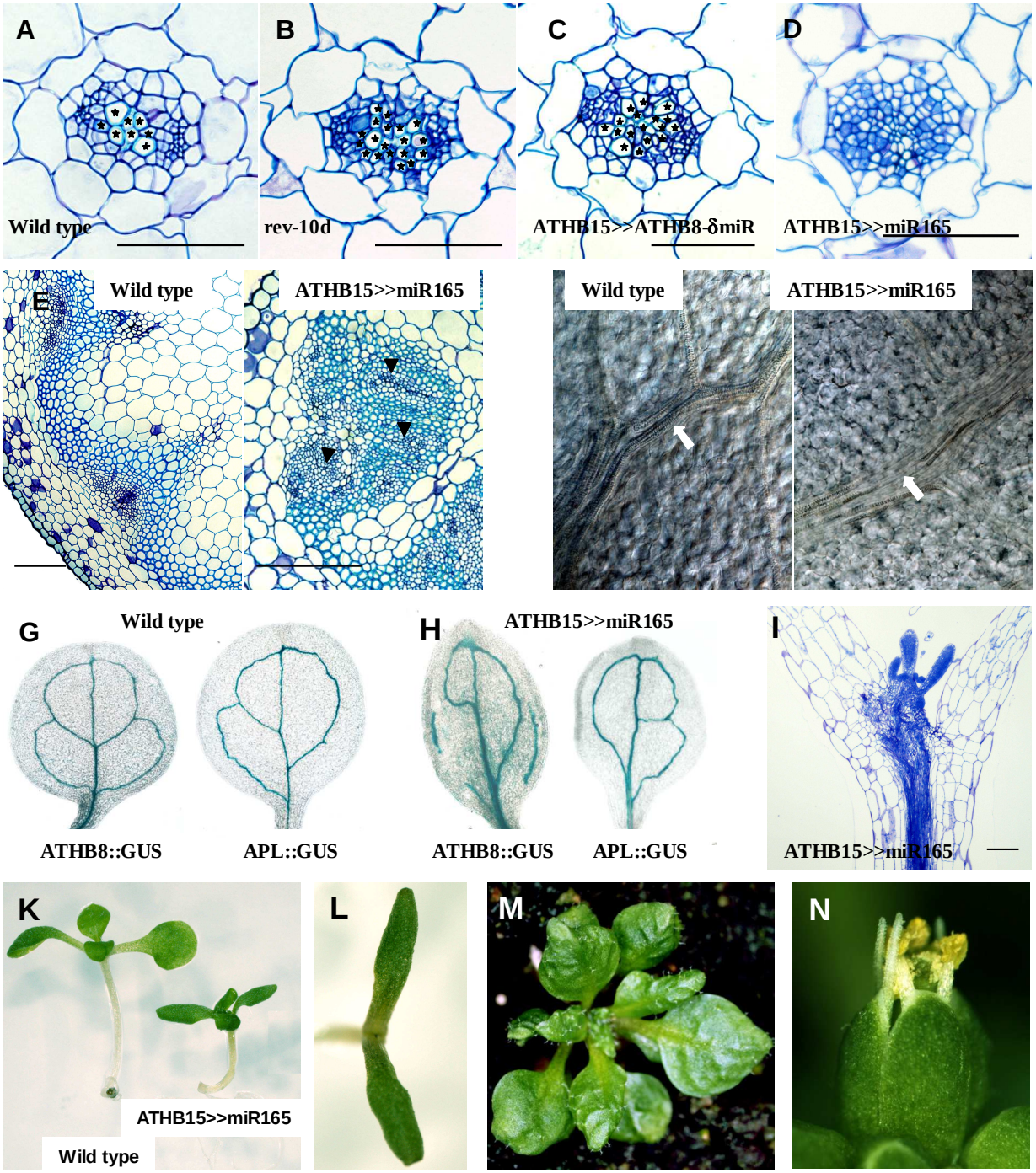
A
Wild type
B
rev-10d
C
ATHB15>>ATHB8-δmiR
D
ATHB15>>miR165
E
Wild type
ATHB15>>miR165
Wild type
ATHB15>>miR165
G
Wild type
ATHB8::GUS
APL::GUS
H
ATHB15>>miR165
ATHB8::GUS
APL::GUS
I
ATHB15>>miR165
K
ATHB15>>miR165
Wild type
L
M
N

Fig. A4

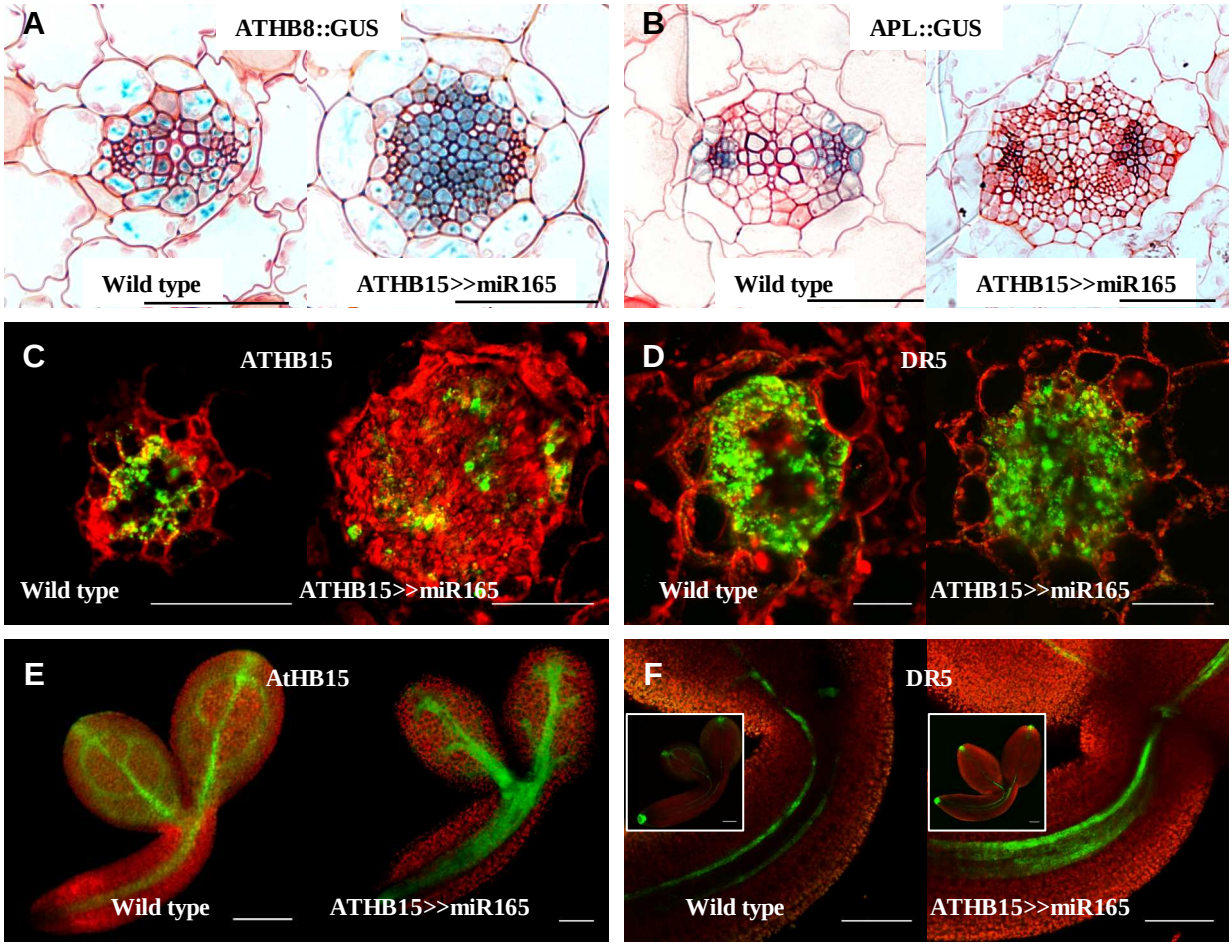
A
ATHB8::GUS
Wild type
ATHB15>>miR165
B
APL::GUS
Wild type
ATHB15>>miR165
C
ATHB15
Wild type
ATHB15>>miR165
D
DR5
Wild type
ATHB15>>miR165
E
AtHB15
Wild type
ATHB15>>miR165
F
DR5
Wild type
ATHB15>>miR165

Fig. A5

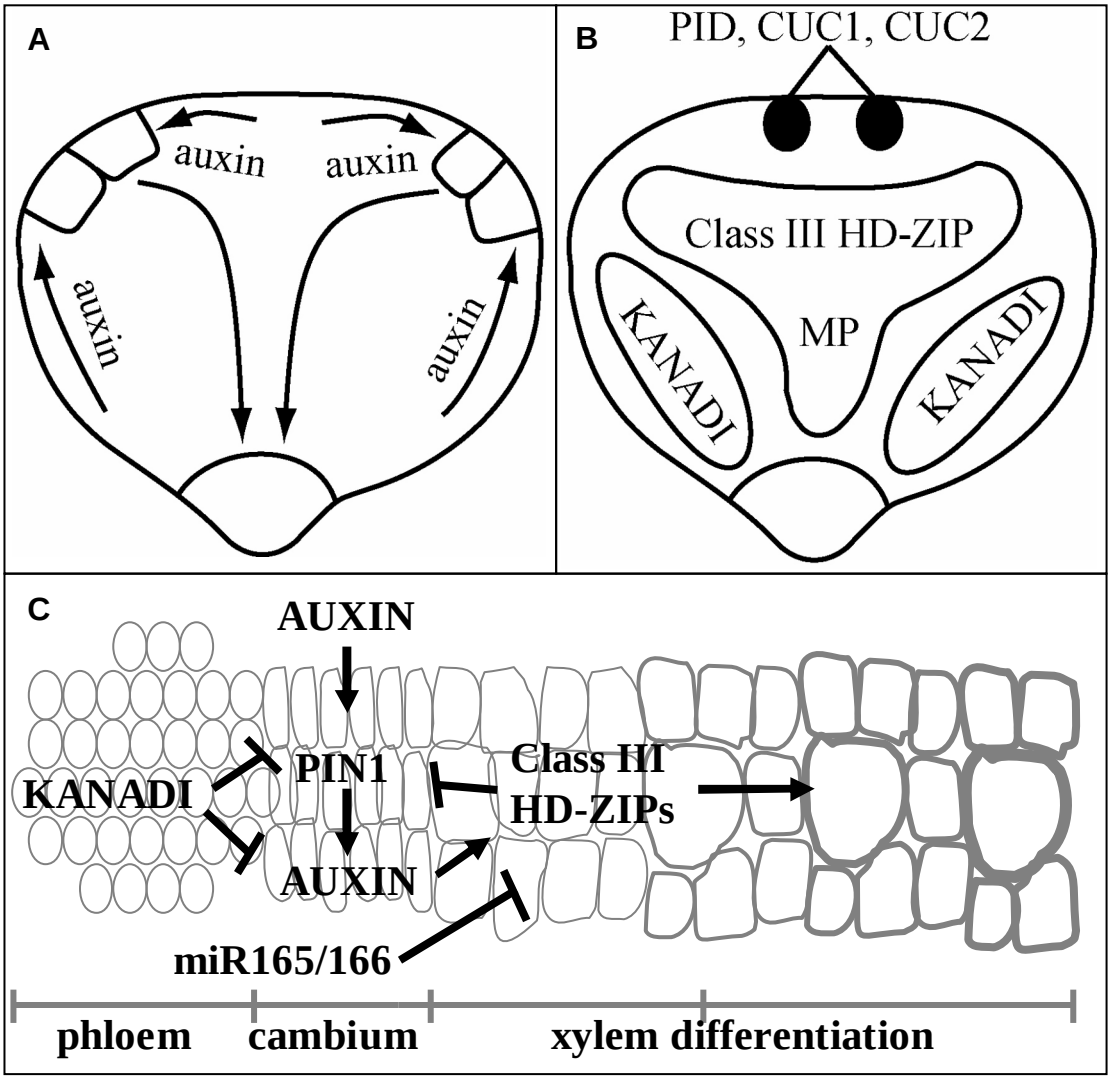
A
auxin
auxin
auxin
auxin
B
PID, CUC1, CUC2
Class III HD-ZIP
KANADI
MP
KANADI
C
AUXIN
KANADI
PIN1
Class III
HD-ZIPs
AUXIN
miR165/166
phloem
cambium
xylem differentiation